Carbon 252 (2026) 121320

Contents lists available at ScienceDirect

Carbon

journal homepage: www.elsevier.com/locate/carbon

Review article

A concise review of recently synthesized 2D carbon allotropes: Amorphous carbon, graphynes, biphenylene and fullerene networks

R. Paupitz [a], A.F. Fonseca [b], M. Bessa [c], G.S.L. Fabris [b], W.F. da Cunha [d], L.D. Machado [c], M.L. Pereira Junior [e,f,*], L.A. Ribeiro Junior [d,g], D.S. Galvão [b,h,*]

[a] Department of Physics, IGCE, São Paulo State University (UNESP), Rio Claro, São Paulo 13506-900, Brazil
[b] Universidade Estadual de Campinas (UNICAMP), Instituto de Física Gleb Wataghin, Departamento de Física Aplicada, 13083-859, Campinas, SP, Brazil
[c] Department of Physics, Federal University of Rio Grande do Norte (UFRN), Natal, Rio Grande do Norte 59078-900, Brazil
[d] Institute of Physics, University of Brasília (UnB), Brasília, Federal District 70910-900, Brazil
[e] Department of Electrical Engineering, College of Technology, University of Brasília (UnB), Brasília, Federal District 70910-900, Brazil
[f] Department of Materials Science and NanoEngineering, Rice University, Houston, TX 77005, United States
[g] Computational Materials Laboratory (LCCMat), Institute of Physics, University of Brasília (UnB), Brasília, Federal District 70910-900, Brazil
[h] Department of Applied Physics and Center for Computational Engineering & Sciences, University of Campinas (UNICAMP), Campinas, São Paulo 13083-970, Brazil

ARTICLE INFO

Keywords:
Two-dimensional carbon allotropes
Amorphous carbon monolayers
Graphynes
Biphenylene-based networks
Fullerene networks
Critical review

ABSTRACT

Two-dimensional (2D) carbon allotropes have received considerable attention due to their unique properties and potential applications in several fields, including electronics, catalysis, energy storage, and sensing. Following the experimental realization of graphene, numerous other 2D carbon structures have been proposed and, in some cases, successfully synthesized. This work presents a concise review of the recently experimentally realized 2D carbon allotropes beyond graphene, including monolayer amorphous carbon, graphynes, biphenylene-, and fullerene-based networks. For each class, we discuss structural characteristics, theoretical predictions, and synthesis methods, with emphasis on the interplay between theory and experiment. We also highlight instances where experimental studies overlooked relevant theoretical contributions. Finally, we identify theoretically predicted structures that remain unexplored experimentally, suggesting opportunities for synthesis-driven investigations.

Contents

* Corresponding authors.
E-mail address: marcelo.lopes@unb.br (M.L. Pereira Junior).

https://doi.org/10.1016/j.carbon.2026.121320
Received 3 September 2025; Received in revised form 12 January 2026; Accepted 27 January 2026
Available online 28 January 2026

1. Introduction

Carbon, in addition to being the backbone of organic compounds, stands out for its remarkable ability to form a wide variety of allotropes across multiple dimensionalities and with distinct atomic hybridizations [1,2]. These structural forms range from zero-dimensional (0D) fullerenes [3,4], one-dimensional (1D) carbon nanotubes [3,5] and nanoribbons, two-dimensional (2D) graphene [6] and graphynes [7], to three-dimensional (3D) graphite [8] and diamond [9], each exhibiting markedly different physical and chemical properties. This versatility makes carbon-based materials highly valuable for a broad range of technological applications, many of which have become the subject of intense recent research.

Among these allotropes, graphene [6] stands out due to its outstanding properties across multiple domains. Despite its simple structure, composed of 2D carbon atoms arranged in a hexagonal lattice, graphene exhibits remarkable electronic and structural characteristics [10]. It is simultaneously lightweight and flexible, while being one of the strongest materials known, enabling its use in mechanically demanding devices [11]. Its high electrical [12] and thermal conductivity [13] make it an excellent candidate for nanoelectronic applications, while its optical transparency opens opportunities in photonics [14]. Furthermore, its high surface-to-volume ratio renders it attractive for energy storage, catalysis, and even biotechnology [15].

Due to these attractive properties, graphene has received considerable attention from materials scientists and engineers. Nevertheless, a key challenge limiting its broader applicability in optoelectronics is its lack of an electronic bandgap [16]. While a tunable bandgap is highly desirable for electronic devices, the intrinsic zero-gap nature of graphene restricts its performance as an active layer in devices such as organic light-emitting diodes (OLEDs) [17], organic photovoltaics (OPVs) [18], and organic field-effect transistors (OFETs) [19]. As a result, substantial efforts have been dedicated to discovering alternative materials that could retain many of graphene's desirable properties while exhibiting a suitable semiconducting bandgap for those applications.

In response, both theorists and experimentalists have worked over the years to evaluate, propose, and experimentally realize new 2D carbon allotropes as potential materials for organic electronic devices [20]. Among these structures, graphene nanoribbons (GNRs) [21] stand out. These narrow strips of graphene, obtained by controlled cutting along specific crystallographic directions, exhibit intrinsic properties distinct from those of their parent material. Depending on their symmetry, GNRs can present a non-zero bandgap. However, the synthesis of GNRs remains technically challenging, particularly in controlling the width, length, edge type, and symmetry at a scale and quality compatible with industrial and device-level applications. All these features directly affect the electronic bandgap and transport behavior [22].

Another example is carbon nanotubes (CNTs) [23], which can be viewed as rolled-up graphene sheets that form cylindrical structures with periodic boundary conditions along their circumference. While they show promise for nanoelectronic and optoelectronic technologies, the production of high-purity, single-walled CNTs with precise chirality and reproducible structural and electronic properties remains a substantial bottleneck [24]. Thus, beyond possessing a suitable bandgap and preserving the desirable properties of graphene, a third critical requirement emerges: the synthesis process must be reliable, reproducible, and scalable.

In this perspective, given the inherent complexity and evolving nature of synthesis techniques, exploring a broad range of theoretically proposed carbon-based 2D materials has proven to be a fruitful strategy. Indeed, notable progress has been made in recent years by following this path [25]. This is evidenced by the increasing number of studies focused on 2D carbon allotropes with diverse topologies and atomic arrangements [26]. Graphene, however, continues to serve as the conceptual and experimental baseline in this area, remaining central to ongoing developments.

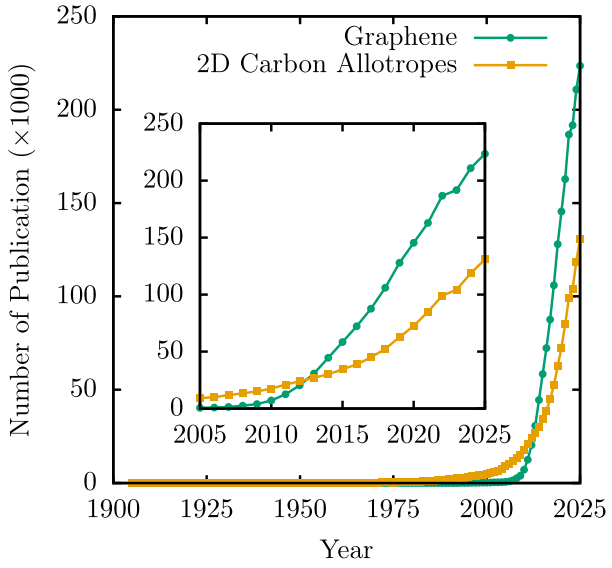

Fig. 1. Time evolution of annual publications mentioning graphene and other 2D carbon allotropes, indexed in the *Scopus* database.

This growing interest is well illustrated by the time evolution of scientific publications on the topic. Fig. 1 shows the annual number of publications indexed in the Scopus database [27] related to graphene and other 2D carbon allotropes. For graphene, a simple Boolean search string was adopted: `"graphene"`. In contrast, retrieving publications concerning 2D carbon allotropes required a broader bibliographic search strategy to capture their structural and terminological diversity. The following Boolean expression was employed: `("carbon allotrope" OR "carbon" OR "carbon network" OR "carbon sheet") AND ("2D" OR "two-dimensional" OR "two dimensional" OR "2-dimensional" OR "layered material" OR "monolayer")`.

The data indicate that until 2012, the number of publications related to 2D carbon allotropes surpassed those focusing exclusively on graphene. From 2013 onwards, graphene became the most frequently published topic annually, a trend that remains consistent. As of the latest query, more than 1.1 million documents related to 2D carbon allotropes are indexed in Scopus, while entries explicitly mentioning graphene total around 1.7 million.

This pattern suggests that interest in 2D carbon systems preceded the consolidation of graphene as a central research object. However, the experimental realization of graphene in 2004 [6] marked a significant turning point. It is also important to note that there is considerable overlap between both datasets, as most publications on 2D allotropes cite graphene, often as a theoretical benchmark or reference material. Therefore, the figures should not be interpreted as indicators of competing research areas but rather as evidence of a coevolutionary and interdependent process. The search for novel carbon allotropes is motivated by the limitations of graphene in specific applications, such as the absence of a bandgap. In contrast, graphene continues to serve as a fundamental material both conceptually and technologically.

In this context, research efforts aimed at developing promising monolayers of 2D carbon allotropes can be generally classified into

two major categories. The first category includes studies that report the experimental synthesis of new carbon allotropes without relying explicitly on theoretical predictions. These discoveries are often followed by detailed characterization efforts using both experimental techniques and computational modeling. An example is the case of graphene itself. Although Wallace first described the electronic band structure of a graphene monolayer in 1947 [28], his work focused on bulk graphite rather than graphene as an isolated 2D system. Later theoretical studies addressed graphene, but often within the scope of specific physical phenomena. For example, Zheng and Ando explored Hall conductivity, referencing graphene only incidentally [29].

It was not until the experimental realization and fundamental characterization of graphene by Novoselov and colleagues in 2004, [6] that graphene emerged as a central topic in materials research, ultimately leading to the Nobel Prize in Physics in 2010. This milestone triggered a surge of theoretical investigations, including the seminal 2009 review by Castro Neto and collaborators [30], which thoroughly examined the electronic properties of graphene.

The second research pathway is more result-oriented and involves experimental synthesis efforts that are explicitly guided by theoretical predictions. This strategy reduces the exploratory cost by targeting materials that have already been identified as promising through simulations. A notable example is the experimental synthesis of graphene nanoribbons, driven by the theoretical insights of Mitsutaka Fujita in 1996 [31], who predicted distinctive electronic behavior arising from edge topologies.

It is essential to note that while studies employing the second approach generally acknowledge prior experimental work that validates their predictions, the reverse is not always the case. Experimental studies sometimes fail to cite earlier theoretical contributions that were available at the time of their discovery. This gap often reflects a lack of integration between theoretical and experimental communities. Closing this gap could accelerate progress in the field. One aspect worth emphasizing in this context is the emergence of machine learning-driven approaches, which have rapidly expanded the computational exploration and optimization of emerging 2D carbon allotropes [32]. Machine learning interatomic potentials (MLIPs), trained on *ab initio* datasets, enable simulations of structural stability, phonon spectra, and thermal expansion with near Density Functional Theory (DFT) accuracy at a fraction of the computational cost. These models have been successfully applied to a wide range of carbon-based systems, including graphene derivatives, haeckelites, phagraphene, and fullerene networks [33]. More recently, transferable MLIPs have been developed, allowing accurate predictions of mechanical failure mechanisms and temperature-dependent responses in nanoporous carbon nitride and related heteroatom-doped frameworks [34]. Together, these advances demonstrate that machine learning approaches bridge the gap between first-principles accuracy and large-scale molecular dynamics (MD) simulations, accelerating the computational design of next-generation carbon nanomaterials.

In recent years, a number of comprehensive reviews have summarized experimental advances and emerging directions in carbon-based materials, providing a broader framework for understanding the rapid evolution of this field. General overviews have discussed the structural diversity, synthesis strategies, and multifunctional properties of carbon materials, ranging from amorphous and porous frameworks to ordered 2D allotropes [32,34–36]. Complementary reviews have focused on specific 2D systems, graphyne derivatives, and heteroatom-doped carbon networks, highlighting advances in low-temperature synthesis, interface engineering, and device integration [37–39]. Other recent perspectives have examined the evolution of carbon allotropes beyond graphene toward sustainable and functional materials, including their prospects in photonics, catalysis, and energy-related applications [40–43]. Together, these studies frame the synthesis breakthroughs discussed in this review within the broader landscape of contemporary carbon materials science.

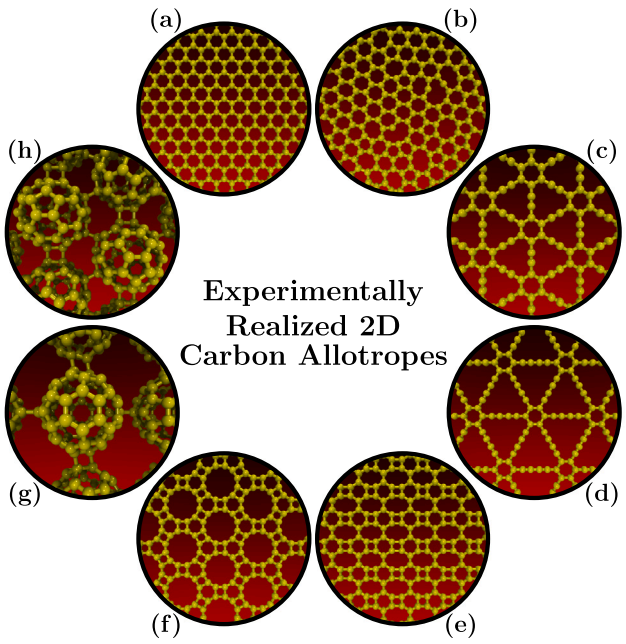

Fig. 2. Experimentally realized 2D carbon allotropes. The panels represent different structures: (a) graphene, (b) monolayer amorphous carbon (MAC), (c) γ-graphyne (GY), (d) γ-graphdiyne (GDY), (e) biphenylene network (BPN), (f) graphenylene network (GP), (g) quasi-tetragonal phase C_{60} ($qTPC_{60}$), (h) quasi-hexagonal phase C_{60} ($qHPC_{60}$).

In this work, we present a critical review of experimentally realized 2D carbon allotropes, emphasizing their atomic structures, synthesis routes, and physical properties. While the primary focus lies on experimentally realized systems, we also consider theoretical contributions that have either guided their discovery or proposed related nanostructures with potential technological relevance. The review is organized as follows. The next section examines 2D amorphous carbon. A discussion of graphyne lattices follows. Subsequently, biphenylene-based carbon networks are analyzed, and 2D fullerene-derived structures are presented. The manuscript concludes with final remarks and perspectives on current challenges and future directions for the field.

All experimentally realized 2D carbon allotropes discussed in the present work are illustrated in Fig. 2. Throughout the text, graphene (Fig. 2(a)) and monolayer amorphous carbon (MAC) (Fig. 2(b)) are discussed in Section 2, γ-graphyne (γ-GY) (Fig. 2(c)) and γ-graphdiyne (γ-GDY) (Fig. 2(d)) are discussed in Section 3, biphenylene-based materials, namely the biphenylene network (BPN) (Fig. 2(e)) and graphenylene (GP) (Fig. 2(f)), are discussed in Section 4, while C_{60}-based networks, namely the quasi-hexagonal ($qHPC_{60}$) (Fig. 2(g)) and quasi-tetragonal ($qTPC_{60}$) (Fig. 2(h)) phases are presented in Section 5. The figure highlights the structural diversity of these materials, including graphene, MAC, graphyne derivatives, biphenylene- and fullerene-networks.

2. Monolayer amorphous carbon

Beyond graphene, MAC is among the most remarkable examples of the recently synthesized 2D carbon allotropes. A direct comparison between Figs. 3(a) and 3(b), corresponding to graphene and MAC, respectively, highlights the fundamental structural contrast between a long-range crystalline lattice and a fully disordered atomic network that nonetheless preserves short-range bonding correlations. In Fig. 3(b), the atomistic model of MAC follows the structural framework originally introduced by Toh et al. [44], which has since become a reference for describing atomically thin amorphous carbon.

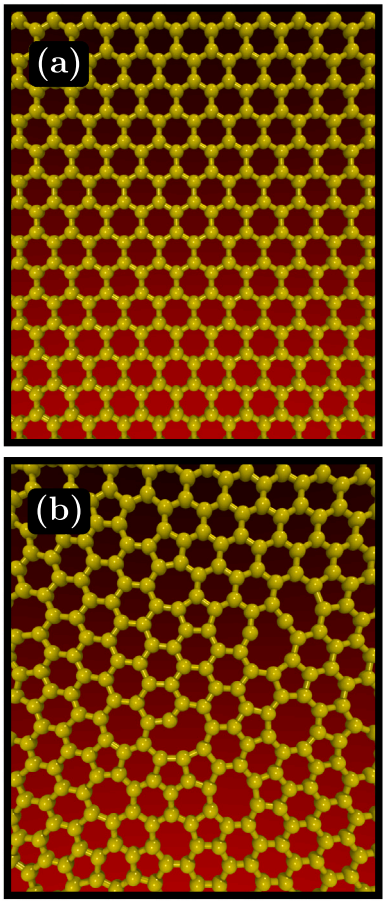

Fig. 3. Atomistic representations of (a) graphene and (b) monolayer amorphous carbon, illustrating the contrast between the long-range crystalline order and the disordered topology.

The synthesis routes leading to these distinct forms of carbon are summarized in Figs. 4 and 5. Graphene synthesis relies on well-established crystalline pathways, including mechanical exfoliation, epitaxial growth on metal or carbide substrates, and chemical vapor deposition, which are designed to preserve long-range order and lattice coherence [45,46]. In contrast, the synthesis of amorphous carbon systems follows a fundamentally different disorder-to-disorder paradigm, in which reactive carbon species generated in a plasma environment reorganize directly into an amorphous monolayer on nanograined Cu substrates, bypassing any intermediate crystalline phase [47]. This mechanism demonstrates that the absence of structural order in both precursor species and substrate plays a key role in stabilizing atomically thin amorphous carbon.

Despite its lack of long-range periodicity, MAC shares several key properties with graphene, including high electrical conductivity, optical transparency, large surface area, and mechanical robustness. Importantly, MAC exhibits a small but finite electronic bandgap, distinguishing it from pristine graphene and expanding its potential for electronic and optoelectronic applications. These features have attracted increasing attention from both experimental [44,48] and theoretical [49–56] communities. In this context, the remainder of this section focuses primarily on MAC, emphasizing its structural characteristics, synthesis mechanisms, and emerging physical properties within the broader landscape of two-dimensional carbon materials.

Unlike crystalline solids, amorphous materials do not exhibit long-range periodicity in their atomic arrangement [57,58]. Although localized regions may resemble crystalline motifs, finite unit cells are insufficient for capturing their structure fully. Techniques such as radial distribution function (RDF) analysis are therefore widely used. Amorphous materials have found broad application in diverse scientific and technological contexts [59–63].

A foundational model for such systems was introduced in 1932 by Zachariasen [64], who proposed the continuous random network (CRN) framework. This model describes disordered yet connected atomic arrangements lacking translational symmetry, and it remains central to understanding amorphous structures [65]. Nevertheless, recent studies suggest deviations from the CRN model in specific systems, motivating the development of refined approaches.

A breakthrough in the field occurred in 2019 when Toh et al. synthesized and characterized MAC [44]. Using laser-assisted chemical vapor deposition (CVD), a continuous monolayer was formed within minutes at relatively low substrate temperatures (approximately 200 °C), in contrast to the higher temperatures typically required for graphene growth [66].

High-resolution transmission electron microscopy (HRTEM) confirmed the absence of crystalline periodicity, revealing a disordered carbon network. The structure is best described by a crystallite-in-Z-CRN model, where nanoscale domains of six-membered rings are embedded in a continuous random network. These domains vary in orientation and strain. The atomic arrangement includes pentagons, heptagons, octagons, distorted hexagons, and regular hexagons, the latter forming crystalline inclusions of approximately 1 nm in diameter. Bond lengths ranged from 0.9 to 1.8 Å, and bond angles spanned 90° to 150°, reflecting significant structural variability.

The material also exhibited excellent film continuity, with no multilayer regions or wrinkles, and remarkable environmental stability, maintaining its structure for over a year.

2.1. *Theoretically predicted properties*

Theoretical modeling of MAC was performed using a kinetic Monte Carlo approach on a 40 × 40 Å^2 supercell with 610 carbon atoms, followed by conjugate gradient relaxation. The AIREBO potential [67] was used for interatomic interactions, implemented in LAMMPS [68]. Among over 60,000 configurations, the one that best matched the HRTEM features was selected as the reference structure.

This model has been employed in multiple studies to explore MAC's mechanical, electronic, optical, and thermal properties [53,55,69–71]. Complementary DFT calculations using VASP [72] and transport simulations with TranSIESTA [73,74] confirmed its room-temperature thermal stability and revealed buckling in non-hexagonal regions. An optical bandgap of approximately 2.1 eV was also identified, underscoring MAC's promise in optoelectronics.

Following this foundational characterization, we extended the analysis to assess MAC's mechanical and thermal behavior in comparison to graphene [53]. Simulations using the same 610-atom MAC model and a 640-atom graphene structure were subjected to uniaxial tension up to a strain of 100%. MAC exhibited a Young's modulus of approximately 323 GPa, compared to 881 GPa for graphene, under the same conditions. While graphene reached a tensile strength of approximately 228 GPa, MAC failed at around 61 GPa. The disordered MAC structure allows more bond rearrangement and accommodates strain more gradually, leading to extensive linear atomic chain (LAC) formation upon rupture.

Thermal ramp simulations, spanning from 100 K to 10,000 K, revealed collapse mechanisms in both systems. LAC formation was observed at temperatures of approximately 4500 K for MAC and 5500 K for graphene. Melting points were estimated to be approximately 3600 K for MAC and 4100 K for graphene.

To explore curvature effects, further investigations examined MAC configured as nanotubes and nanoscrolls [55]. Density Functional-based Tight Binding (DFTB) and DFT calculations revealed that rolling the sheet resulted in small bandgap openings (90, 13, and 18 meV for

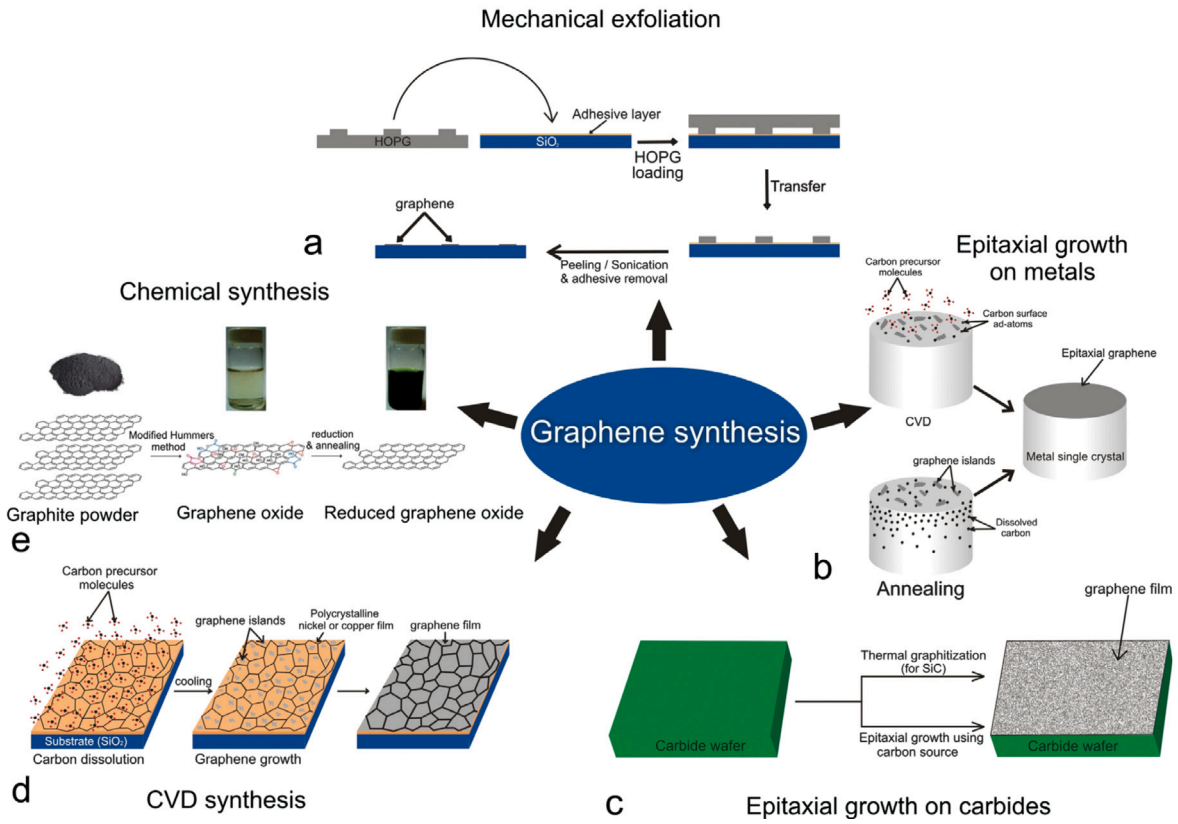

Fig. 4. Representative synthesis routes for graphene and related crystalline two-dimensional carbon materials, including mechanical exfoliation, epitaxial growth on metals and carbides, and chemical vapor deposition.
Source: Reproduced with permission from Refs. [45,46] under the Creative Commons CC BY license.

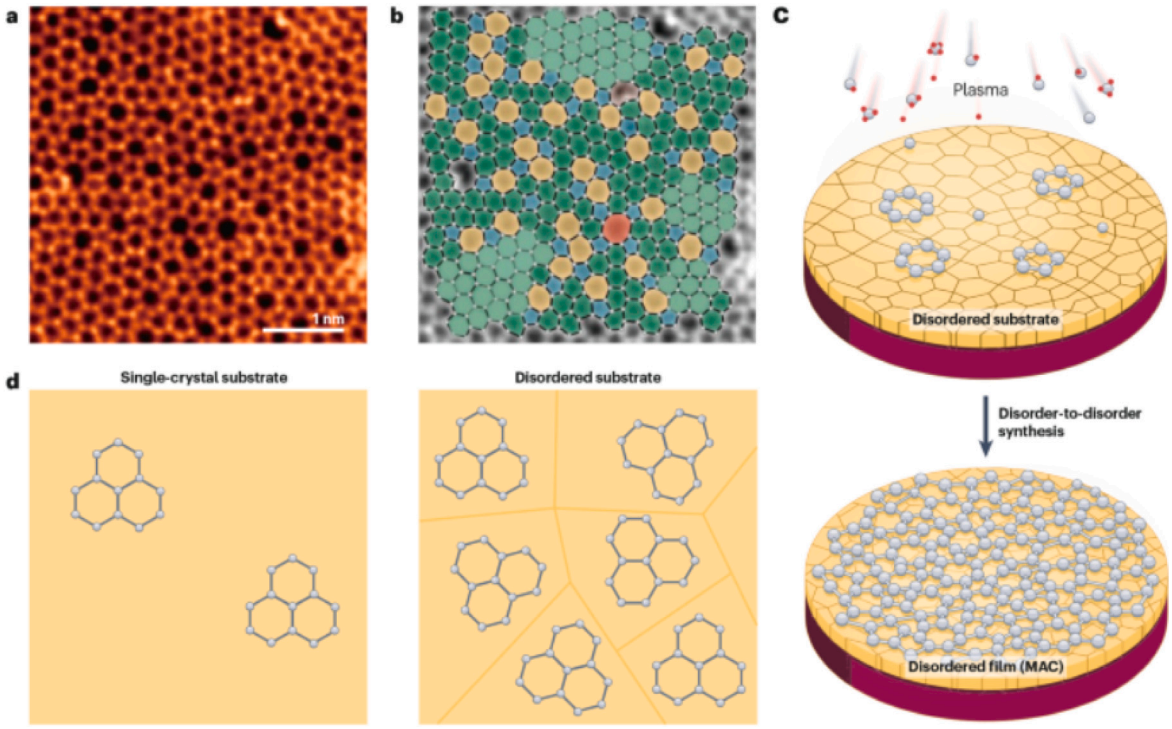

Fig. 5. Disorder-to-disorder synthesis of ultraclean monolayer amorphous carbon (MAC), illustrating plasma-assisted growth on nanograined Cu substrates and the resulting topologically disordered atomic network.
Source: Reproduced with permission from Ref. [47]

tubes and scrolls). These systems absorb light from the infrared (IF) to ultraviolet (UV), with reflectivity decreasing as the wavelength moves toward the UV. Scrolls showed the largest optical response.

Using larger supercells (3660 atoms), MD simulations assessed the thermal and mechanical properties of MAC-based nanotubes and nanoscrolls [69]. Results confirmed that MAC exhibits comparable mechanical behavior to its crystalline counterpart under curvature. Melting temperatures varied between 5100 K and 5900 K, depending on the geometry and strain distribution.

In addition to these characteristics, MAC presents a percolating π network sustained by short-range order, which yields a finite density of states at the Fermi level and metallic-like transport. This electronic behavior enables applications as transparent and flexible conductors [44]. By contrast, amorphous BN is best described as a compositionally disordered pseudo-continuous random network containing pseudocrystallites and noncanonical B–B and N–N linkages. Despite the pronounced structural disorder, it remains insulating and thermally stable at room temperature, which favors applications as ultrathin dielectric or barrier layers rather than conductive films [75]. A distinct disorder paradigm is observed in amorphous MoS_2, where operando experiments and theoretical studies reveal shortened Mo-S and Mo–Mo bonds together with edge-like motifs that persist under electrochemical bias. These structural features impart metallic character and enhanced charge-transfer kinetics, which underpin high catalytic activity for the hydrogen evolution reaction [76]. Taken together, these examples demonstrate that disorder can either suppress or enable electronic conduction depending critically on the bonding topology and chemical composition, thereby delineating complementary functional niches for amorphous two-dimensional materials.

3. Graphyne families materials

One of the earliest predictions of a one-atom-thick 2D carbon allotrope family distinct from graphene is the structures named graphynes (GY). In 1987, Baughman, Eckhardt, and Kertesz [7] proposed seven new structures of periodic 2D carbon phases formed by acetylenic chains (−C≡C−), connecting aromatic rings or carbon–carbon bonds. These can be conceptualized as systematic substitutions of carbon–carbon bonds in graphene by acetylenic groups. There are innumerable ways to generate structural GY motifs by connecting acetylenic chains directly to themselves or through aromatic rings and sp^2 carbon–carbon bonds. Among the seven GY structures originally proposed, those designated as α-, β-, γ-, and 6,6,12-GY are the most investigated. The first three members of the graphyne family exhibit hexagonal symmetry, with γ-GY being the densest of the graphyne family.

The GY structures can be created with different numbers of acetylenic chains, n ($(-C\equiv C-)_n$, $n \geq 1$), without changing the structural symmetry. Structures having $n = 2, 3, 4$, are designated as graphdiyne (GDY), graphtriyne, graphtetrayne (GTY), and so forth, respectively. Fig. 6 presents the most representative GY structures. The atomic arrangements of γ-GY, -GDY, and -GTY are shown in Figs. 6(a-c), while the theoretical phases α-, β-, and 6,6,12-GY structures are shown in Figs. 6(d-f), highlighting the diversity of ring topology and acetylenic bonding motifs within the graphyne family.

3.1. Theoretically predicted properties

Interest in GYs emerged decades later, based on several works that predicted that the physical properties of GYs are not only as special as those of graphene [77], but in some aspects even more distinctive. Similar to graphene, GYs have been predicted to exhibit high charge carrier mobility, ranging from 0.2 to 5.4×10^5 $cm^2V^{-1}s^{-1}$ [78,79], in contrast to values on the order of 2×10^5 $cm^2V^{-1}s^{-1}$ reported for graphene [77]. Their mechanical response is also remarkable, with predicted Young's modulus values spanning from 0.1 to 0.7 TPa for GYs [80,81], compared to approximately 1.1 TPa for graphene [77]. Different from graphene, GYs present relatively low thermal conductivity, with reported values ranging from 18 to 82 $Wm^{-1}K^{-1}$ [78,82], in contrast to the high thermal conductivity of graphene, which can reach values around 5000 $Wm^{-1}K^{-1}$ [77]. In addition, GYs are intrinsically porous [83] and exhibit a non-zero electronic bandgap [84–86], features that are particularly attractive for electronic and optoelectronic applications. Furthermore, their electronic properties can be tuned [87], which also allows the design of new applications in electronic devices. Finally, asymmetric GYs display null and negative linear compressibilities [88,89], a property that could be exploited for applications such as sensors and other mechanical actuators. These properties underscore the rationale for considering GYs as a substitute for graphene in electronic and other applications [90,91].

Recent literature has predicted that GYs possess additional attractive properties, including negative thermal expansion [92,93], Poisson's ratio greater than 0.5 [88,93], interesting optoelectronic properties [94], magnetic hystereses [95], thermoelectric features [96,97], enhanced elastocaloric effect [98] and thermal stability up to about 1000 K [99]. A number of computational studies have been conducted to explore the existence and properties of GY scrolls [99], nanoribbons [98,100], and nanotubes [101].

These theoretical works have contributed to the study of potentially new applications of GYs. Examples include the development of nanotransistors [102], gas separation and desalination [103–107], anticancer and antibacterial agents [108,109], anodes for batteries [110,111], hydrogen storage [112], supercapacitor electrodes [113,114], and others [115–118].

3.2. Synthesized graphynes

Following the seminal contributions of Baughman, Eckhardt, and Kertesz [7], numerous attempts have been documented in the literature to synthesize GYs. The synthesis of GY oligomers and ethynylene-linked molecules has been achieved. However, the yield has been limited to small fragments [119–125].

The first successful experimental achievement of the GY family was reported in 2010 by Liu et al. [126], with the γ-GDY synthesis on a Cu foil accomplished through the implementation of an *in situ* Glaser-Hay coupling reaction [127–129] of hexaethynylbenzene (HEB) monomers with pyridine as the organic solvent. The efficacy of Liu's methodology for obtaining γ-GDYs can be attributed to the catalytic properties of Cu ions dispersed in pyridine, which facilitate the Glaser reaction of the HEB monomers. Additionally, the Cu foil serves as a template for the growth of γ-GDY, contributing to the method's success.

After the initial report by Liu et al. research on γ-GDYs has undergone exponential growth, encompassing the development of novel growth methods [130–134]. Several innovative synthetic strategies have been developed to overcome the limitations of early GDY growth methods, particularly for the experimentally realized γ phase. Matsuoka et al. [130] reported liquid–liquid and gas–liquid interfacial synthetic routes that promote carbon–carbon coupling reactions from HEB monomers, enabling the formation of significantly thinner stacks at room temperature. Zuo et al. [131] introduced a metal-catalyst-free approach to synthesize γ-GDY in air through a so-called popcorn-like explosion phenomenon, in which rapid dehydrogenation-driven coupling of HEB monomers occurs at temperatures as low as 90 °C. Zhou et al. [132] employed an alternative coupling strategy based on hexakis-[(trimethylsilyl)ethynyl]benzene (HEB-TMS) monomers on graphene substrates, yielding γ-GDY layers with thicknesses below 3 nm. Subsequently, Yin et al. [134] developed another catalyst-free route in which a microwave-induced temperature gradient is applied to a solution of HEB monomers dissolved in a toluene-hexane mixture on a solid NaCl substrate, producing ultrathin films with thicknesses below 2 nm. While Gao et al. [133] provided a comprehensive review of synthesis methods and potential applications of γ-GDY, Kuang et al. [135] have recently demonstrated an ultrafast, second-scale synthesis of large

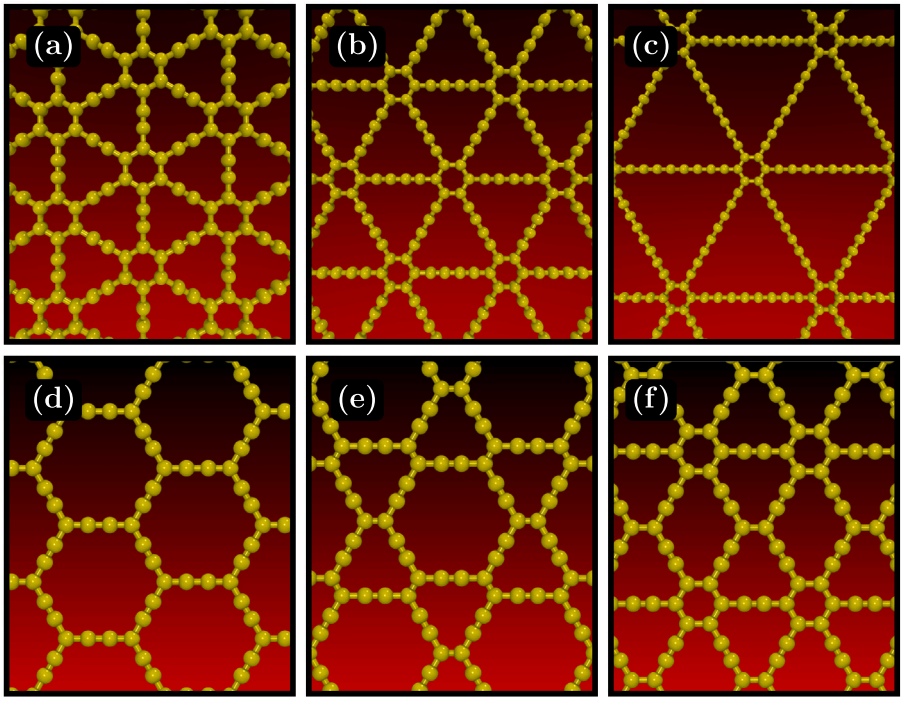

Fig. 6. Representative atomic structures of graphyne-based allotropes. Panels show (a) γ-GY, (b) -GDY, and (c) -GTY. (d) α-, (e) β-, and (f) 6,6,12-GY. The different arrangements of acetylenic linkages and polygonal rings illustrate the structural diversity within the graphyne family.

quantities of this material via electron-beam irradiation of HEB-TMS compounds, using copper(II) acetate and N,N-dimethylformamide as catalyst and solvent, respectively.

The synthesis of γ-GTY, i.e., a GY with $n = 4$ in the γ-phase, was reported almost a decade later by Gao et al. [136] and Pan et al. [137]. These works have received comparatively less attention in the literature than those of γ-GDY, which may be attributable to the challenges associated with their synthesis. The Sonogashira reaction method [138] was employed in both works to describe an intermediate step analogous to that utilized in the synthesis of γ-GDY. This step involves the synthesis of monomers composed of a carbon ring with four acetylenic arms. Subsequently, the γ-GTY were grown on copper foils through reactions analogous to Glaser-Hay.

The synthesis of γ-GDY and γ-GTY represents a significant breakthrough in the field. However, their large porous nature imposes certain limitations on their properties. Nevertheless, the difficulties associated with synthesizing graphyne with $n = 1$, have been recently surmounted. Li et al. [139] were the first to report the synthesis of γ-GY ($n = 1$), through a mechanochemical synthesis method.

Four years later, in 2022, Barua, Saraswat, and Rao [140], and Rodionov et al. [141] reported successful synthetic approaches, based on Sonogashira crosslinking reactions, for the production of the γ-GY. The synthesis of another form of GY with $n = 1$, termed Holey γ-GY, has also been reported by Liu et al. [142]. In a recent study, Song et al. [143] reported the wet chemistry synthesis of γ-GY based on a metal-free crosslinking method. This method involves the combination of fluoro-(hetero)arenes and alkynyl silanes in the presence of tetrabutylammonium fluoride. According to Song et al. their method is capable of producing γ-GY, ranging from grams to the sub-microscopic level.

Li and Han [118] posit that among the various methods of synthesizing γ-GY, the mechanochemical approach is suboptimal due to its inability to adequately control reactions and remove impurities, resulting in substandard product quality.

In a recent study, Rodionov et al. [144] tried to replicate the mechanochemical method for synthesizing γ-GY. The validity of the achievement was challenged by showing that applying the same method under equivalent conditions yielded disordered structures in the absence of carbon–carbon triple bonds. Consequently, the Sonogashira reaction methods can be regarded as the most suitable approach to obtain high-quality γ-GY samples [118]. Nevertheless, Li and Han [118] have noted that a methodology for producing γ-GY with a variable number of layers, size, and stacking modes remains to be developed.

The synthesis of the other members of the GY family remains to be achieved. However, the identification of a method for producing the other structures could be expedited by that of γ-GY. The synthesis of the Holey γ-GY [142] and the recent production of precursors of the 6,6,12-GY [145,146] suggest the feasibility of synthesizing additional $n = 1$ GYs. Fig. 7 depicts the schemes of the main synthetic routes to produce γ-GY and -GDY. At the top, a schematic illustration of one synthetic route to the production of large-area γ-GDY films via a cross-coupling reaction using hexaethynylbenzene is shown [126]. In the middle of the figure, the illustration shows a proposed synthetic route to obtain γ-GY under mild conditions through a cross-linking strategy [140]. On the bottom of Fig. 7, one can see a simplified representation of the synthesis of graphynes through a crystallization-assisted irreversible cross-coupling polymerization [141].

A fast and scalable synthesis of large-area γ-GDY has been achieved [126,135]. Despite the successful synthesis of small-domain γ-GYs and extended GDY sheets, the scalable growth of crystalline graphyne-based materials remains a key bottleneck. The bottom-up *in situ* coupling of acetylene-rich precursors often suffers from slow reaction kinetics and limited molecular diffusion, restricting domain sizes to the micrometer scale [139,141,147]. Recent studies suggest that interfacial coupling synthesis at liquid–liquid or gas–solid boundaries, as well as on-surface polymerization on Cu or Ag substrates, can significantly improve lateral uniformity and control over stoichiometry, approaching the requirements for wafer-scale fabrication [139,141,147]. The most proximate achievements in γ-GY have been reported by Song et al. [143], who reported the synthesis of high quantities (on a gram scale) of γ-GY, albeit in the form of stacks, not single layers.

Although experimental data on key physical quantities, such as the band gap, elastic modulus, and coefficient of thermal expansion, for

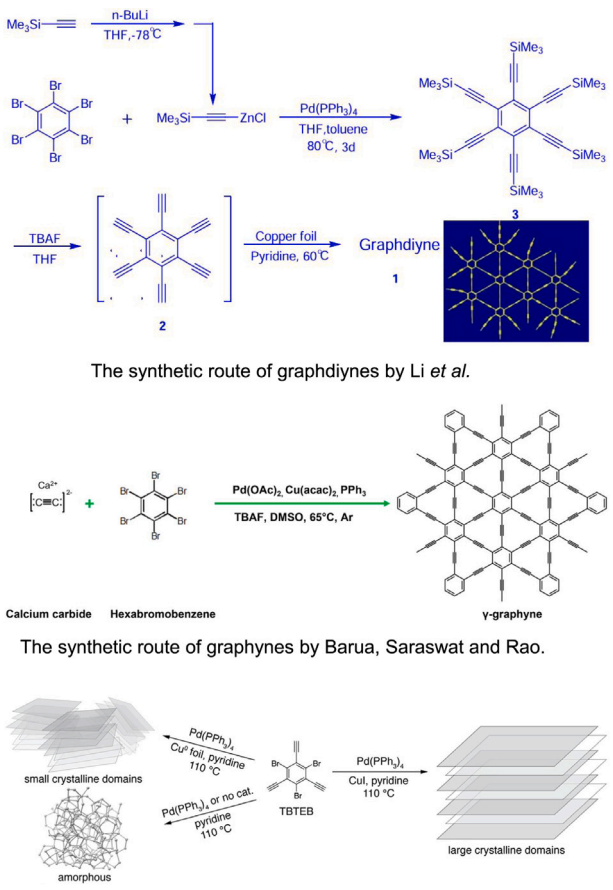

Fig. 7. Schemes of the main synthetic routes to produce γ-GY and -GDY. *Source:* The scheme on top is reproduced from Ref. [126] with permission from the Royal Society of Chemistry. Scheme in the middle is reprinted with permission from Ref. [140], Copyright 2022, Elsevier. Figure at the bottom is reproduced with permission from Ref. [141], Copyright 2022, American Chemical Society.

GYs are scarce, a comparative analysis between predicted and measured properties of the GY structures can be made.

The band gap of γ-GY (γ-GDY) has been theoretically predicted to range from 0.454 to 2.23 eV [78,133] (from 0.44 to 1.47 eV [133]). Experimentally, the three most significant works reporting the synthesis of γ-GY measured band-gap values of 2.23 eV [140], 0.48 eV [141], and 0.62 eV [143]. For γ-GDY, experimental band-gap values of 1.47 eV [134] and 1.48 eV [132] have been reported.

The only mechanical property of γ-GDY that has been measured experimentally is the elastic modulus of thin γ-GDY films, as reported by Xiao et al. [148]. Using atomic force microscopy, a mean Young's modulus of 218.5 GPa was determined for γ-GDY films with thicknesses ranging from 10 to 30 nm. In contrast, classical MD simulations predict substantially higher elastic moduli for graphyne-based systems. Cranford and Buehler [80] and Zhang, Pei, and Wang [81] reported values between 500 and 700 GPa for different graphyne lattices, while Kanegae and Fonseca [88] obtained a Young's modulus of 341.2 GPa for γ-GDY using a similar classical MD approach.

Thermal properties further illustrate the gap between theory and experiment. Hernandez and Fonseca [93] predicted negative linear thermal expansion coefficients for γ-GY and -GDY, with values of -1.2×10^{-5} K^{-1} and -2.05×10^{-5} K^{-1}, respectively. More recently, Kong et al. [149] experimentally measured the thermal expansion coefficient of γ-GDY, obtaining a value of -0.718×10^{-5} K^{-1}. This experimentally determined value is approximately half the magnitude of classical simulation predictions, underscoring the need for further experimental validation.

In Section 3.1, some predicted applications of GYs and GDYs were cited. Here, we present several examples of experimentally demonstrated applications developed to realize these predictions.

For instance, in 2011 Long et al. [102] predicted the semiconducting properties of GDYs, highlighting their potential for nanotransistor applications. Five years later, Qian et al. [150] developed a synthesis route to produce γ-GDY films on arrays of ZnO nanorods, demonstrating high carrier mobility and the feasibility of fabricating field-effect transistors (FETs). Subsequently, Li et al. [151] refined this approach by producing γ-GDY-based FETs with carrier modulation induced by light and heat. Zhang et al. [152] introduced GDY inks and demonstrated direct printing of GDY-based FETs on flexible substrates. More recently, Liu et al. [153] developed organic FETs in which γ-GDY particles function as nano-floating gates.

The intrinsic porosity of γ-GY and -GDY renders them suitable for applications in gas separation and desalination [103–107]. Zhou et al. [154] were the first to investigate gas permeation through γ-GDY membranes. Liu et al. [155] developed a γ-GDY-based filter capable of completely removing lead ions from contaminated water. A combined theoretical and experimental study by Yuan, Xiong, and Shen [156] demonstrated that γ-GDY shows strong potential for selective separation of actinides and lanthanides in the nuclear fuel cycle. Chen et al. [157] succeeded in producing porous submicrometer-thick γ-GDY membranes on porous copper hollow fibers, achieving 99.9% NaCl rejection with ultrahigh water permeability. A recent review by Li, Zhao, and Wang [158] provides further insight into advances in this field.

With respect to the potential of γ-GDY as antibacterial agents [108,109], research in this area remains at an early stage. Two independent studies report contrasting conclusions regarding antibacterial activity. Zhang et al. [159] reported superior antibacterial performance of γ-graphdiyne oxide (γ-GDYO) against *Escherichia coli* and *Staphylococcus aureus*. In contrast, Zhu et al. [160] demonstrated that pristine γ-GDY exhibits higher antibacterial efficiency, suggesting that excessive oxidation may suppress the intrinsic catalytic activity of graphdiyne-based systems. Bi et al. [161] further showed that boron-doped GDY (B-γ-GDY) is effective against both Gram-positive and Gram-negative bacteria, an effect attributed to enhanced catalytic activity induced by boron incorporation [162]. Wang et al. [163] demonstrated the efficacy of γ-GDY-TiO_2 composites in preventing orthopedic implant-associated infections.

Regarding anticancer applications, one of the earliest studies involved the synthesis of bovine serum albumin (BSA)-modified γ-GDY nanoparticles [164]. These nanoparticles were shown to eliminate free radicals, reduce radiation-induced DNA damage, and prolong cell survival under ionizing radiation. Subsequent studies have explored γ-GDY-based systems for therapies targeting glioblastoma [165] and prostate cancer [166]. Despite the early stage of this research area, it is regarded as promising due to the optical properties of γ-GDY that enable photothermal degradation of cancer cells [167]. Comprehensive discussions can be found in recent reviews by Huang et al. [168], Yu et al. [169], and Wu et al. [170].

Energy-related applications represent one of the most actively investigated directions for γ-GDY. Their potential as advanced anode materials has attracted considerable attention [110,111]. γ-GDY have also been explored for hydrogen storage [112] and as supercapacitor electrodes [113,114]. Shen et al. [171] demonstrated that nitrogen-doped γ-GDY-based lithium-ion and sodium-ion capacitors exhibit energy densities exceeding those of pristine γ-GDY and many other carbon materials. Wang et al. [172] investigated aminated γ-GDY for methanol fuel cell applications. Liu, Wang, and Jin [173] synthesized γ-GDY nanolamella electrodes for supercapacitors, which retained their capacitance after more than 11,000 charge–discharge cycles. A recent review

by Xie, Jia, and Huang [174] summarizes advances in GDY-based energy conversion and storage technologies.

Despite these advances, the scalable growth of crystalline GY-based materials remains a central challenge. While γ-GDY films with centimeter-scale lateral dimensions and gram-scale yields have been reported [126,135], the controlled synthesis of large-area, single-layer γ-GY and -GDY with long-range order is still limited by slow coupling kinetics, precursor diffusion constraints, and substrate effects. Recent strategies based on interfacial synthesis, on-surface polymerization on Cu or Ag substrates, and irradiation-assisted routes have shown promise in improving lateral uniformity and throughput, pointing toward feasible pathways for wafer-scale fabrication [139,141,143,147].

Comprehensive overviews of the potential and experimentally realized applications of γ-GDY can also be found in recent reviews [147,175,176].

In relation to the thermal metastability of γ-GY [99], a recent study has demonstrated that stacks of γ-phase undergo an irreversible transformation into planar, nongraphitic, pure sp^2 carbon crystals [177]. The transformation occurs exothermically at ambient pressure over the temperature range 160 °C to 310 °C. This finding suggests a novel approach for synthesizing new 2D carbon phases.

4. Biphenylene based monolayers

The molecule known as biphenylene consists of two hexagonal carbon rings connected by two covalent bonds that form a 4-membered ring. Due to its single and double bonds configuration, it combines aromatic and anti-aromatic properties [178,179], being at the same time chemically stable [180] and presenting interesting physicochemical properties, which several authors explored in the last decades [181–185].

BPN exhibit an intrinsic metallic character together with predicted Young's modulus values in the range of 0.61–0.72 TPa [35]. These values are comparable to those reported for graphynes and only slightly lower than those of graphene, reflecting a balance between mechanical rigidity and structural flexibility arising from the mixed 4–6–8 ring topology. Moreover, the metallic density of states and optical absorption coefficients on the order of 2.5×10^4 cm^{-1} [186] underscore the potential of BPN for applications such as transparent electrodes, nanoelectronic interconnects, and gas sensors, where the simultaneous presence of electrical conductivity and mechanical robustness is a key requirement.

This, along with the rise of interest in 2D materials, motivated several groups, both theoretical and experimental, to investigate the possibility of obtaining technologically promising materials based on periodically arranged 2D structures formed using biphenylene as the repeating unit. It is worth noting that, in 1968 and 1989, Balaban and collaborators proposed several carbon-based structures that were later "reinvented" with different names in more recent studies. Among the various theoretically predicted configurations, two will be discussed in this section, BPN [187,188] and GP [189,190] shown in Figs. 8(a) and 8(b) respectively, as described in detail in the next section.

4.1. Theoretically predicted properties

Different 2D lattices can be constructed by periodically connecting biphenylene units, leading to distinct biphenylene-based carbon networks. Two experimentally realized configurations are exemplified in Fig. 8. In Fig. 8(a), the BPN forms an extended lattice composed of alternating four-, six-, and eight-membered rings, resulting in a metallic and topologically nontrivial framework. In contrast, Fig. 8(b) shows GP, in which biphenylene motifs are arranged into a porous lattice dominated by six- and twelve-membered rings, yielding a semiconducting structure with regularly spaced pores.

The material known as BPN is shown in Fig. 8(a), forming a rectangular lattice in which the repeating unit is a biphenylene molecule. The lattice constants are 3.75 Å and 4.52 Å in the horizontal and vertical directions in Fig. 8(a), respectively. The lattice is found to be relatively stable, with cohesive energy $E_{coh} = -7.55$ eV/atom, although being less stable than graphene, and its work function is estimated as $\Phi = 4.30$ eV [186]. BPN is predicted to be a better fit for lithium-ion batteries than most 2D carbon materials, since the adsorption of that metal would be more energetically favored than in graphene or graphyne, for instance [191].

The unique combination of 4-, 6-, and 8-membered rings in BPN introduces pronounced topological and electronic anisotropy that is absent in conventional hexagonal carbon allotropes [192]. This diversity of polygonal motifs modulates the π-conjugation and generates distinct electron delocalization pathways along the armchair and zigzag directions [193]. As a result, BPN exhibits anisotropic charge transport and direction-dependent current–voltage characteristics. Quantum-transport calculations predict a monotonic increase of current along the zigzag direction and the emergence of negative differential resistance along the armchair direction, arising from variations in band dispersion and effective mass associated with different ring domains [193]. Substitutional doping with boron or nitrogen has been shown to further tune the electronic structure, enabling a transition from metallic to semiconducting behavior and broadening the range of potential device applications [194,195]. Although the atomic structure of BPN has been experimentally realized [196], most insights into its electronic anisotropy and transport properties remain theoretical and await direct experimental validation.

As an experimentally synthesized material, the interest in BPN-like structures has increased. In the last few years, several studies have been reported on experimental methods for their synthesis and possible technological applications [192,196–199].

It is interesting to note that these materials behave like a metal when presented as a sheet or a nanotube. In contrast, they become semiconductors when functionalized or cut as nanoribbons [200,201]. This tunability of physical properties makes them versatile candidates for various applications, including gas storage, gas separation, and optical sensors [202], as well as nanoelectronic devices and nanosensors of different types.

On the theoretical side, studies regarding BPN have shown that armchair and zigzag nanoribbons [203] have distinctive electronic and optical properties compared to other carbon allotropes. Armchair nanoribbons can present conducting or semiconducting character, with high mobility (~ 57.174 $cm^2V^{-1}s^{-1}$) depending on the number of unit cells [204]. GW and Bethe–Salpeter-based calculations suggest that, for BPN nanoribbons, absorption peaks due to excitons are located in the visible range. Additionally, the more relevant bound excitons are found to present a strong electron–hole interaction, which can be relevant for photovoltaic applications [203,205].

Other works suggest their electronic properties can be engineered, achieving a strain-induced metal–insulator transition at relatively high strain values, opening a Γ-X indirect electronic band gap [206]. Furthermore, BPN networks demonstrate high mechanical stability and flexibility [207,208]. Additionally, the high anisotropy of its thermoelectric properties has been highlighted [206], reinforcing its potential for electronic applications.

Another relevant 2D lattice created using biphenylenes and already experimentally realized is shown in Fig. 8(b), known as GP. This material features a unique geometrical structure composed of four-, six-, and twelve-membered rings. Its unit cell belongs to the P6/mmm space group with one irreducible atom. The central nanopore, formed by a dodecagon ring, has a diameter of 5.47 Å [209]. Its cohesive energy (−9.7 eV) is close to values found for graphene (−10.4 eV), suggesting slightly lower stability [210].

The GP structure reveals seven high-symmetry points, including hollow adsorption sites within the rings and edges between rings.

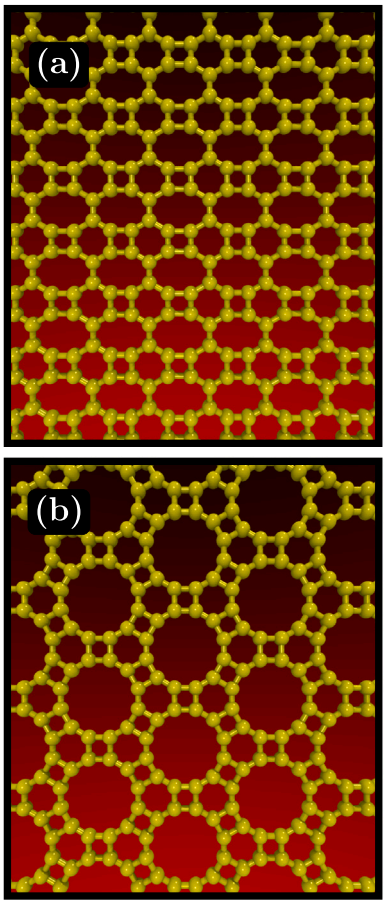

Fig. 8. Two experimentally obtained biphenylene-based 2D materials. (a) Biphenylene Network, where it is possible to identify the four-, six-, and eight-membered rings. (b) Graphenylene lattice, composed of four-, six-, and twelve-membered rings.

These sites are critical for applications such as gas separation and sensing, as they influence the diffusion barriers that ions, atoms, or molecules encounter as they pass through pores. The interaction of chemical species with these sites can also influence the adsorption energies of small molecules or atoms interacting with the membrane, thereby altering the material's adsorption capacity. Mechanically, GP demonstrates remarkable properties, surpassing some 2D materials due to its symmetry-driven elastic constants, which yield a Young's Modulus of 648.8 GPa and a Poisson's ratio of 0.259. Although GP's modulus is lower than that of graphene (1 TPa), its mechanical versatility remains significant [209].

Mechanical stability is a key factor governing the practical use of porous 2D carbon networks in devices such as gas-separation membranes and electrodes for energy storage. MD studies [211,212] indicate that graphenylene exhibits a high in-plane Young's modulus in the range of 0.45–0.65 TPa, while preserving flexibility and elastic recoverability up to approximately 10% strain before structural failure. This combination of stiffness and elastic resilience allows graphenylene membranes to withstand pressures exceeding 10 MPa without pore collapse, supporting their operation under moderate to high pressure conditions relevant to selective gas permeation [212,213]. In electrochemical applications, this mechanical robustness is also advantageous for maintaining structural integrity under repeated charge–discharge cycles.

A clear contrast is observed when comparing BPN with its structural counterpart composed of larger polygonal rings, such as GP. The presence of 12-membered rings, in contrast to the 8-membered rings in BPN, leads to significant differences in C–C bond angles, thereby modifying steric repulsion and aromaticity. These geometric variations are sufficient to induce fundamental changes in the electronic structure, rendering GP semiconducting, in contrast to the metallic character predicted for BPN. In the literature, GP is reported to present a direct electronic bandgap below 1 eV [189,190] at the K point, differing fundamentally from graphene's Dirac cone structure. Its electronic bands, being almost parabolic close to the K point, result in excellent electronic mobility, with effective masses for electrons ($m^*/m_e = 0.26$) and holes ($m^*/m_h = 0.33$), making GP a promising intrinsic semiconductor [189].

This 2D porous material exhibits two important characteristics [189] that should be observed in an ideal carbon-based 2D semiconductor: on one side, an intrinsic electronic bandgap close to that of usual semiconductors; on the other side, GP presents a reasonable electronic dispersion, resulting in electronic delocalization and high charge mobility. Excitonic properties of GP were also investigated, revealing that its optical excitation can lead to bright and dark excitons with binding energies of 530 meV, indicating BP as a candidate for applications in solar energy and quantum information technology [214].

The dodecahedral pore of GP exceeds the kinetic diameter of certain molecules, enabling efficient gas diffusion. Song et al. [215] concluded, via DFT calculations, that H_2 exhibits a low energy barrier (0.20 eV) for diffusion, unlike CO (0.99 eV), CO_2 (1.05 eV), and N_2 (1.01 eV). GP also shows promise in cryogenics, particularly for separating helium isotopes (^{3}He and ^{4}He) owing to its high permeance and quantum-tunneling properties. It was also confirmed that GP outperforms inorganic graphenylene (IGP) [216], with superior separation factors and permeance (10^{-8} mol m^{-2} s^{-1} bar^{-1}) at high temperatures [217]. Moreover, improved separation efficiency under steady-state conditions poses IGP as more effective than GP at elevated temperatures. Strain tuning further enhances GP's performance. Zhu et al. [218] demonstrated a sixfold increase in H_2 permeance (2.6×10^{-2} mol s^{-1} m^{-2} Pa^{-1}) under 3.04% strain, strains of 3.04%–4.20% enable CO_2 separation, while 5.12–10.78% improves methane (CH_4) separation. These findings suggest GP has great potential as a tunable material for technological applications.

Addressing high non-renewable energy consumption and toxic gas removal is critical, and carbon-based catalysts, enhanced by anchored metals, are effective in mitigating atmospheric pollutants.[219,220] Chen et al. [221] demonstrated via first-principles calculations that GP doped with single Ru and Mo atoms, facilitates CO and NO oxidation through the Eley–Rideal (ER) mechanism, which is more efficient than the Langmuir–Hinshelwood (LH) model. Tang et al. [222] showed that Pt and Pd anchored on GP exhibit low energy barriers (< 0.35 eV) for the ER mechanism during CO_2 and N_2 production. Transition metals (Mn, Co, Ni, Cu) also function effectively as single-atom catalysts on GP surfaces [223]. Furthermore, Fe anchored on GP demonstrates strong catalytic performance in CO oxidation and multifunctional gas sensing (CO, NO, NO_2, O_2) due to its magnetic and electronic properties.

The limitations of traditional anode materials, such as graphite, with a specific capacity of 372 mAh g^{-1}, highlight the need for alternatives. Yu [224] demonstrated that graphenylene (GP) offers superior lithium mobility and storage capacities – 1116 mAh g^{-1} (Li_3C_6) and 930 mAh g^{-1} ($Li_{2.5}C_6$) – through DFT studies. However, single-sided Li adsorption reduces capacity to 487 mAh g^{-1}. GP also shows promise for sodium-ion batteries (SIBs), achieving 729.89 mAh g^{-1} (NaC_3),[225] which surpasses graphite (100 mAh g^{-1}) and doped graphene (308 mAh g^{-1}).[226] Additionally, Hussain et al. [227] found that GP doped with alkali metals stabilizes 20 H_2 molecules, enhancing hydrogen storage. In water desalination, fluorinated GP membranes achieve high water permeability (11.032 L m^{-2} h^{-1} bar^{-1}) and 99.4% salt rejection, proving their efficacy for water cleaning applications [228]. Jahangirzadeh et al. [212] showed that GP has an excellent ability to separate salt ions under high pressures, with a permeability of 251.351 L m^{-2} h^{-1} bar^{-1} and salt rejection of 98.8%.

Another realm in which GP can be considered a promising alternative to standard materials is the construction of nanoscale electronic devices. Villegas-Lelovsky and Paupitz [229] demonstrated that doping GP enables electronic transport tuning, forming *pn* junctions suitable for low-dimensional devices such as diodes, with a conducting threshold of $\sim$ 1.5 eV. The possibility of Zener-like configurations was also discussed in that paper. Additionally, *ab initio* calculations highlight GP/MoX_2 van der Waals heterostructures (X = S, Te, Se) for diodes with high rectification factors (10^3-10^4) and optical absorption spectrum in the range of visible light, making them promising for photonics and nanoelectronics [230]. Liu et al. [231] showed GP's functionalization via hydrogenation and halogenation, achieving band gap energy ranges of 0.075–4.98 eV and 0.024–4.87 eV, respectively, posing GP as a versatile material for band gap engineering.

GP and similar materials have also been identified as high-order topological insulators [232]. Due to a zero dipolar moment, their characterization is somewhat more sophisticated than that of regular topological insulators, bringing the necessity of taking into account higher order moments, like quadrupoles and octupoles [232–235]. Furthermore, these materials are promising for the study of higher-order topological superconductors. Such a rich set of topological properties suggests that this class of materials should be considered in future investigations regarding the proposition of nanodevices, especially those designed for the use of topological properties in quantum computing [236,237].

4.2. Synthesis of biphenylene-based networks

A bottom-up synthesis of the BPN was attempted by several groups over several years, yielding several studies reporting interesting but only partial experimental realizations. Despite theoretical proposals for its practical synthesis, such as using uniaxial tension to convert penta-graphene into BPN [208], these approaches have not yet been experimentally demonstrated. Early experimental efforts predominantly yielded linear structures or narrow nanoribbons, which typically exhibit semiconducting behavior, in contrast to the metallic characteristics predicted for an extended two-dimensional BPN lattice [197,201].

A major breakthrough in this field was achieved in 2021, when Fan and co-workers [196] successfully synthesized extended, atomically precise BPN monolayers on a gold surface using an interpolymer dehydrofluorination reaction, commonly referred to as HF-zipping. As illustrated in Fig. 9, this strategy relies on a two-step, surface-confined process. Initially, dihalogenated terphenyl (DHTP) monomers undergo Ullmann coupling on the metal surface, thereby forming aligned polyphenylene chains. Subsequently, an HF-zipping reaction between adjacent chains induces the formation of four-membered carbon rings, giving rise to the characteristic 4–6–8 ring topology of BPN. This approach represented a decisive advance compared to earlier on-surface synthesis attempts, such as those reported by Schlüter et al. [197], which were limited to short BPN segments formed from tribromoterphenyl (TTBP) monomers on Cu(111). Fig. 9 further contrasts the atomic structural model of BPN with the corresponding STM images, highlighting the close agreement between theoretical lattice models and experimentally resolved atomic arrangements.

Beyond the initial realization of monolayer BPN, subsequent studies have explored the response of this non-benzenoid carbon lattice to external stimuli. In particular, pressure-dependent investigations have revealed that BPN undergoes significant structural and electronic modifications under compression [238]. More recently, alternative synthesis routes have been proposed, including polymerization processes triggered at room temperature by applied pressure, which can induce additional structural transformations at elevated pressures around 3 GPa and 14 GPa [198]. These findings underscore the structural flexibility of BPN and suggest that pressure may serve as an effective parameter for tuning its properties and possibly enabling the synthesis of larger-area sheets.

In parallel with the development of BPN, considerable attention has been devoted to the synthesis of GP. The concept of GP was first proposed by Balaban and collaborators in 1968 [239]. Later theoretical analyses by Baughman et al. suggested that its formation from graphyne would be thermodynamically unfavorable [240]. Following the experimental realization of graphene [6], renewed interest in alternative carbon allotropes motivated further theoretical studies of graphenylene and related porous networks [189,190,241].

Experimental progress toward GP-like structures was significantly stimulated by the synthesis of a porous, one-atom-thick polyphenylene network reported by Bieri and co-workers in 2009 [242]. This insulating molecular network was fabricated via surface-assisted aryl-aryl coupling of hexaiodo-substituted cyclohexa-*m*-phenylene (CHP) on an Ag(111) substrate. STM measurements revealed an ordered superlattice with a uniform nanopore spacing of approximately 7 Å and an average pore diameter of 5.8 Å. Subsequent theoretical works proposed that this polyphenylene network could, in principle, transform into a carbon allotrope composed of alternating hexagonal and square rings [189,243].

A decisive experimental realization of this concept was reported in 2017 by Du et al. [244], who synthesized a crystalline two-dimensional carbon material consisting of four- and six-membered rings, which they termed 4–6 carbophene. As summarized in Fig. 10, the synthesis proceeds via dehydration reactions of 1,3,5-trihydroxybenzene and can follow two distinct pathways. In the intramolecular dehydration route (left side, panel (a)), dehydration generates reactive fragments that combine into graphenylene-like building blocks. In the intermolecular dehydration route (left side, panel (b)), dehydration occurs between neighboring molecules, thereby enabling rapid coupling, whereas panel (c) illustrates a representative crystalline structure formed by the bonding of such fragments. The synthesis was carried out under an argon atmosphere at temperatures between 350 and 380 °C in a quartz tube furnace, using γ-Al_2O_3 as a dehydrating agent [245,246].

Fig. 10 compiles the key experimental evidence supporting the formation, transfer, and structural integrity of graphenylene (4–6 carbophene) films. Figs. 10(a) and 10(b) schematically illustrate the two possible polymerization pathways based on intra- and intermolecular dehydration of 1,3,5-trihydroxybenzene mediated by Al_2O_3 at 350 °C, while panel (c) depicts the resulting crystalline 4–6 ring network. Optical photographs in Fig. 10(d) show a clean copper foil and a foil partially covered by the GP film, evidencing successful growth on the metallic substrate, whereas Fig. 10(e) presents a pristine quartz glass sheet alongside a quartz substrate partially covered by the transferred GP film. Scanning electron microscopy images in Figs. 10(f) and 10(g) further document the morphology and continuity of the detached membranes, including GP films separated from copper and freestanding GP membranes after transfer from quartz substrates. Finally, panels (h) and (i) of Fig. 10 show macroscopic images of the transferred 4–6 carbophene films, confirming their mechanical integrity, continuity, and stability after handling and transfer.

Together, these experimental advances establish biphenylene-based networks as a rapidly evolving family of non-benzenoid two-dimensional carbon allotropes. While the controlled synthesis of large-area, defect-free sheets remains a central challenge, the demonstrated feasibility of BPN and graphenylene highlights the expanding structural landscape accessible through on-surface chemistry and solid-state polymerization strategies.

5. Fullerene based 2D networks

2D Fullerene networks are formed by joining fullerene molecules into a monolayer of interconnected units. Depending on the intermolecular connection, different phases can be obtained, such as rhombohedral (R), quasi-hexagonal ($qHPC_{60}$), tetragonal (T), or quasi-tetragonal

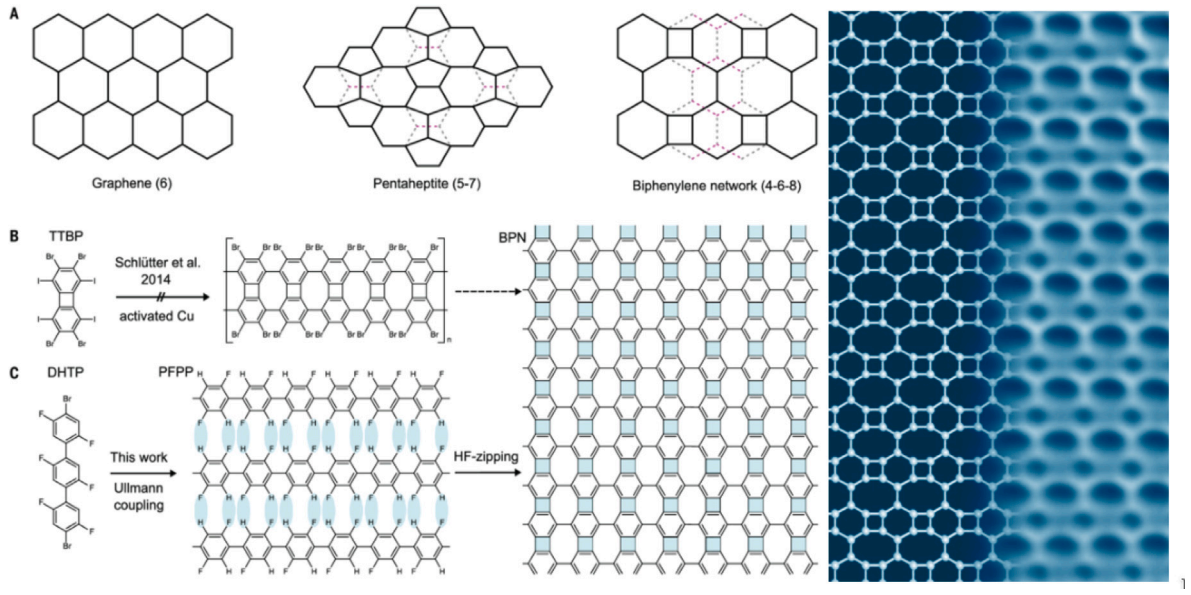

Fig. 9. Representative synthesis routes and structural relationships involved in the formation of biphenylene-based two-dimensional networks.
Source: Reproduced with permission from Ref. [196] and adapted from Ref. [46].

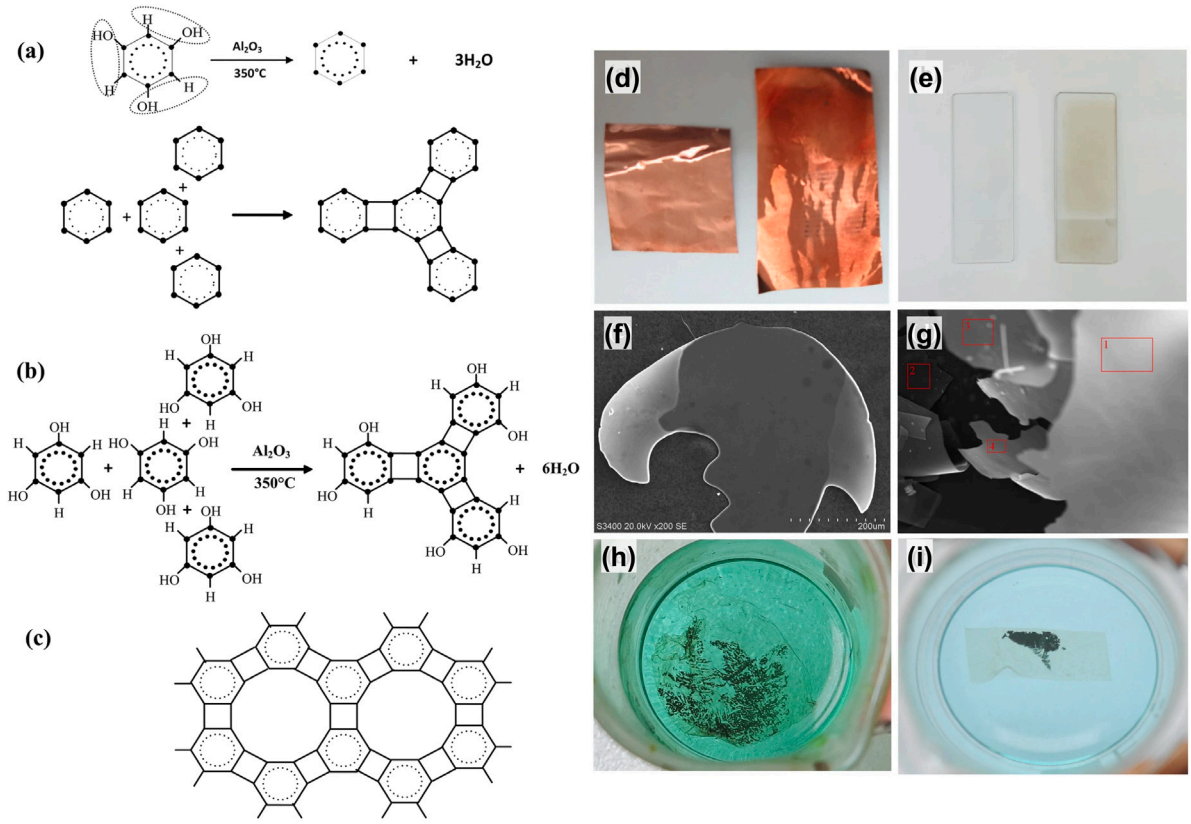

Fig. 10. Synthesis and characterization of GP (4–6 carbophene), including schematic dehydration pathways and representative photographs/SEM images of film growth and transfer.
Source: Reproduced with permission from Ref. [244], under the Creative Commons CC BY license.

($qTPC_{60}$) ones [247–250]. There are different methods to induce the polymerization of adjacent C_{60} units to create a network [251], using, for example, photons [252,253], electron-beam [254], plasma [255, 256], pressure, and pressure–temperature [257–259]. Fig. 11 displays the structure of two experimentally obtained 2D fullerene networks, which are discussed in the present work.

Fig. 11 provides a top view of the atomic structures of the two experimentally realized monolayer fullerene networks. Panels (a) and (b) correspond to the qH and qT phases, respectively. The $qTPC_{60}$ phase is characterized by [2+2] cycloaddition bonds extending along both in-plane directions, giving rise to a nearly square lattice. In contrast, the qH phase exhibits [2 + 2] cycloaddition bonds along a single direction,

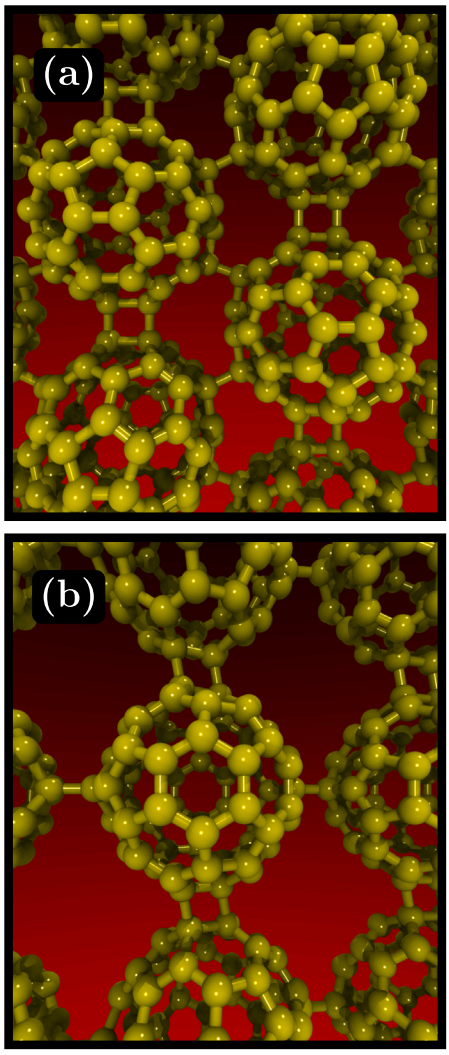

Fig. 11. Top view of the atomic structure of the two experimentally obtained monolayer fullerene networks. (a) and (b) display the qHP and qTP monolayers, respectively.

combined with diagonal σ bonds between carbon atoms, resulting in a hexagonal arrangement [260]. In both phases, the [2+2] cycloaddition bonds connect adjacent C_{60} units through four-membered rings, as highlighted in the figure [249].

5.1. Theoretically predicted properties

From 1993 to 1995, theoretical studies investigated the polymerization of C_{60} molecules, although the formation of dimers, trimers, tetramers, or 3D FCC solids dominated the early research [261–266]. However, the experimental synthesis of a structure composed of stacked planes of polymerized fullerene molecules (similar to graphite) [257,267], stimulated theoretical investigation on a 2D rhombohedral phase of interconnected fullerenes [247]. Using a carbon tight-binding potential, the authors predicted a semiconductor behavior for the lowest energy configuration of this phase. The structure had energy 2.71 eV/molecule higher than pristine C_{60} and an equilibrium distance of 9.17 Å, in close agreement with the experimental value of 9.22 Å [257]. Subsequently, theoretical predictions on the energetic stability and the electronic structure of R and *T* phases of C_{60} polymers were conducted by Okada and Saito [268], using DFT calculations. According to their results, networks in both phases are semiconductors with small indirect gaps. In addition, due to the small interlayer distance, both networks feature a 3D electronic structure, in agreement with the results of Davydov and colleagues [269].

More recently, after the successful synthesis of $qHPC_{60}$, several theoretical studies considered various properties and applications of this material. For example, using DFT, Tromer et al. [270,271] investigated the mechanical and optoelectronic properties of the $qHPC_{60}$ monolayer. Their calculations revealed that this fullerene network exhibits an anisotropic elastic modulus and predicted that it could be utilized as a UV collector for photon energies up to 5.5 eV. In the same year, Yu et al. [272] also investigated this same structure. Their DFT simulations predicted a direct electronic band gap of 1.55 eV, which is consistent with the experimental results. They also observed that the optical, thermoelectric, and mechanical properties of $qHPC_{60}$ are anisotropic. In addition, they identified that this anisotropy was due to asymmetry in the bridging of C_{60} units.

Posterior theoretical calculations suggested the use of monolayer qTP- and $qHPC_{60}$ as photocatalysts for water splitting [273]. Using semilocal DFT and hybrid functional simulations, this work found that the monolayer could act as either an electronic donor (qHP) or a receptor (qTP) in photocatalysis. Both materials exhibited excellent exciton binding energies, and it was verified that the overall water splitting could occur spontaneously in $qTPC_{60}$ upon photon excitation at room temperature and acidic conditions. Furthermore, Y. Tong et al. [274] examined the suitability of the tetragonal phase fullerene monolayer for hydrogen separation. The authors found that it exhibited the best pore size match and entropic selectivity, suggesting promise for this material in applications such as H_2 purification and water splitting.

Recently, using first-principles calculations, Peng and Pizzochero [260] tested and confirmed the outstanding, and highly tunable, properties of experimentally observed fullerene structures. In that study, the authors investigated the structural stability of monolayer phases, thermal expansion behavior, and several mechanical properties. Furthermore, that study investigates the photocatalytic properties of such systems, which are supported by experimental evidence.

The effect of external electric field modulation on the photoelectric properties of the qTP- and $qHPC_{60}$ monolayers was also investigated [275]. The authors observed the sensitivity of the optoelectronic properties of the monolayers to an applied voltage, finding a transition from a semiconducting to a conducting state for voltages of 25.5 V (qHP) and 30 V (qTP). Their results showed that the visible light absorption peak in a qT phase was first redshifted and then blueshifted as the electric field intensity increased. Meanwhile, for the qH phase, the UV peak was blueshifted. Their results show that both materials could potentially be employed in optoelectronic devices, as external electric fields modulate their photoelectric properties.

Later theoretical works also confirmed the superior mechanical [276,277] and thermoelectric properties [248] of monolayer fullerene networks. Furthermore, recent studies have significantly advanced the understanding of the properties and possible applications of monolayer C_{60} phases [278–286].

In the theoretical field, machine learning techniques are becoming essential tools for predicting the structural, thermal, mechanical, electronic, and optical properties of 2D fullerene networks [277,286–289]. Mortazavi et al. employed a combined framework based on DFT, classical MD, and MLIP to investigate the thermal and mechanical responses of a large set of 2D fullerene networks, selected from thousands of candidates according to their energetic stability [277]. Their results revealed lattice thermal conductivities on the order of 10 $W\,m^{-1}\,K^{-1}$ across several low-energy structures, highlighting the suitability of these networks for thermal-management and thermoelectric applications.

More recently, Alekseev et al. [286] employed MD simulations with machine learning–based interatomic potentials, specifically the Gaussian approximation potential GAP-20, to investigate the thermal stability and fracture behavior of qTP and qHP monolayers. In contrast

to earlier theoretical expectations, the qT phase was found to be slightly more thermally stable than qHP. Both phases were reported to decompose into individual C_{60} cages at temperatures on the order of 1200 K, with decomposition temperatures of approximately 1050 K for qHP and 1100 K for qTP.

Machine learning approaches have also been used to explore fullerene formation mechanisms. Han et al. [289] investigated the formation and interconversion of fullerenes under different growth environments, including carbon vapor and iron–carbon systems. Their results showed that fullerene formation is favored in low-density carbon vapor environments, whereas higher carbon densities promote the formation of amorphous carbon particles, providing valuable insight into the growth pathways of fullerene-based nanostructures.

Beyond structural and thermal considerations, the qHP and qT phases of 2D fullerene networks exhibit distinct electronic and optical characteristics. The qH phase is generally predicted to display a smaller band gap and a higher elastic modulus than qTP, and most studies indicate that qHP remains stable up to higher temperatures, with only isolated exceptions reported in the literature [286]. From an optical perspective, theoretical calculations predict weak anisotropy in the absorbance of qHP, in contrast to the pronounced anisotropy expected for qTP. In addition, optical absorption is typically suppressed below approximately 1.5 eV for qHP and 2.0 eV for qTP, reflecting differences in their electronic structures and suggesting distinct optoelectronic response regimes for the two phases [273].

5.2. Synthesized fullerene networks

The first report on polymerized fullerene networks dates back to 1993, when Rao et al. reported the creation of a covalently bonded FCC structure from C_{60} molecules through photopolymerization induced by visible or UV light [252]. In the following year, Iwasa et al. [257] achieved the synthesis of 3D fullerene networks through a high-pressure, high-temperature (HPHT) route. Using a cubic-anvil apparatus, pristine C_{60} was subjected to pressures of 5 GPa and temperatures ranging from 300 to 800 °C, leading to the formation of two distinct metastable polymerized phases. A face-centered cubic phase (FCC-pC_{60}) was obtained between 300–400 °C, with a lattice parameter a = 13.6 Å, while a rhombohedral phase (rh-pC_{60}) formed between 500–800 °C, characterized by lattice parameters a = 9.22 Å and c = 24.6 Å. In both cases, the intermolecular distances were sufficiently reduced to promote covalent bonding between adjacent C_{60} cages, resulting in partially cross-linked fullerene frameworks. Spectroscopic analyses using infrared, Raman, and ^{13}C nuclear magnetic resonance techniques confirmed a pronounced reduction in the original icosahedral symmetry of the C_{60} molecules, together with the emergence of new vibrational features consistent with polymerization. These HPHT-derived networks exhibit enhanced structural rigidity and reduced solubility, are metastable, and revert to pristine C_{60} upon annealing above 300 °C, representing a key milestone toward the realization of 3D covalently bonded fullerene architectures.

In 1995, Nuñez et al. [267] were one of the first to report the synthesis of 2D fullerene phases. They obtained three new C_{60} phases, which included an orthorhombic (O) 1D chain (spacegroup *Immm*). The other phases were 2D: one rhombohedral (*Immm*) and one tetragonal ($R\bar{3}m$). Synthesis was achieved through a 2 + 2 cycloaddition reaction of double bonds, utilizing moderately high pressures and temperatures. This resulted in a product with a mixture of phases, which was resolved by electron diffraction patterns and X-ray techniques.

In 1998, the tetragonal phase was investigated by Davydov et al. [290,291]. Until then, the *T* phase was obtained only in mixtures containing O and R phases and was considered metastable. By using different temperature and pressure paths, targeted at 873 K and 2.2 GPa, the authors successfully synthesized a 3D solid composed almost entirely of T-phase layers [291]. In the following years, Chen et al. performed the first single-crystal X-ray refinement on the structure of both T [292] and R [293] phases. For the *T* phase, their X-ray structural analysis revealed that the polymer actually crystallized in the orthorhombic space group (*Immm*). For the R phase, they found that C_{60} polymerization occurred two-dimensionally along the (111)-plane of the FCC lattice, suggesting that this process should proceed rapidly once it starts at high pressure and temperature.

In 2003, Narymbetov et al. [259] obtained single crystals of the 2D polymerized C_{60} T phase without oriented domains under high temperature and pressure. They obtained interlayer distances between *T* films contrary to previous theoretical predictions [247,294,295], due to partial disorder in the structure, which consisted of 84% $P4_2/mmc$ and 16% *Immm* layers. In 2009, Kazachenko and Ryazanov [296] investigated fullerene thin films obtained via the electron-beam dispersion (EBD) method, which combined an electron-induced sublimation of the C_{60} solid (fullerite) with an electron-assisted polymerization. They obtained thin films with varying proportions of polymerized and nearly pristine C_{60}s.

By 2010, structures composed of polymerized fullerenes were well-established. However, a number of those were not pure C_{60} polymers, having other species (as alkali metals) or polymers inducing the connection between C_{60} units [250,254,293,297,298]. Furthermore, an all-carbon network had not been isolated as a 2D material or produced in significant quantities [249,293].

It was only in 2022 that the synthesis of a pure carbon 2D fullerene network was successful when Hou et al. obtained large single-crystals of monolayer quasi-hexagonal-phase fullerene (qHPC_{60}). In the same article, they also reported the synthesis of a few-layer quasi-tetragonal phase fullerene (qTPC_{60}) [249]. This study proposed an organic cation slicing procedure to exfoliate the 2D layers from the bulk material, as it cannot be mechanically exfoliated nor cleaved in polar solvents due to the strong Mg-C interaction. Note that the Mg ions were introduced during the synthesis of the bulk crystal, thereby linking adjacent layers, but were removed during exfoliation.

The key experimental routes leading to the realization of covalently bonded fullerene networks are summarized in Fig. 12. Panel (a) illustrates the organic cation slicing strategy introduced by Hou et al. [249], in which a layered bulk precursor of polymerized C_{60} is exfoliated into monolayer sheets through electrostatic stabilization by tetrabutylammonium (TBA^+) cations. In this approach, magnesium ions are incorporated during bulk crystal growth, promoting interlayer coupling, and are subsequently removed during exfoliation, yielding negatively charged polymeric C_{60}^{n-} nanosheets arranged in qHP and qTP lattices. This method enabled, for the first time, the isolation of large-area monolayer fullerene networks composed exclusively of carbon.

Fig. 12(b) presents a complementary synthesis route based on chemical vapor transport (CVT), reported by Roy et al. [299]. In this process, reactions between C_{60} powder and magnesium vapor at temperatures between 500 and 600 °C lead to the crystallization of layered Mg_xC_{60} graphullerene structures. Atomic-resolution inverse fast Fourier transform (iFFT) images and atomic force microscopy (AFM) topography confirm the layered morphology, while temperature-dependent electrical conductivity measurements reveal thermally activated transport with an activation energy of approximately 121 meV, consistent with semiconducting behavior in covalently bonded fullerene networks. Together, these approaches demonstrate how molecular fullerenes can be transformed into extended 2D and 3D carbon frameworks through controlled covalent polymerization.

In 2023, evidence for the excellent performance of few-layer fullerene networks as catalysts for water splitting into H_2 was reported by Wang and colleagues [300]. In their work, they synthesized the 2D qHPC_{60} network following the method by Hou et al. and then conducted photocatalytic experiments in pure water. They confirmed that qHPC_{60} nanosheets display great activity, unlike both pristine C_{60} and bulk Mg_4-C_{60}. Their results confirmed the theoretical predictions of Peng [273] and Tong [274]. In the same year, another breakthrough

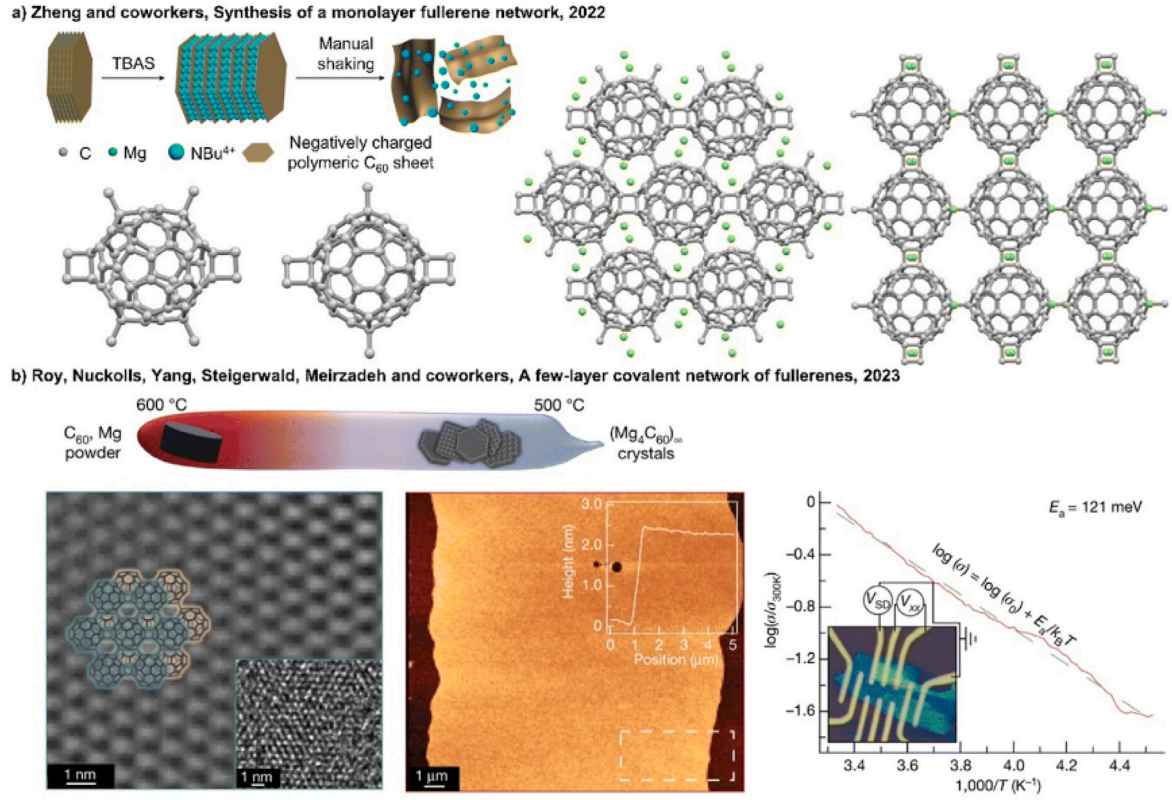

Fig. 12. Representative synthesis routes and structural characterization of covalently bonded fullerene networks. (a) Organic cation slicing approach for monolayer C_{60} networks. (b) Chemical vapor transport growth of layered Mg_xC_{60} graphullerene structures.
Source: Reproduced with permission from Ref. [299], under the Creative Commons CC BY license.

was reported by Meirzadeh and colleagues [301]. They developed a chemical strategy to grow macroscopic thin flakes of the qH phase that could be mechanically exfoliated. They called these monolayers, which have crystal sizes in the order of hundreds of micrometers, graphullerene.

Another exciting discovery occurred in 2024 when X. Chen et al. [302] reported the experimental synthesis of a porous fullerene membrane. This was achieved by modifying a qHP sheet, using 600 °C heating to promote depolymerization of Mg-intercalated $qHPC_{60}$. Their process introduced nanopores with diameters ranging from 1.2 to 5.3 nm, enabling ultrafast permeation of organic solvents. A similar process was also reported by Pan et al. [303]. He and collaborators [304] reported further advancements in the synthesis of nanoporous fullerene networks, where a centimeter-sized nanoporous 2D carbon monolayer was obtained by rapid pyrolysis of a fullerene monolayer.

Most recently, in 2025, Zhang et al. [305] reported a facile electrochemical process for the gram-scale synthesis of C_{60} monolayers. The process was similar to that employed by Hou et al. [249], with the addition of a hydrogen-assisted electrochemical exfoliation strategy. The authors reported high-quality, high-yield production of $qHPC_{60}$. Their scalable process achieved production rates of up to 5 g/day, enabling large-scale exploration of C_{60} polymeric monolayers. Advances in synthesis methods, coupled with declining C_{60} prices (20 USD/gram in 2024 [299]), are driving research on 2D fullerene networks.

These systems exhibit excellent optoelectronic properties [270,272], in addition to remarkable structural and thermal stability [248,271,276,277]. As a result, they have been proposed for use in optical devices such as UV collectors, photocatalysts for water splitting, and solar cells, as well as in thermoelectric devices and membranes for hydrogen separation [270,273,274]. Furthermore, owing to their tunable electronic band gaps and relatively high carrier mobility, monolayer fullerene networks are also promising candidates for semiconducting and optoelectronic device applications [260,275].

6. Conclusions

The field of 2D carbon allotropes has evolved significantly beyond graphene, encompassing a growing family of experimentally realized networks with diverse structural and electronic characteristics. In this review, we have discussed the experimentally realized 2D carbon materials, including MAC, γ-GY and -GDY, BPN and GP, and $qTPC_{60}$ and $qHPC_{60}$. Each of these materials exhibits unique topological motifs, synthesis routes, and physical properties, thereby expanding the design space for carbon-based nanotechnologies.

To provide a concise comparative overview of the discussed two-dimensional materials, Table 1 summarizes representative structural, mechanical, electronic, and optical properties reported for the monolayers. The listed parameters include lattice symmetry, Young's modulus, electronic band gap, optical absorption range, carrier mobility, and effective mass values, which were compiled from experimental and theoretical studies. Whenever applicable, intrinsic monolayer values at zero strain and room temperature are reported, with ranges indicating variability across different methods or measurements. This comparison highlights the diversity of mechanical, electronic, and optical responses among emerging 2D carbon allotropes and related materials.

The diverse structural motifs and bonding configurations of recently synthesized 2D carbon allotropes lead to distinct technological prospects. MAC combines metallic character, isotropic flexibility, and optical transparency, making it particularly promising for flexible electronics, transparent conductive films, and wearable devices, where mechanical resilience and electrical conductivity must coexist [44,326,327]. In contrast, γ-GY exhibits direction-dependent charge transport and a moderate, tunable band gap [87], supporting applications in high-speed field-effect transistors [328], chemical sensors [329], and energy storage devices [79,330]. BPN network display intrinsic metallic conductivity together with exceptional mechanical stiffness, offering immediate potential for transparent electrodes [322],

Table 1
Representative structural, mechanical, electronic, and optical properties of the 2D carbon allotropes discussed in this work. The table compiles reported values for monolayers at room temperature, including lattice symmetry, Young's modulus, band gap, optical absorption range, carrier mobility, and effective masses, with ranges reflecting variations across experimental and theoretical studies. Representative literature sources are cited for each entry.

Material	Symmetry	Y (TPa)	Band gap (eV)	Absorption (10^4 cm^{-1})	μ (cm^2 V^{-1} s^{-1})	m_{eff} ($\times m_0$)
Graphene	Hexagonal (D_{6h}, P6/mmm) [306]	$\simeq$ 1 [307]	Gapless [6]	$\sim$ 3.9 UV region [308]	2×10^3–3.5×10^5 [10,240,309]	Massless [310] (0.01–0.04) [311]
MAC	–	$\sim$ 0.3 [53]	Metallic [52]	1.6–1.8 Visible [52]	–	–
γ-GY	Hexagonal (P6m) [312]	$\sim$ 0.3–0.7 [93,313,314]	$\sim$ 0.4–1.2 [141,315]	$\sim$ 0.1–0.36 Near-IR [316]	~ 0.2–5.4×10^5 [78,79]	$m_e \sim$ 0.07–0.41 $m_h \sim$ 0.1–1.24 [317]
γ-GDY	Hexagonal (P6m) [318]	$\sim$ 0.3–0.45 [88,93]	$\sim$ 0.47–1.47 [132,134,319]	2.17 Visible and near-UV [320]	2.0×10^4–2.0×10^5 [102]	$m_e \sim$ 0.08–0.17 $m_h \sim$ 0.14–0.24 [102,321]
BPN	Orthorhombic (Pmmm) [322]	$\sim$ 0.61–0.72 [35,237]	Metallic [186]	$\sim$ 2.5 UV [186]	$\sim$ 57.2 [233]	$m_e \sim$ 0.18–0.22 $m_h \sim$ 0.20–7.70 [323]
GP	Hexagonal P6/mmm [209]	$\sim$ 0.65 [209]	0.83–1.05 [209,214]	$\sim$ 1.61 Visible [214]	$\mu_e \sim (0.6-1.4)\times10^5$ $\mu_h \sim (1.0-2.0)\times10^3$ [324]	$m_e \simeq$ 0.26 $m_h \simeq$ 0.33 [189]
qHPC$_{60}$/qTPC$_{60}$	qTPC$_{60}$ (P2/m) qHPC$_{60}$ (Pc) [303]	$\sim$ 0.2–0.4 [298,300]	1.6–1.9 [298,303]	2.6–2.8 Visible and near-UV [303]	7.20 [291]	$m_e \sim$ 1.40–1.64 $m_h \sim -(0.58-0.10)$ [325]

nanoelectronic interconnects [193], supercapacitor electrodes [331], and sensing applications [332,333]. GP, characterized by its regularly spaced pores, has been proposed as a promising material for lithium and sodium storage as well as for water desalination, owing to its high ionic mobility and storage capacity [212,224,228]. In addition, its intrinsic semiconducting nature and optical absorption profile make it attractive for photonic and nanoscale electronic devices [189,190,214,229]. Recent studies have further identified specific BPN-based structures as high-order topological insulators [232], opening additional opportunities in quantum and topological electronics. Finally, qHPC$_{60}$ and qTPC$_{60}$ networks exhibit semiconducting band gaps and strong visible-light absorption, positioning them as suitable candidates for photovoltaic and optoelectronic applications, hydrogen storage, photocatalysis, advanced lithium-sulfur and sodium-sulfur batteries, volatile organic compound sensing, and thermoelectric devices [303,334–337]. Together, these allotropes expand the design space of carbon-based nanomaterials, providing complementary platforms ranging from metallic conductors to semiconductors for next-generation technologies.

Looking ahead, recent experimental advances suggest that several newly discovered 2D carbon allotropes may progress beyond laboratory-scale demonstrations toward practical device applications. As synthesis methodologies mature, including bottom-up coupling, interfacial polymerization, and scalable chemical vapor deposition, the transition from proof-of-concept studies to functional devices is expected to accelerate. Among the allotropes reviewed here, GDY appears particularly promising in the near term due to its tunable electronic gap, rich surface chemistry, and growing number of experimentally demonstrated electronic, sensing, and energy-related applications. BPN networks also stand out for their combination of intrinsic metallic conductivity and mechanical robustness, making them attractive for interconnects and transparent electrodes. Monolayer amorphous carbon, with its metallic transparency and mechanical flexibility, may enable earlier adoption in flexible and transparent electronic platforms. While further advances in large-area synthesis, stability, and integration are still required, the complementary properties of these materials indicate that carbon-based 2D technologies are likely to expand beyond graphene toward more diverse device architectures in the near future.

Taking into account the discussions presented throughout this review, it is clear that the past decade has witnessed remarkable advances in the synthesis and characterization of new 2D carbon allotropes, progressively bridging the gap between theoretical predictions and experimental realizations. Nevertheless, several key challenges must still be addressed before these materials can reach technological maturity.

Across all these material classes, cross-cutting challenges include the incorporation of machine-learning-driven materials design, the implementation of in situ and operando characterization techniques, and the development of scalable fabrication strategies compatible with flexible, hybrid, and large-area devices. Together, these directions outline a realistic roadmap for advancing 2D carbon allotropes from laboratory-scale demonstrations toward functional technologies.

Overall, the growing landscape of 2D carbon allotropes presents a rich platform for fundamental research and emerging technologies, marking a golden new era in carbon-based materials science.

CRediT authorship contribution statement

R. Paupitz: Writing – original draft, Validation, Supervision, Methodology, Investigation, Funding acquisition, Formal analysis. **A.F. Fonseca:** Writing – original draft, Validation, Methodology, Investigation, Funding acquisition, Formal analysis. **M. Bessa:** Writing – original draft, Investigation, Formal analysis. **G.S.L. Fabris:** Writing – original draft, Methodology, Investigation, Formal analysis. **W.F. da Cunha:** Writing – original draft. **L.D. Machado:** Writing – original draft, Validation, Methodology, Investigation, Funding acquisition, Formal analysis. **M.L. Pereira:** Writing – review & editing, Visualization, Project administration, Funding acquisition, Formal analysis. **L.A. Ribeiro:** Writing – original draft, Validation, Investigation, Funding acquisition, Formal analysis. **D.S. Galvão:** Writing – review & editing, Validation, Supervision, Project administration, Funding acquisition, Conceptualization.

Declaration of competing interest

The authors declare the following financial interests/personal relationships which may be considered as potential competing interests:

Ricardo Pauptiz reports financial support was provided by State of Sao Paulo Research Foundation. Alexandre Fontes da Fonseca reports was provided by State of Sao Paulo Research Foundation. Alexandre Fontes da Fonseca reports was provided by National Council for Scientific and Technological Development. Mizraim Bessa reports was provided by National Council for Scientific and Technological Development. Leonardo Dantas Machado reports was provided by National Council for Scientific and Technological Development. Guilherme da Silva Lopes Fabris reports was provided by State of Sao Paulo Research Foundation. Marcelo Lopes Pereira Junior reports was provided by Foundation for Research Support of the Federal District. Marcelo Lopes Pereira Junior reports was provided by National Council for Scientific and Technological Development. Marcelo Lopes Pereira Junior reports was provided by Coordination for the improvement of Higher Education Personnel. Luiz Antonio Ribeiro Junior reports was provided by Foundation for Research Support of the Federal District. Luiz Antonio Ribeiro Junior reports was provided by National Council for Scientific and Technological Development. Luiz Antonio Ribeiro Junior reports was provided by Coordination for the improvement of Higher Education Personnel. Douglas Soares Galvao reports was provided by State of Sao Paulo Research Foundation. If there are other authors, they declare that they have no known competing financial interests or personal relationships that could have appeared to influence the work reported in this paper.

Acknowledgments

This work was partially supported by the Brazilian Coordination for the Improvement of Higher Education Personnel (CAPES), the National Council for Scientific and Technological Development (CNPq), the Research Support Foundation of the Federal District (FAPDF), and the São Paulo Research Foundation (FAPESP). R.P. acknowledges financial support from FAPESP (grant No. 2021/14977-2) and CNPq (grant No. 313592/2023-3). A.F.F. is a fellow of CNPq (grant No. 302009/2025-6) and acknowledges additional support from FAPESP (grant No. 2024/14403-4). M.B. and L.D.M. acknowledge support from CAPES and CNPq (grant No. 313065/2023-3). G.S.L.F. acknowledges a postdoctoral fellowship funded by FAPESP (grant No. 2024/03413-9). M.L.P.J. acknowledges financial support from FAPDF (grant No. 00193-00001807/2023-16), CNPq (grant Nos. 444921/2024-9 and 308222/2025-3), and CAPES (grant No. 88887.005164/2024-00). L.A.R.J. acknowledges financial support from FAPDF (grant Nos. 00193-00001808/2022-71 and 00193-00001857/2023-95), the FAPDF-PRONEM program (grant No. 00193-00001247/2021-20), CNPq (grant Nos. 350176/2022-1, 167745/2023-9, and 444111/2024-7), and the PDPG-FAPDF-CAPES Centro-Oeste program (grant No. 00193-00000867/2024-94). D. S. G. acknowledges support from INEO/CNPq and FAPESP (grant No. 2025/27044-5). The authors also acknowledge the Coaraci Supercomputer Center for computational time, supported by FAPESP (grant No. 2019/17874-0), and the Center for Computing in Engineering and Sciences at Unicamp, supported by FAPESP (grant No. 2013/08293-7).

References

[1] Santosh K. Tiwari, Vijay Kumar, Andrzej Huczko, R. Oraon, A. De Adhikari, G.C. Nayak, Magical allotropes of carbon: prospects and applications, Crit. Rev. Solid State Mater. Sci. 41 (4) (2016) 257–317.

[2] Chandra Shekhar Yadav, Iqbal Azad, Abdul Rahman Khan, Prashant Singh, Carbon allotropes: Past to present aspects, in: Biosensors Based on Graphene, Graphene Oxide and Graphynes for Early Detection of Cancer, CRC Press, 2025, pp. 1–23.

[3] Ali Mostofizadeh, Yanwei Li, Bo Song, Yudong Huang, Synthesis, properties, and applications of low-dimensional carbon-related nanomaterials, J. Nanomater. 2011 (1) (2011) 685081.

[4] Richard E. Smalley, Discovering the fullerenes, Rev. Modern Phys. 69 (3) (1997) 723.

[5] Rizwan Shoukat, Muhammad Imran Khan, Carbon nanotubes: a review on properties, synthesis methods and applications in micro and nanotechnology, Microsyst. Technol. (2021) 1–10.

[6] K.S. Novoselov, A.K. Geim, S.V. Morozov, D. Jiang, Y. Zhang, S.V. Dubonos, I.V. Grigorieva, A.A. Firsov, Electric field effect in atomically thin carbon films, Science 306 (5696) (2004) 666–669, http://dx.doi.org/10.1126/science.1102896.

[7] Ray Baughman, H. Eckhardt, Miklos Kertesz, Structure-property predictions for new planar forms of carbon: Layered phases containing sp2 and sp atoms, J. Chem. Phys. 87 (1987) 6687–6699, http://dx.doi.org/10.1063/1.453405.

[8] John Desmond Bernal, The structure of graphite, Proc. R. Soc. Lond. Ser. A, Contain. Pap. A Math. Phys. Character 106 (740) (1924) 749–773.

[9] William Henry Bragg, William Lawrence Bragg, The structure of the diamond, Proc. R. Soc. Lond. Ser. A, Contain. Pap. A Math. Phys. Character 89 (610) (1913) 277–291.

[10] Akanksha R. Urade, Indranil Lahiri, K.S. Suresh, Graphene properties, synthesis and applications: a review, Jom 75 (3) (2023) 614–630.

[11] Aamir Razaq, Faiza Bibi, Xiaoxiao Zheng, Raffaello Papadakis, Syed Hassan Mujtaba Jafri, Hu Li, Review on graphene-, graphene oxide-, reduced graphene oxide-based flexible composites: From fabrication to applications, Materials 15 (3) (2022) 1012.

[12] Farooq Ahmad, Muhammad Zahid, Huma Jamil, Muhammad Ahmed Khan, Shahid Atiq, Mubashira Bibi, Kanwal Shahbaz, Muhammad Adnan, Muhammad Danish, Fazal Rasheed, et al., Advances in graphene-based electrode materials for high-performance supercapacitors: A review, J. Energy Storage 72 (2023) 108731.

[13] Huicheng Lin, Qifei Jian, Xingying Bai, Deqiang Li, Zhe Huang, Wentao Huang, Shengsen Feng, Zongyi Cheng, Recent advances in thermal conductivity and thermal applications of graphene and its derivatives nanofluids, Appl. Therm. Eng. 218 (2023) 119176.

[14] Seyedeh Nastaran Talebzadeh, Saeed Golmohammadi, Seyyedeh Ladan Talebzadeh, A review for graphene, graphene-based materials, and their applications in photonics and optoelectronic devices, in: 2024 6th Iranian International Conference on Microelectronics, IICM, IEEE, 2024, pp. 1–5.

[15] Jiuhui Han, Isaac Johnson, Mingwei Chen, 3D continuously porous graphene for energy applications, Adv. Mater. 34 (15) (2022) 2108750.

[16] Jiayang Wu, Han Lin, David J Moss, Kian Ping Loh, Baohua Jia, Graphene oxide for photonics, electronics and optoelectronics, Nat. Rev. Chem. 7 (3) (2023) 162–183.

[17] Jinlei Miao, Tingting Fan, Flexible and stretchable transparent conductive graphene-based electrodes for emerging wearable electronics, Carbon 202 (2023) 495–527.

[18] Yifan Yin, Yuchen Zhou, Miriam H Rafailovich, Chang-Yong Nam, Recent advances of two-dimensional material additives in hybrid perovskite solar cells, Nanotechnology 34 (17) (2023) 172001.

[19] Qian Cai, Jiachi Ye, Belal Jahannia, Hao Wang, Chandraman Patil, Rasul Al Foysal Redoy, Abdulrahman Sidam, Sinan Sameer, Sultan Aljohani, Muhammed Umer, et al., Comprehensive study and design of graphene transistor, Micromachines 15 (3) (2024) 406.

[20] Susmita Jana, Arka Bandyopadhyay, Sujoy Datta, Debaprem Bhattacharya, Debnarayan Jana, Emerging properties of carbon based 2D material beyond graphene, J. Phys.: Condens. Matter. 34 (5) (2021) 053001.

[21] Haomin Wang, Hui Shan Wang, Chuanxu Ma, Lingxiu Chen, Chengxin Jiang, Chen Chen, Xiaoming Xie, An-Ping Li, Xinran Wang, Graphene nanoribbons for quantum electronics, Nat. Rev. Phys. 3 (12) (2021) 791–802.

[22] R.S. Koen Houtsma, Joris de la Rie, Meike Stöhr, Atomically precise graphene nanoribbons: interplay of structural and electronic properties, Chem. Soc. Rev. 50 (11) (2021) 6541–6568.

[23] Pulickel M. Ajayan, Otto Z. Zhou, Applications of carbon nanotubes, Carbon Nanotub.: Synth. Struct. Prop. Appl. (2001) 391–425.

[24] Zhenxing Zhu, Chaojie Cui, Yunxiang Bai, Jun Gao, Yaxin Jiang, Bofan Li, Yao Wang, Qiang Zhang, Weizhong Qian, Fei Wei, Advances in precise structure control and assembly toward the carbon nanotube industry, Adv. Funct. Mater. 32 (11) (2022) 2109401.

[25] Md Mohi Uddin, Mohammad Humaun Kabir, Md Ashraf Ali, Md Mukter Hossain, Mayeen Uddin Khandaker, Sumit Mandal, A. Arifutzzaman, Debnarayan Jana, Graphene-like emerging 2D materials: recent progress, challenges and future outlook, RSC Adv. 13 (47) (2023) 33336–33375.

[26] Wentao Li, Promising 2D carbon allotropes with intrinsic bandgaps based on bilayer α-graphyne, Phys. Status Solidi (B) 262 (3) (2025) 2400488.

[27] Elsevier, Scopus: Scientific Abstract and Citation Database, Elsevier, Netherlands, 2025, https://www.scopus.com (Accessed: 29 June 2025).

[28] Zhen Zhen, Hongwei Zhu, Structure and properties of graphene, in: Graphene, Elsevier, 2018, pp. 1–12.

[29] Yisong Zheng, Tsuneya Ando, Hall conductivity of a two-dimensional graphite system, Phys. Rev. B 65 (24) (2002) 245420.

[30] Antonio H Castro Neto, Francisco Guinea, Nuno MR Peres, Kostya S Novoselov, Andre K Geim, The electronic properties of graphene, Rev. Mod. Phys. 81 (1) (2009) 109–162.

[31] Mitsutaka Fujita, Katsunori Wakabayashi, Kyoko Nakada, Koichi Kusakabe, Peculiar localized state at zigzag graphite edge, J. Phys. Soc. Japan 65 (7) (1996) 1920–1923.

[32] Bohayra Mortazavi, Recent advances in machine learning-assisted multiscale design of energy materials, Adv. Energy Mater. 15 (9) (2024) http://dx.doi.org/10.1002/aenm.202403876.

[33] Bohayra Mortazavi, Ali Rajabpour, Xiaoying Zhuang, Timon Rabczuk, Alexander V. Shapeev, Exploring thermal expansion of carbon-based nanosheets by machine-learning interatomic potentials, Carbon 186 (2022) 501–508, http://dx.doi.org/10.1016/j.carbon.2021.10.059.

[34] Bohayra Mortazavi, Timon Rabczuk, Xiaoying Zhuang, Exploring the structural stability, thermal and mechanical properties of nanoporous carbon nitride nanosheets using a transferrable machine learning interatomic potential, Mach. Learn. Comput. Sci. Eng. 1 (1) (2024) http://dx.doi.org/10.1007/s44379-024-00008-6.

[35] Bohayra Mortazavi, Alexander V. Shapeev, Anisotropic mechanical response, high negative thermal expansion, and outstanding dynamical stability of biphenylene monolayer revealed by machine-learning interatomic potentials, FlatChem 32 (2022) 100347, http://dx.doi.org/10.1016/j.flatc.2022.100347.

[36] Zhaolong Li, Kaiming Peng, Nannan Ji, Wenlong Zhang, Wenrou Tian, Zhenfei Gao, Advanced mechanisms and applications of microwave-assisted synthesis of carbon-based materials: a brief review, Nanoscale Adv. 7 (2) (2025) 419–432, http://dx.doi.org/10.1039/d4na00701h.

[37] Yan Fang, Yuxin Liu, Lu Qi, Yurui Xue, Yuliang Li, 2D graphdiyne: an emerging carbon material, Chem. Soc. Rev. 51 (7) (2022) 2681–2709, http://dx.doi.org/10.1039/d1cs00592h.

[38] Xuchen Zheng, Siao Chen, Jinze Li, Han Wu, Chao Zhang, Danyan Zhang, Xi Chen, Yang Gao, Feng He, Lan Hui, Huibiao Liu, Tonggang Jiu, Ning Wang, Guoxing Li, Jialiang Xu, Yurui Xue, Changshui Huang, Chunying Chen, Yanbing Guo, Tong-Bu Lu, Dan Wang, Lanqun Mao, Jin Zhang, Yue Zhang, Lifeng Chi, Wanlin Guo, Xian-He Bu, Hongjie Zhang, Liming Dai, Yuliang Zhao, Yuliang Li, Two-dimensional carbon graphdiyne: Advances in fundamental and application research, ACS Nano 17 (15) (2023) 14309–14346, http://dx.doi.org/10.1021/acsnano.3c03849.

[39] Farooq Ahmad, Asif Mahmood, Tahir Muhmood, Carbon allotropes: Basics, properties and applications, in: Heteroatom-Doped Carbon Allotropes: Progress in Synthesis, Characterization, and Applications, American Chemical Society, 2024, pp. 1–18, http://dx.doi.org/10.1021/bk-2024-1491.ch001.

[40] Susmita Jana, Arka Bandyopadhyay, Sujoy Datta, Debaprem Bhattacharya, Debnarayan Jana, Emerging properties of carbon based 2D material beyond graphene, J. Phys.: Condens. Matter. 34 (5) (2021) 053001, http://dx.doi.org/10.1088/1361-648x/ac3075.

[41] Chandra Shekhar Yadav, Iqbal Azad, Abdul Rahman Khan, Prashant Singh, Carbon allotropes: past to present aspects, in: Biosensors Based on Graphene, Graphene Oxide and Graphynes for Early Detection of Cancer, CRC Press, 2024, pp. 1–23.

[42] Andreas Hirsch, The era of carbon allotropes, Nat. Mater. 9 (11) (2010) 868–871, http://dx.doi.org/10.1038/nmat2885.

[43] Jiang Li, Deqiang Yin, Yi Qin, Carbon materials: structures, properties, synthesis and applications, Manuf. Rev. 10 (2023) 13, http://dx.doi.org/10.1051/mfreview/2023011.

[44] Chee Tat Toh, Hongji Zhang, Junhao Lin, Alexander S. Mayorov, Yun-Peng Wang, Carlo M. Orofeo, Darim Badur Ferry, Henrik Andersen, N. Kakenov, Zenglong Guo, Irfan Haider Abidi, Hunter Sims, Kazu Suenaga, Sokrates T. Pantelides, Barbaros Özyilmaz, Synthesis and properties of free-standing monolayer amorphous carbon, Nature 577 (2020) 199–203.

[45] Coster Kumunda, Abolanle S. Adekunle, Bhekie B. Mamba, Ntuthuko W. Hlongwa, Thabo T.I. Nkambule, Electrochemical detection of environmental pollutants based on graphene derivatives: A review, Front. Mater. 7 (2021) http://dx.doi.org/10.3389/fmats.2020.616787.

[46] Sci News News Staff, Scientists synthesize new allotrope of carbon, 2021, URL https://www.sci.news/othersciences/chemistry/biphenylene-network-09686.html (Accessed 28 Nov 2025).

[47] Hyeongjoon Kim, Kyuyeon Won, Hyeon Suk Shin, Engineering disorder with monolayer amorphous carbon growth, Nature Nanotechnology 20 (10) (2025) 1357–1358, http://dx.doi.org/10.1038/s41565-025-01986-1.

[48] J. Kotakoski, A.V. Krasheninnikov, U. Kaiser, J.C. Meyer, From point defects in graphene to two-dimensional amorphous carbon, Phys. Rev. Lett. 106 (2011) 105505, http://dx.doi.org/10.1103/PhysRevLett.106.105505.

[49] V. Kapko, D.A. Drabold, M.F. Thorpe, Electronic structure of a realistic model of amorphous graphene, Phys. Status Solidi (B) 247 (5) (2010) 1197–1200, http://dx.doi.org/10.1002/pssb.200945581.

[50] Erik Holmström, Jonas Fransson, Olle Eriksson, Raquel Lizárraga, Biplab Sanyal, Sumanta Bhandary, Mikhail I. Katsnelson, Disorder-induced metallicity in amorphous graphene, Phys. Rev. B 84 (2011) 205414, http://dx.doi.org/10.1103/PhysRevB.84.205414.

[51] Jiani Hu, Mouyang Cheng, Erxun Han, Han Li, Lei Liu, Ji Chen, Simulated atomistic growth of amorphous monolayer carbon, J. Phys. Chem. Lett. 16 (2025) 6866–6873.

[52] Emanuel J.A. Dos Santos, Marcelo L. Pereira, Raphael M. Tromer, Douglas S. Galvão, Luiz A. Ribeiro, Exploring the electronic and mechanical properties of the recently synthesized nitrogen-doped amorphous monolayer carbon, Nanoscale 17 (12) (2025) 7253–7263.

[53] Levi C. Felix, Raphael M. Tromer, Pedro A.S. Autreto, Luiz A. Ribeiro Junior, Douglas S. Galvao, On the mechanical properties and thermal stability of a recently synthesized monolayer amorphous carbon, J. Phys. Chem. C 124 (27) (2020) 14855–14860.

[54] Marcelo Lopes Pereira Junior, Wiliam Ferreira da Cunha, Douglas Soares Galvão, Luiz Antonio Ribeiro Junior, A reactive molecular dynamics study on the mechanical properties of a recently synthesized amorphous carbon monolayer converted into a nanotube/nanoscroll, Phys. Chem. Chem. Phys. 23 (15) (2021) 9089–9095.

[55] Raphael M. Tromer, Levi C. Felix, Luiz A. Ribeiro, Douglas S. Galvao, Optoelectronic properties of amorphous carbon-based nanotube and nanoscroll, Phys. E: Low-Dimensional Syst. Nanostructures 130 (2021) 114683.

[56] Raphael M. Tromer, Marcelo L. Pereira Júnior, Luiz A. Ribeiro Júnior, Douglas S. Galvão, Structural and electronic properties of amorphous silicon and germanium monolayers and nanotubes: A DFT investigation, Chem. Phys. Lett. 856 (2024) 141647.

[57] D.A. Drabold, Topics in the theory of amorphous materials, Eur. Phys. J. B 68 (2009) 1–21.

[58] Martin C. Wilding, Mark Wilson, Paul F. McMillan, Structural studies and polymorphism in amorphous solids and liquids at high pressure, Chem. Soc. Rev. 35 (10) (2006) 964–986.

[59] Stanford R. Ovshinsky, David Adler, Progress in the science and application of amorphous materials, J. Non-Cryst. Solids 90 (1–3) (1987) 229–241.

[60] T. Meydan, Application of amorphous materials to sensors, J. Magn. Magn. Mater. 133 (1–3) (1994) 525–532.

[61] Wu-Xing Zhou, Yuan Cheng, Ke-Qiu Chen, Guofeng Xie, Tian Wang, Gang Zhang, Thermal conductivity of amorphous materials, Adv. Funct. Mater. 30 (8) (2020) 1903829.

[62] F.C. Li, T. Liu, J.Y. Zhang, S. Shuang, Q. Wang, A.D. Wang, J.G. Wang, Y. Yang, Amorphous–nanocrystalline alloys: fabrication, properties, and applications, Mater. Today Adv. 4 (2019) 100027.

[63] Yongshuai Wang, Qing Zhang, Lin Li, Fan Wu, Dechao Geng, Wenping Hu, Turning defects into advantages: Structures, synthesis, and applications of 2D amorphous carbon, Adv. Funct. Mater. (2025) e09481.

[64] William Houlder Zachariasen, The atomic arrangement in glass, J. Am. Chem. Soc. 54 (10) (1932) 3841–3851.

[65] Lei Shi, Yafeng Zhang, Biqin Dong, Tianrong Zhan, Xiaohan Liu, Jian Zi, Amorphous photonic crystals with only short-range order, Adv. Mater. 25 (37) (2013) 5314–5320, http://dx.doi.org/10.1002/adma.201301909.

[66] Won-Jae Joo, Jae-Hyun Lee, Yamujin Jang, Seog-Gyun Kang, Young-Nam Kwon, Jaegwan Chung, Sangyeob Lee, Changhyun Kim, Tae-Hoon Kim, Cheol-Woong Yang, et al., Realization of continuous zachariasen carbon monolayer, Sci. Adv. 3 (2) (2017) e1601821.

[67] Steven J. Stuart, Alan B. Tutein, Judith A. Harrison, A reactive potential for hydrocarbons with intermolecular interactions, J. Chem. Phys. 112 (14) (2000) 6472–6486.

[68] Steve Plimpton, Fast parallel algorithms for short-range molecular dynamics, J. Comput. Phys. 117 (1995) 1–19, http://dx.doi.org/10.1006/jcph.1995.1039.

[69] M.L. Pereira, W.F. da Cunha, R.T. de Sousa, G.D. Amvame Nze, D.S. Galvão, L.A. Ribeiro, On the mechanical properties and fracture patterns of the nonbenzenoid carbon allotrope (biphenylene network): a reactive molecular dynamics study, Nanoscale 14 (8) (2022) 3200–3211.

[70] Wenhui Xie, Yujie Wei, Roughening for strengthening and toughening in monolayer carbon based composites, Nano Lett. 21 (11) (2021) 4823–4829.

[71] Wenhui Xie, Xibei Zhang, Yujie Wei, Huajian Gao, Toughening two dimensional materials through lattice disorder, Carbon 213 (2023) 118268.

[72] Georg Kresse, Jürgen Furthmüller, Efficient iterative schemes for ab initio total-energy calculations using a plane-wave basis set, Phys. Rev. B 54 (16) (1996) 11169.

[73] Mads Brandbyge, José-Luis Mozos, Pablo Ordejón, Jeremy Taylor, Kurt Stokbro, Density-functional method for nonequilibrium electron transport, Phys. Rev. B 65 (16) (2002) 165401.

[74] José M Soler, Emilio Artacho, Julian D Gale, Alberto García, Javier Junquera, Pablo Ordejón, Daniel Sánchez-Portal, The SIESTA method for ab initio order-n materials simulation, J. Phys.: Condens. Matter. 14 (11) (2002) 2745.

[75] Yu-Tian Zhang, Yun-Peng Wang, Xianli Zhang, Yu-Yang Zhang, Shixuan Du, Sokrates T. Pantelides, Structure of amorphous two-dimensional materials: Elemental monolayer amorphous carbon versus binary monolayer amorphous boron nitride, Nano Lett. 22 (19) (2022) 8018–8024, http://dx.doi.org/10.1021/acs.nanolett.2c02542, URL http://dx.doi.org/10.1021/acs.nanolett.2c02542.

[76] Longfei Wu, Alessandro Longo, Nelson Y. Dzade, Akhil Sharma, Marco M.R.M. Hendrix, Ageeth A. Bol, Nora H. de Leeuw, Emiel J.M. Hensen, Jan P. Hofmann, The origin of high activity of amorphous MoS2 in the hydrogen evolution reaction, ChemSusChem 12 (19) (2019) 4383–4389, http://dx.doi.org/10.1002/cssc.201901811.

[77] Vestince B. Mbayachi, Euphrem Ndayiragije, Thirasara Sammani, Sunaina Taj, Elice R. Mbuta, Atta ullah khan, Graphene synthesis, characterization and its applications: A review, Results Chem. 3 (2021) 100163, http://dx.doi.org/10.1016/j.rechem.2021.100163.

[78] Jun Kang, Zhongming Wei, Jingbo Li, Graphyne and its family: Recent theoretical advances, ACS Appl. Mater. & Interfaces 11 (3) (2019) 2692–2706, http://dx.doi.org/10.1021/acsami.8b03338, PMID: 29663794.

[79] Jianming Chen, Jinyang Xi, Dong Wang, Zhigang Shuai, Carrier mobility in graphyne should be even larger than that in graphene: A theoretical prediction, J. Phys. Chem. Lett. 4 (9) (2013) 1443–1448, http://dx.doi.org/10.1021/jz4005587, PMID: 26282296.

[80] Steven W. Cranford, Markus J. Buehler, Mechanical properties of graphyne, Carbon 49 (13) (2011) 4111–4121, http://dx.doi.org/10.1016/j.carbon.2011.05.024, URL https://www.sciencedirect.com/science/article/pii/S0008622311003861.

[81] Y.Y. Zhang, Q.X. Pei, C.M. Wang, Mechanical properties of graphynes under tension: A molecular dynamics study, Appl. Phys. Lett. 101 (8) (2012) 081909, http://dx.doi.org/10.1063/1.4747719.

[82] Xiao-Ming Wang, Dong-Chuan Mo, Shu-Shen Lu, On the thermoelectric transport properties of graphyne by the first-principles method, J. Chem. Phys. 138 (20) (2013) 204704, http://dx.doi.org/10.1063/1.4806069, URL https://doi.org/10.1063/1.4806069.

[83] Guilherme B. Kanegae, Alexandre F. Fonseca, Density dependence of elastic properties of graphynes, MRS Adv. 8 (7) (2023) 355–360, http://dx.doi.org/10.1557/s43580-023-00529-x.

[84] N. Narita, S. Nagai, S. Suzuki, K. Nakao, Optimized geometries and electronic structures of graphyne and its family, Phys. Rev. B 58 (16) (1998) 11009–11014, http://dx.doi.org/10.1103/PhysRevB.58.11009.

[85] Daniel Malko, Christian Neiss, Francesc Viñes, Andreas Görling, Competition for graphene: Graphynes with direction-dependent Dirac cones, Phys. Rev. Lett. 108 (2012) 086804, http://dx.doi.org/10.1103/PhysRevLett.108.086804.

[86] Wenzhi Wu, Wanlin Guo, Xiao Cheng Zeng, Intrinsic electronic and transport properties of graphyne sheets and nanoribbons, Nanoscale 5 (2013) 9264–9276, http://dx.doi.org/10.1039/C3NR03167E.

[87] J.E. Padilha, A. Fazzio, Antônio J.R. da Silva, Directional control of the electronic and transport properties of graphynes, J. Phys. Chem. C 118 (32) (2014) 18793–18798, http://dx.doi.org/10.1021/jp5062804.

[88] Guilherme B. Kanegae, Alexandre F. Fonseca, Effective acetylene length dependence of the elastic properties of different kinds of graphynes, Carbon Trends 7 (2022) 100152, http://dx.doi.org/10.1016/j.cartre.2022.100152, URL https://www.sciencedirect.com/science/article/pii/S2667056922000086.

[89] Guilherme B. Kanegae, Alexandre F. Fonseca, Angular dependence of four mechanical properties of graphynes, MRS Adv. 10 (12) (2025) 1487–1492, http://dx.doi.org/10.1557/s43580-025-01124-y.

[90] Michael Schirber, Graphyne may be better than graphene, Physics 5 (2012) 24, URL https://physics.aps.org/articles/v5/24.

[91] Jon Cartwright, Graphyne could be better than graphene, Science (2012) URL https://www.science.org/content/article/graphyne-could-be-better-graphene.

[92] Cheol-Woon Kim, Seoung-Hun Kang, Young-Kyun Kwon, Rigid unit modes in $sp-sp^2$ hybridized carbon systems: Origin of negative thermal expansion, Phys. Rev. B 92 (2015) 245434, http://dx.doi.org/10.1103/PhysRevB.92.245434.

[93] Sergio A. Hernandez, Alexandre F. Fonseca, Anisotropic elastic modulus, high Poisson's ratio and negative thermal expansion of graphynes and graphdiynes, Diam. Relat. Mater. 77 (2017) 57–64, http://dx.doi.org/10.1016/j.diamond.2017.06.002, URL https://www.sciencedirect.com/science/article/pii/S0925963517301747.

[94] Dani George, H.R. Chandan, R. Shwetharani, M. Faisal, Jahir Ahmed, Farid A. Harraz, R. Geetha Balakrishna, Understanding graphyne; theoretical insights and its optoelectronic behaviour, Mater. Sci. Semicond. Process. 187 (2025) 109113, http://dx.doi.org/10.1016/j.mssp.2024.109113, URL https://www.sciencedirect.com/science/article/pii/S1369800124010096.

[95] Ersin Kantar, Investigating the magnetic and hysteretic properties of graphyne-based nanostructures: a comparative study of shape effects on critical temperatures, coercivity, and remanence, Phys. Scr. 99 (3) (2024) 035965, http://dx.doi.org/10.1088/1402-4896/ad2b40.

[96] Xiao-Ming Wang, Dong-Chuan Mo, Shu-Shen Lu, On the thermoelectric transport properties of graphyne by the first-principles method, J. Chem. Phys. 138 (20) (2013) 204704, http://dx.doi.org/10.1063/1.4806069.

[97] Nihan Kosku Perkgöz, Cem Sevik, Vibrational and thermodynamic properties of α-, β-, γ-, and 6, 6, 12-graphyne structures, Nanotechnology 25 (18) (2014) 185701, http://dx.doi.org/10.1088/0957-4484/25/18/185701.

[98] Guilherme B. Kanegae, Marcelo L. Pereira Junior, Douglas S. Galvão, Luiz A. Ribeiro Junior, Alexandre F. Fonseca, Enhanced elastocaloric effects in γ-graphyne, ACS Appl. Mater. & Interfaces 17 (9) (2025) 13074–13082, http://dx.doi.org/10.1021/acsami.4c03302, PMID: 38706297.

[99] Daniel A. Solis, Daiane D. Borges, Cristiano F. Woellner, Douglas S. Galvão, Structural and thermal stability of graphyne and graphdiyne nanoscroll structures, ACS Appl. Mater. & Interfaces 11 (3) (2019) 2670–2676, http://dx.doi.org/10.1021/acsami.8b03481.

[100] Qiaohan Liu, Xiaorong Wang, Jing Yu, Jingang Wang, Graphyne and graphdiyne nanoribbons: from their structures and properties to potential applications, Phys. Chem. Chem. Phys. 26 (2024) 1541–1563, http://dx.doi.org/10.1039/D3CP04393B.

[101] V.R. Coluci, S.F. Braga, S.B. Legoas, D.S. Galvão, R.H. Baughman, Families of carbon nanotubes: Graphyne-based nanotubes, Phys. Rev. B 68 (2003) 035430, http://dx.doi.org/10.1103/PhysRevB.68.035430.

[102] Mengqiu Long, Ling Tang, Dong Wang, Yuliang Li, Zhigang Shuai, Electronic structure and carrier mobility in graphdiyne sheet and nanoribbons: Theoretical predictions, ACS Nano 5 (4) (2011) 2593–2600, http://dx.doi.org/10.1021/nn102472s.

[103] Shangchao Lin, Markus J. Buehler, Mechanics and molecular filtration performance of graphyne nanoweb membranes for selective water purification, Nanoscale 5 (2013) 11801–11807, http://dx.doi.org/10.1039/C3NR03241H.

[104] Jianlong Kou, Xiaoyan Zhou, Hangjun Lu, Fengmin Wu, Jintu Fan, Graphyne as the membrane for water desalination, Nanoscale 6 (2014) 1865–1870, http://dx.doi.org/10.1039/C3NR04984A.

[105] Jingjie Yeo, Gang Seob Jung, Francisco J. Martín-Martínez, Jennifer Beem, Zhao Qin, Markus J. Buehler, Multiscale design of graphyne-based materials for high-performance separation membranes, Adv. Mater. 31 (42) (2019) 1805665, http://dx.doi.org/10.1002/adma.201805665.

[106] Hu Qiu, Minmin Xue, Chun Shen, Zhuhua Zhang, Wanlin Guo, Graphynes for water desalination and gas separation, Adv. Mater. 31 (42) (2019) 1803772, http://dx.doi.org/10.1002/adma.201803772, URL https://advanced.onlinelibrary.wiley.com/doi/abs/10.1002/adma.201803772.

[107] Khatereh Azizi, S. Mehdi Vaez Allaei, Arman Fathizadeh, Ali Sadeghi, Muhammad Sahimi, Graphyne-3: a highly efficient candidate for separation of small gas molecules from gaseous mixtures, Sci. Rep. 11 (1) (2021) 16325, http://dx.doi.org/10.1038/s41598-021-95304-z.

[108] Tingting Zheng, Yu Gao, Xiaoxiao Deng, Huibiao Liu, Jian Liu, Ran Liu, Jingwei Shao, Yuliang Li, Lee Jia, Comparisons between graphene oxide and graphdiyne oxide in physicochemistry biology and cytotoxicity, ACS Appl. Mater. & Interfaces 10 (39) (2018) 32946–32954, http://dx.doi.org/10.1021/acsami.8b06804.

[109] Jyotirmoy Deb, Ajit Kundu, Nandini Garg, Utpal Sarkar, Brahmananda Chakraborty, Copper decorated graphyne as a promising nanocarrier for cisplatin anti-cancer drug: A DFT study, Appl. Surf. Sci. 622 (2023) 156885, http://dx.doi.org/10.1016/j.apsusc.2023.156885.

[110] Ryota Sakamoto, Naoya Fukui, Hiroaki Maeda, Ryota Matsuoka, Ryojun Toyoda, Hiroshi Nishihara, The accelerating world of graphdiynes, Adv. Mater. 31 (42) (2019) 1804211, http://dx.doi.org/10.1002/adma.201804211, URL https://advanced.onlinelibrary.wiley.com/doi/abs/10.1002/adma.201804211.

[111] Massimiliano Bartolomei, Giacomo Giorgi, Sodium into γ-graphyne multilayers: An intercalation compound for anodes in metal-ion batteries, ACS Mater. Lett. 6 (10) (2024) 4682–4689, http://dx.doi.org/10.1021/acsmaterialslett.4c01119.

[112] C. Quej, J. Medina, G. Canto, M.L. Casais-Molina, C. Cab, A. Tapia, Electronic and structural properties of hydrogen adsorption on γ-graphyne and γ-bnyne, Comput. Mater. Sci. 232 (2024) 112677, http://dx.doi.org/10.1016/j.commatsci.2023.112677, URL https://www.sciencedirect.com/science/article/pii/S0927025623006717.

[113] Xiaojie Chen, Wenxian Xu, Bin Song, Pimo He, First-principles study of stability, electronic structure and quantum capacitance of B-, N- and O-doped graphynes as supercapacitor electrodes, J. Phys.: Condens. Matter. 32 (21) (2020) 215501, http://dx.doi.org/10.1088/1361-648X/ab6e8d.

[114] Henrique de Araujo Chagas, Thaciana Malaspina, Eudes Eterno Fileti, Guilherme Colherinhas, Performance analysis of supercapacitors with graphene and graphyne electrodes, Energy Storage 7 (1) (2025) e70114, http://dx.doi.org/10.1002/est2.70114.

[115] A.L. Ivanovskii, Graphynes and graphdyines, Progr. Solid State Chem. 41 (1–2) (2013) 1–19, http://dx.doi.org/10.1016/j.progsolidstchem.2012.12.001.

[116] Yongjun Li, Liang Xu, Huibiao Liu, Yuliang Li, Graphdiyne and graphyne: from theoretical predictions to practical construction, Chem. Soc. Rev. 43 (2014) 2572–2586, http://dx.doi.org/10.1039/C3CS60388A.

[117] Binquan Luan, Tien Huynh, Ruhong Zhou, Potential interference of protein–protein interactions by graphyne, J. Phys. Chem. B 120 (9) (2016) 2124–2131, http://dx.doi.org/10.1021/acs.jpcb.5b11449, PMID: 26885561.

[118] Jiaqiang Li, Yu Han, Artificial carbon allotrope γ-graphyne: Synthesis, properties, and applications, Giant 13 (2023) 100140, http://dx.doi.org/10.1016/j.giant.2023.100140, URL https://www.sciencedirect.com/science/article/pii/S2666542523000024.

[119] Matthew R. Callstrom, Thomas X. Neenan, George M. Whitesides, Poly[ethynylene(3-n-butyl-2,5-thiophenediyl)-ethynylene]: a soluble polymer containing diacetylene units and its conversion to a highly cross-linked organic solid, Macromolecules 21 (12) (1988) 3528–3530, http://dx.doi.org/10.1021/ma00190a034.

[120] Sara Eisler, Rik R. Tykwinski, Expanded radialenes: Modular synthesis and characterization of cross-conjugated enyne macrocycles, Angew. Chem. Int. Ed. 38 (13–14) (1999) 1940–1943.

[121] Joshua M. Kehoe, James H. Kiley, Jamieson J. English, Charles A. Johnson, Ryan C. Petersen, Michael M. Haley, Carbon networks based on dehydrobenzoannulenes. 3. Synthesis of graphyne Substructures1, Org. Lett. 2 (7) (2000) 969–972, http://dx.doi.org/10.1021/ol005623w, PMID: 10768199.
[122] Wei Zhang, Scott M. Brombosz, Jose L. Mendoza, Jeffrey S. Moore, A high-yield, one-step synthesis of o-phenylene ethynylene cyclic trimer via precipitation-driven alkyne metathesis, J. Org. Chem. 70 (24) (2005) 10198–10201, http://dx.doi.org/10.1021/jo0517803, PMID: 16292873.
[123] Charles A. Johnson, Yunyi Lu, Michael M. Haley, Carbon networks based on benzocyclynes. 6. Synthesis of graphyne substructures via directed alkyne metathesis, Org. Lett. 9 (19) (2007) 3725–3728, http://dx.doi.org/10.1021/ol7014253, PMID: 17705499.
[124] Michael M. Haley, Synthesis and properties of annulenic subunits of graphyne and graphdiyne nanoarchitectures, Pure Appl. Chem. 80 (3) (2008) 519–532, http://dx.doi.org/10.1351/pac200880030519.
[125] François Diederich, Milan Kivala, All-carbon scaffolds by rational design, Adv. Mater. 22 (7) (2010) 803–812, http://dx.doi.org/10.1002/adma.200902623.
[126] Guoxing Li, Yuliang Li, Huibiao Liu, Yanbing Guo, Yongjun Li, Daoben Zhu, Architecture of graphdiyne nanoscale films, "Chem. Commun." 46 (2010) 3256–3258, http://dx.doi.org/10.1039/B922733D.
[127] C. Glaser, Beiträge zur kenntniss des acetenylbenzols, Berichte der Dtsch. Chem. Ges. 2 (1) (1869) 422–424, http://dx.doi.org/10.1002/cber.186900201183.
[128] Jie Jack Li, Glaser coupling, in: Name Reactions: A Collection of Detailed Reaction Mechanisms, Springer Berlin Heidelberg, Berlin, Heidelberg, 2006, pp. 263–264, http://dx.doi.org/10.1007/3-540-30031-7_117.
[129] Allan S. Hay, Oxidative coupling of acetylenes. II1, J. Org. Chem. 27 (9) (1962) 3320–3321, http://dx.doi.org/10.1021/jo01056a511, URL https://doi.org/10.1021/jo01056a511.
[130] Ryota Matsuoka, Ryota Sakamoto, Ken Hoshiko, Sono Sasaki, Hiroyasu Masunaga, Kosuke Nagashio, Hiroshi Nishihara, Crystalline graphdiyne nanosheets produced at a gas/liquid or liquid/liquid interface, J. Am. Chem. Soc. 139 (8) (2017) 3145–3152, http://dx.doi.org/10.1021/jacs.6b12776, PMID: 28199105.
[131] Zicheng Zuo, Hong Shang, Yanhuan Chen, Jiaofu Li, Huibiao Liu, Yongjun Li, Yuliang Li, A facile approach for graphdiyne preparation under atmosphere for an advanced battery anode, Chem. Commun. 53 (2017) 8074–8077, http://dx.doi.org/10.1039/C7CC03200E.
[132] Jingyuan Zhou, Ziqian Xie, Rong Liu, Xin Gao, Jiaqiang Li, Yan Xiong, Lianming Tong, Jin Zhang, Zhongfan Liu, Synthesis of ultrathin graphdiyne film using a surface template, ACS Appl. Mater. & Interfaces 11 (3) (2019) 2632–2637, http://dx.doi.org/10.1021/acsami.8b02612.
[133] Xin Gao, Huibiao Liu, Dan Wang, Jin Zhang, Graphdiyne: synthesis, properties, and applications, Chem. Soc. Rev. 48 (2019) 908–936, http://dx.doi.org/10.1039/C8CS00773J.
[134] Chen Yin, Jiaqiang Li, Tianran Li, Yue Yu, Ya Kong, Peng Gao, Hailin Peng, Lianming Tong, Jin Zhang, Catalyst-free synthesis of few-layer graphdiyne using a microwave-induced temperature gradient at a solid/liquid interface, Adv. Funct. Mater. 30 (23) (2020) 2001396, http://dx.doi.org/10.1002/adfm.202001396, URL https://advanced.onlinelibrary.wiley.com/doi/abs/10.1002/adfm.202001396.
[135] Junhua Kuang, Jia Yu, Qiaoyu Zhang, Shihang Zhu, Ruoxuan Wang, Junchi Ma, Jinlong Wan, Han Han, Zhifeng He, Nuowen Ma, Yuting Zhang, Liuxuan Cao, Shisheng Zheng, Binju Wang, Li Peng, Shuliang Yang, Jian-Feng Li, Weiguo Song, Yuliang Li, Graphdiyne production in a flash: High-yield direct synthesis by electron beam irradiation, Adv. Mater. 37 (40) (2025) 2506979, http://dx.doi.org/10.1002/adma.202506979.
[136] Juan Gao, Jiaofu Li, Yanhuan Chen, Zicheng Zuo, Yongjun Li, Huibiao Liu, Yuliang Li, Architecture and properties of a novel two-dimensional carbon material-graphtetrayne, Nano Energy 43 (2018) 192–199, http://dx.doi.org/10.1016/j.nanoen.2017.11.005, URL https://www.sciencedirect.com/science/article/pii/S2211285517306845.
[137] Qingyan Pan, Siqi Chen, Chenyu Wu, Feng Shao, Jing Sun, Lishui Sun, Zhaohui Zhang, Yixiao Man, Zhibo Li, Lixia He, Yingjie Zhao, Direct synthesis of crystalline graphtetrayne—A new graphyne allotrope, CCS Chem. 3 (4) (2021) 1368–1375, http://dx.doi.org/10.31635/ccschem.020.202000377.
[138] Rafael Chinchilla, Carmen Nájera, The sonogashira reaction: A booming methodology in synthetic organic chemistry, Chem. Rev. 107 (3) (2007) 874–922, http://dx.doi.org/10.1021/cr050992x, PMID: 17305399.
[139] Qiaodan Li, Yong Li, Yang Chen, Lulu Wu, Chaofan Yang, Xiaoli Cui, Synthesis of γ-graphyne by mechanochemistry and its electronic structure, Carbon 136 (2018) 248–254, http://dx.doi.org/10.1016/j.carbon.2018.04.081, URL https://www.sciencedirect.com/science/article/pii/S0008622318304421.
[140] Manaswee Barua, Aditi Saraswat, C.N.R. Rao, A novel method for synthesis of γ-graphyne and their charge transfer properties, Carbon 200 (2022) 247–252, http://dx.doi.org/10.1016/j.carbon.2022.08.061, URL https://www.sciencedirect.com/science/article/pii/S0008622322006844.
[141] Victor G. Desyatkin, William B. Martin, Ali E. Aliev, Nathaniel E. Chapman, Alexandre F. Fonseca, Douglas S. Galvão, Ericka Roy Miller, Kevin H. Stone, Zhong Wang, Dante Zakhidov, F. Ted Limpoco, Sarah R. Almahdali, Shane M. Parker, Ray H. Baughman, Valentin O. Rodionov, Scalable synthesis and characterization of multilayer γ-graphyne, new carbon crystals with a small direct band gap, J. Am. Chem. Soc. 144 (39) (2022) 17999–18008, http://dx.doi.org/10.1021/jacs.2c06583, PMID: 36130080.
[142] Xinghui Liu, Soo Min Cho, Shiru Lin, Zhongfang Chen, Wooseon Choi, Young-Min Kim, Eunbhin Yun, Eun Hee Baek, Do Hyun Ryu, Hyoyoung Lee, Constructing two-dimensional holey graphyne with unusual annulative π-extension, Matter 5 (7) (2022) 2306–2318, http://dx.doi.org/10.1016/j.matt.2022.04.033.
[143] Tao Song, Hong Liu, Haiyuan Zou, Cheng Wang, Siyan Shu, Hao Dai, Lele Duan, Metal-free wet chemistry for the fast gram-scale synthesis of γ-graphyne and its derivatives, Angew. Chem. Int. Ed. 63 (50) (2024) e202411228, http://dx.doi.org/10.1002/anie.202411228.
[144] Ezra R. Kone, Sarah Nasri, Grace L. Parker, Victor G. Desyatkin, William B. Martin, John F. Trant, Valentin O. Rodionov, Replication of mechanochemical syntheses of γ-graphyne from calcium carbide fails to produce the claimed product, Carbon 232 (2025) 119808, http://dx.doi.org/10.1016/j.carbon.2024.119808, URL https://www.sciencedirect.com/science/article/pii/S0008622324010273.
[145] Martin Drøhse Kilde, Adrian H. Murray, Cecilie Lindholm Andersen, Freja Eilsø Storm, Katrin Schmidt, Anders Kadziola, Kurt V. Mikkelsen, Frank Hampel, Ole Hammerich, Rik R. Tykwinski, Mogens Brøndsted Nielsen, Synthesis of radiaannulene oligomers to model the elusive carbon allotrope 6,6,12-graphyne, Nat. Commun. 10 (1) (2019) 3714, http://dx.doi.org/10.1038/s41467-019-11700-0.
[146] Peter Lundg° ard Krøll, Magnus Bukhave Johansen, Andreas Erbs Hillers-Bendtsen, Ahmed Ali El-Sayed, Mathias Dowds, Andrea Knakkergaard Knub, Viktor Bliksted Roug Pedersen, Kurt V. Mikkelsen, Mogens Brøndsted Nielsen, Synthesis and properties of acetylenic scaffolds modeling segments of 6,6,12-graphyne, Chem. – A Eur. J. n/a (n/a) (2025) e202500360, http://dx.doi.org/10.1002/chem.202500360.
[147] Arnet Maria Antony, Raja Gopal Peri, Siddappa A. Patil, Akshaya K. Samal, Beyond graphene: a review of graphene's lesser-known yne relatives and their energy applications, J. Mater. Chem. A (2025) http://dx.doi.org/10.1039/D5TA04704H.
[148] Kailu Xiao, Jiaofu Li, Xianqian Wu, Huibiao Liu, Chenguang Huang, Yuliang Li, Nanoindentation of thin graphdiyne films: Experiments and molecular dynamics simulation, Carbon 144 (2019) 72–80, http://dx.doi.org/10.1016/j.carbon.2018.12.029, URL https://www.sciencedirect.com/science/article/pii/S0008622318311606.
[149] Ya Kong, Yuling Yin, Xueting Feng, Zixuan Zhang, Feng Ding, Lianming Tong, Jin Zhang, Negative thermal expansion behaviour of graphdiyne, Nano Today 48 (2023) 101695, http://dx.doi.org/10.1016/j.nantod.2022.101695, URL https://www.sciencedirect.com/science/article/pii/S1748013222003231.
[150] Xuemin Qian, Huibiao Liu, Changshui Huang, Songhua Chen, Liang Zhang, Yongjun Li, Jizheng Wang, Yuliang Li, Self-catalyzed growth of large-area nanofilms of two-dimensional carbon, Sci. Rep. 5 (1) (2015) 7756, http://dx.doi.org/10.1038/srep07756.
[151] Yuan Li, Mingjia Zhang, Xiuli Hu, Xinhui Fan, Lingmin Yu, Changshui Huang, Light and heat triggering modulation of the electronic performance of a graphdiyne-based thin film transistor, J. Phys. Chem. Lett. 11 (6) (2020) 1998–2005, http://dx.doi.org/10.1021/acs.jpclett.0c00113.
[152] Mingjia Zhang, Yuan Li, Xiaodong Li, Naiyin Wang, Changshui Huang, Graphdiyne ink for ionic liquid gated printed transistor, Adv. Electron. Mater. 6 (7) (2020) 2000157, http://dx.doi.org/10.1002/aelm.202000157.
[153] Yuyu Liu, Zhen Shao, Xiang Yu, Dong Guo, Shasha Wang, Linyi Bian, Yanhuan Chen, Huibiao Liu, Haifeng Ling, Linghai Xie, Graphdiyne particles as nano-floating gates for high-performance nonvolatile organic field-effect transistor memory, Org. Electron. 128 (2024) 107027, http://dx.doi.org/10.1016/j.orgel.2024.107027.
[154] Zhihua Zhou, Yongtao Tan, Qian Yang, Achintya Bera, Zecheng Xiong, Mehmet Yagmurcukardes, Minsoo Kim, Yichao Zou, Guanghua Wang, Artem Mishchenko, Ivan Timokhin, Canbin Wang, Hao Wang, Chongyang Yang, Yizhen Lu, Radha Boya, Honggang Liao, Sarah Haigh, Huibiao Liu, Francois M. Peeters, Yuliang Li, Andre K. Geim, Sheng Hu, Gas permeation through graphdiyne-based nanoporous membranes, Nat. Commun. 13 (1) (2022) 4031, http://dx.doi.org/10.1038/s41467-022-31779-2.
[155] Rong Liu, Jingyuan Zhou, Xin Gao, Jiaqiang Li, Ziqian Xie, Zhenzhu Li, Shuqing Zhang, Lianming Tong, Jin Zhang, Zhongfan Liu, Graphdiyne filter for decontaminating lead-ion-polluted water, Adv. Electron. Mater. 3 (11) (2017) 1700122, http://dx.doi.org/10.1002/aelm.201700122.
[156] Tianyu Yuan, Shijie Xiong, Xinghai Shen, Coordination of actinide single ions to deformed graphdiyne: Strategy on essential separation processes in nuclear fuel cycle, Angew. Chem. Int. Ed. 59 (40) (2020) 17719–17725, http://dx.doi.org/10.1002/anie.202008165, URL https://onlinelibrary.wiley.com/doi/abs/10.1002/anie.202008165.
[157] Huiling Chen, Xing Liu, Dian Gong, Chang Zhu, Guojuan Liu, Jingrui Fan, Ping Wu, Zhi Li, Yichang Pan, Guosheng Shi, Yuhan Sun, Gaofeng Zeng, Ultrahigh-water-flux desalination on graphdiyne membranes, Nat. Water 1 (9) (2023) 800–807, http://dx.doi.org/10.1038/s44221-023-00123-3.
[158] Siyuan Li, Yasong Zhao, Dan Wang, Progress in graphdiyne-based membrane for gas separation and water purification, ChemPhysMater 4 (3) (2025) 234–250, http://dx.doi.org/10.1016/j.chphma.2025.02.007, URL https://www.sciencedirect.com/science/article/pii/S2772571525000208.

[159] Yana Zhang, Wenxin Liu, Yongjun Li, Ying-Wei Yang, Alideertu Dong, Yuliang Li, 2D graphdiyne oxide serves as a superior new generation of antibacterial agents, IScience 19 (2019) 662–675, http://dx.doi.org/10.1016/j.isci.2019.08.019, URL https://www.sciencedirect.com/science/article/pii/S2589004219302974.

[160] Zhiling Zhu, Qiang Bai, Shuo Li, Siheng Li, Manhong Liu, Fanglin Du, Ning Sui, William W. Yu, Antibacterial activity of graphdiyne and graphdiyne oxide, Small 16 (34) (2020) 2001440, http://dx.doi.org/10.1002/smll.202001440.

[161] Xuelong Bi, Qiang Bai, Lina Wang, Fanglin Du, Manhong Liu, William W. Yu, Siheng Li, Jiaqiang Li, Zhiling Zhu, Ning Sui, Jin Zhang, Boron doped graphdiyne: A metal-free peroxidase mimetic nanozyme for antibacterial application, Nano Res. 15 (2) (2022) 1446–1454, http://dx.doi.org/10.1007/s12274-021-3685-4.

[162] Hetong Qi, Yuxi Tong, Mengyue Zhang, Xuemei Wu, Ling Yue, Boron-doped and ketonic carbonyl group-enriched graphdiyne as a dual-site carbon nanozyme with enhanced peroxidase-like activity, Anal. Chem. 94 (49) (2022) 17272–17278, http://dx.doi.org/10.1021/acs.analchem.2c04239.

[163] Rui Wang, Miusi Shi, Feiyan Xu, Yun Qiu, Peng Zhang, Kailun Shen, Qin Zhao, Jiaguo Yu, Yufeng Zhang, Graphdiyne-modified TiO2 nanofibers with osteoinductive and enhanced photocatalytic antibacterial activities to prevent implant infection, Nat. Commun. 11 (1) (2020) 4465, http://dx.doi.org/10.1038/s41467-020-18267-1.

[164] Jiani Xie, Ning Wang, Xinghua Dong, Chengyan Wang, Zhen Du, Linqiang Mei, Yuan Yong, Changshui Huang, Yuliang Li, Zhanjun Gu, Yuliang Zhao, Graphdiyne nanoparticles with high free radical scavenging activity for radiation protection, ACS Appl. Mater. & Interfaces 11 (3) (2019) 2579–2590, http://dx.doi.org/10.1021/acsami.8b00949.

[165] Ling-Xiao Zhao, Zhi-Qiang Gong, Qi Zhang, Da-Long He, Ri-Le Ge, Jin Meng, Hang Ren, Yong-Gang Fan, Zhan-You Wang, Graphdiyne nanoplatforms for photothermal-ferroptosis combination therapy against glioblastoma, J. Control. Release 359 (2023) 12–25, http://dx.doi.org/10.1016/j.jconrel.2023.05.035, URL https://www.sciencedirect.com/science/article/pii/S0168365923003486.

[166] W. Xie, Y. Wang, Q. Xu, G. Zhong, J. Lin, H. He, Q. Du, H. Tan, M. Chen, Z. Wu, Y. Deng, Z. Han, J. Lu, J. Ye, F. Zou, Y. Zhuo, W Zhong, A unique approach: Biomimetic graphdiyne-based nanoplatform to treat prostate cancer by combining cuproptosis and enhanced chemodynamic therapy, Int. J. Nanomedicine 19 (2024) 3957–3972, http://dx.doi.org/10.2147/IJN.S455355.

[167] Jun Jin, Mengyu Guo, Jiaming Liu, Jing Liu, Huige Zhou, Jiayang Li, Liming Wang, Huibiao Liu, Yuliang Li, Yuliang Zhao, Chunying Chen, Graphdiyne nanosheet-based drug delivery platform for photothermal/chemotherapy combination treatment of cancer, ACS Appl. Mater. & Interfaces 10 (10) (2018) 8436–8442, http://dx.doi.org/10.1021/acsami.7b17219.

[168] Z. Huang, G. Chen, F. Deng, Y. Li, Nanostructured graphdiyne: Synthesis and biomedical applications, Int. J. Nanomedicine 17 (2022) 6467–6490, http://dx.doi.org/10.2147/IJN.S383707.

[169] Wen Yu, Gang Song, Fengting Lv, Yiming Huang, Haotian Bai, Shu Wang, Recent advances in graphdiyne materials for biomedical applications, Nano Today 46 (2022) 101616, http://dx.doi.org/10.1016/j.nantod.2022.101616, URL https://www.sciencedirect.com/science/article/pii/S1748013222002444.

[170] Xiaojie Wu, Yaning Lu, Peipei Li, Qiudi Shen, Douxin Xiao, Haixia Wu, Jing Kang, Yansong Qi, Alideertu Dong, Current advances in the synthesis, properties, and biomedical applications of two-dimensional graphdiyne: A review, ACS Appl. Nano Mater. 7 (3) (2024) 2461–2493, http://dx.doi.org/10.1021/acsanm.3c05068.

[171] Xiangyan Shen, Ze Yang, Kun Wang, Ning Wang, Jianjiang He, Huiping Du, Changshui Huang, Nitrogen-doped graphdiyne as high-capacity electrode materials for both lithium-ion and sodium-ion capacitors, ChemElectroChem 5 (11) (2018) 1435–1443, http://dx.doi.org/10.1002/celc.201800300, URL https://chemistry-europe.onlinelibrary.wiley.com/doi/abs/10.1002/celc.201800300.

[172] Fan Wang, Zicheng Zuo, Liang Li, Kuo Li, Feng He, Zhongqing Jiang, Yuliang Li, Large-area aminated-graphdiyne thin films for direct methanol fuel cells, Angew. Chem. Int. Ed. 58 (42) (2019) 15010–15015, http://dx.doi.org/10.1002/anie.201910588.

[173] Guiquan Liu, Guorong Wang, Zhiliang Jin, Subtly synthesized graphdiyne nanolamellas as stable electrode material for supercapacitors, Electrochim. Acta 464 (2023) 142866, http://dx.doi.org/10.1016/j.electacta.2023.142866, URL https://www.sciencedirect.com/science/article/pii/S001346862301040X.

[174] Haiyan Xie, Pengwei Jia, Hongwei Huang, Multidimensional graphdiyne structures and beyond for energy conversion and storage, Adv. Funct. Mater. n/a (n/a) (2025) e10586, http://dx.doi.org/10.1002/adfm.202510586, URL https://advanced.onlinelibrary.wiley.com/doi/abs/10.1002/adfm.202510586.

[175] Mengke Wang, Junmei Pu, Yi Hu, You Zi, Zheng-Guang Wu, Weichun Huang, Functional graphdiyne for emerging applications: Recent advances and future challenges, Adv. Funct. Mater. 34 (4) (2024) 2308601, http://dx.doi.org/10.1002/adfm.202308601.

[176] Dinh Phuc Do, Eunji Lee, Viet Q. Bui, Hyoyoung Lee, Recent progress in two-dimensional graphdiyne: Synthesis, characterization, and applications, ChemPhysMater 4 (2) (2025) 91–107, http://dx.doi.org/10.1016/j.chphma.2024.09.005, URL https://www.sciencedirect.com/science/article/pii/S2772571524000585.

[177] Ali E. Aliev, Yongzhe Guo, Alexandre F. Fonseca, Joselito M. Razal, Zhong Wang, Douglas S. Galvão, Claire M. Bolding, Nathaniel E. Chapman-Wilson, Victor G. Desyatkin, Johannes E. Leisen, Luiz A. Ribeiro Junior, Guilherme B. Kanegae, Peter Lynch, Jizhen Zhang, Mia A. Judicpa, Aaron M. Parra, Mengmeng Zhang, Enlai Gao, Lifang Hu, Valentin O. Rodionov, Ray H. Baughman, A planar-sheet nongraphitic zero-bandgap sp^2 carbon phase made by the low-temperature reaction of γ-graphyne, Proc. Natl. Acad. Sci. 122 (5) (2025) e2413194122, http://dx.doi.org/10.1073/pnas.2413194122.

[178] R. Totani, C. Grazioli, T. Zhang, I. Bidermane, J. Lüder, M. de Simone, M. Coreno, B. Brena, L. Lozzi, C. Puglia, Electronic structure investigation of biphenylene films, J. Chem. Phys. 146 (5) (2017) http://dx.doi.org/10.1063/1.4975104.

[179] Fritz Vögtle, Fascinating molecules in organic chemistry, 1992, (No Title).

[180] Anne I.S. Holm, Henrik A.B. Johansson, Henrik Cederquist, Henning Zettergren, Dissociation and multiple ionization energies for five polycyclic aromatic hydrocarbon molecules, J. Chem. Phys. 134 (4) (2011).

[181] T. Elsaesser, F. Lärmer, W. Kaiser, Bernhard Dick, M. Niemeyer, W. Lüttke, Picosecond spectroscopy of electronically excited singlet states in biphenylene, Chem. Phys. 126 (2–3) (1988) 405–416.

[182] T.C.W. Mak, J. Trotter, 1. The crystal and molecular structure of biphenylene, J. Chem. Soc. (Resumed) (1962) 1, http://dx.doi.org/10.1039/jr9620000001.

[183] M.E. Beck, R. Rebentisch, G. Hohlneicher, M.P. Fülscher, L. Serrano-Andrés, B.O. Roos, Vertical and adiabatic electronic excitations in biphenylene: A theoretical study, J. Chem. Phys. 107 (22) (1997) 9464–9474.

[184] Ralf Zimmermann, A theoretical study on the molecular structure of biphenylene in its first excited singlet and triplet states: quantum chemical calculations on the structural changes of an antiaromatic molecule upon excitation, J. Mol. Struct. 377 (1) (1996) 35–46.

[185] Tianyang Liu, Yu Jing, Yafei Li, Two-dimensional biphenylene: A graphene allotrope with superior activity toward electrochemical oxygen reduction reaction, J. Phys. Chem. Lett. 12 (51) (2021) 12230–12234, http://dx.doi.org/10.1021/acs.jpclett.1c03851.

[186] A. Bafekry, M. Faraji, M.M. Fadlallah, H.R. Jappor, S. Karbasizadeh, M. Ghergherehchi, D. Gogova, Biphenylene monolayer as a two-dimensional non-benzenoid carbon allotrope: a first-principles study, J. Phys.: Condens. Matter. 34 (1) (2021) 015001, http://dx.doi.org/10.1088/1361-648x/ac2a7b.

[187] A.T. Balaban, Co C. Rentia, E. Ciupitu, Chemical graphs. 6. Estimation of relative stability of several planar and tridimensional lattices for elementary carbon, Rev. Roum. Chim 13 (2) (1968) 231–247.

[188] A.T. Balaban, Carbon and its nets, in: Symmetry 2, Elsevier, 1989, pp. 397–416.

[189] G. Brunetto, P.A.S. Autreto, L.D. Machado, B.I. Santos, R.P.B. dos Santos, D.S. Galvao, Nonzero gap two-dimensional carbon allotrope from porous graphene, J. Phys. Chem. C 116 (23) (2012) 12810–12813, http://dx.doi.org/10.1021/jp211300n.

[190] Qi Song, Bing Wang, Ke Deng, Xinliang Feng, Manfred Wagner, Julian D. Gale, Klaus Müllen, Linjie Zhi, Graphenylene, a unique two-dimensional carbon network with nondelocalized cyclohexatriene units, J. Mater. Chem. C 1 (2013) 38–41, http://dx.doi.org/10.1039/C2TC00006G.

[191] Pablo A. Denis, Federico Iribarne, Hydrogen storage in doped biphenylene based sheets, Comput. Theor. Chem. 1062 (2015) 30–35, http://dx.doi.org/10.1016/j.comptc.2015.03.012, URL https://www.sciencedirect.com/science/article/pii/S2210271X15001188.

[192] Hideaki Takano, Takeharu Ito, Kyalo Stephen Kanyiva, Takanori Shibata, Recent advances of biphenylene: Synthesis, reactions and uses, Eur. J. Org. Chem. 2019 (18) (2019) 2871–2883, http://dx.doi.org/10.1002/ejoc.201900111.

[193] Guogang Liu, Tong Chen, Xiaohui Li, Zhonghui Xu, Xianbo Xiao, Electronic transport in biphenylene network monolayer: Proposals for 2D multifunctional carbon-based nanodevices, Appl. Surf. Sci. 599 (2022) 153993, http://dx.doi.org/10.1016/j.apsusc.2022.153993.

[194] F.F. Monteiro, W.F. Giozza, R.T. de Sousa Júnior, P.H. de Oliveira Neto, L.A. Ribeiro Júnior, M.L. Pereira Júnior, On the mechanical, electronic, and optical properties of the boron nitride analog for the recently synthesized biphenylene network: a DFT study, J. Mol. Model. 29 (7) (2023) http://dx.doi.org/10.1007/s00894-023-05606-4.

[195] Xue-Dan Ma, Zhen-Wei Tian, Ran Jia, Fu-Quan Bai, BN counterpart of biphenylene network: A theoretical investigation, Appl. Surf. Sci. 598 (2022) 153674, http://dx.doi.org/10.1016/j.apsusc.2022.153674, URL https://www.sciencedirect.com/science/article/pii/S0169433222012247.

[196] Qitang Fan, Linghao Yan, Matthias W. Tripp, Ondrej Krejci, Stavrina Dimosthenous, Stefan R. Kachel, Mengyi Chen, Adam S. Foster, Ulrich Koert, Peter Liljeroth, J. Michael Gottfried, Biphenylene network: A nonbenzenoid carbon allotrope, Science 372 (6544) (2021) 852+, http://dx.doi.org/10.1126/science.abg4509.

[197] Florian Schlütter, Tomohiko Nishiuchi, Volker Enkelmann, Klaus Müllen, Octafunctionalized biphenylenes: molecular precursors for isomeric graphene nanostructures, Angew. Chem. 126 (6) (2014) 1564–1568.

[198] Zilin Zhao, Guangwei Che, Fang Li, Yunfan Fei, Hao Luo, Puyi Lang, Qingchao Zeng, Hongcun Bai, Yajie Wang, Ho-kwang Mao, Haiyan Zheng, Kuo Li, Synthesis of a biphenylene nanoribbon by compressing biphenylene under extreme conditions, Phys. Chem. Chem. Phys. 27 (12) (2025) 6072–6078, http://dx.doi.org/10.1039/d5cp00083a.

[199] Vinod Kumar, Surender Pratap, Brahmananda Chakraborty, 2D biphenylene: exciting properties, synthesis & applications, J. Phys.-Condens Matter 37 (11) (2025) http://dx.doi.org/10.1088/1361-648X/ada70f.

[200] Mathew A. Hudspeth, Brandon W. Whitman, Veronica Barone, Juan E. Peralta, Electronic properties of the biphenylene sheet and its one-dimensional derivatives, ACS Nano 4 (8) (2010) 4565–4570, http://dx.doi.org/10.1021/nn100758h.

[201] Pablo A. Denis, Stability and electronic properties of biphenylene based functionalized nanoribbons and sheets, J. Phys. Chem. C 118 (43) (2014) 24976–24982, http://dx.doi.org/10.1021/jp5069895.

[202] Shudong Wang, Optical response and excitonic effects in graphene nanoribbons derived from biphenylene, Mater. Lett. 167 (2016) 258–261, http://dx.doi.org/10.1016/j.matlet.2016.01.017, URL https://www.sciencedirect.com/science/article/pii/S0167577X16300179.

[203] Hazem Abdelsalam, Omar H. Abd-Elkader, Mahmoud A.S. Sakr, Ghada M. Abdelrazek, Yushen Liu, Qinfang Zhang, Insights into the electronic, optical, and catalytic properties of finite biphenylene nanoribbons: First-principles study, Comput. Theor. Chem. 1236 (2024) 114600, http://dx.doi.org/10.1016/j.comptc.2024.114600.

[204] Hongyu Ge, Guo Wang, Yi Liao, A theoretical investigation on the transport properties of armchair biphenylene nanoribbons, Chem. Phys. Lett. 648 (2016) 97–101, http://dx.doi.org/10.1016/j.cplett.2016.02.011.

[205] Shudong Wang, Optical response and excitonic effects in graphene nanoribbons derived from biphenylene, Mater. Lett. 167 (2016) 258–261, http://dx.doi.org/10.1016/j.matlet.2016.01.017, URL https://www.sciencedirect.com/science/article/pii/S0167577X16300179.

[206] Gözde Özbal Sargin, Salih Demirci, Kai Gong, V. Ongun Özçelik, Ultrathin carbon biphenylene network as an anisotropic thermoelectric material with high temperature stability under mechanical strain, Phys. Rev. Mater. 9 (2025) 024003, http://dx.doi.org/10.1103/PhysRevMaterials.9.024003, URL https://link.aps.org/doi/10.1103/PhysRevMaterials.9.024003.

[207] M.L. Pereira, W.F. da Cunha, R.T. de Sousa, G.D. Amvame Nze, D.S. Galvão, L.A. Ribeiro, On the mechanical properties and fracture patterns of the nonbenzenoid carbon allotrope (biphenylene network): a reactive molecular dynamics study, Nanoscale 14 (8) (2022) 3200–3211, http://dx.doi.org/10.1039/d1nr07959j.

[208] Obaidur Rahaman, Bohayra Mortazavi, Arezoo Dianat, Gianaurelio Cuniberti, Timon Rabczuk, Metamorphosis in carbon network: From penta-graphene to biphenylene under uniaxial tension, FlatChem 1 (2017) 65–73, http://dx.doi.org/10.1016/j.flatc.2016.12.001.

[209] G.S.L. Fabris, N.L. Marana, E. Longo, J.R. Sambrano, Theoretical study of porous surfaces derived from graphene and boron nitride, J. Solid State Chem. 258 (2018) 247–255, http://dx.doi.org/10.1016/j.jssc.2017.10.025.

[210] Guilherme S.L. Fabris, Carlos A. Paskocimas, Julio R. Sambrano, Ricardo Paupitz, One- and two-dimensional structures based on gallium nitride, J. Solid State Chem. 303 (2021) 122513, http://dx.doi.org/10.1016/j.jssc.2021.122513, URL https://www.sciencedirect.com/science/article/pii/S0022459621005582.

[211] Saeed Rouhi, Ali Ghasemi, Investigation of the elastic properties of graphenylene using molecular dynamics simulations, Mater. Res. 20 (1) (2016) 1–9, http://dx.doi.org/10.1590/1980-5373-mr-2015-0742.

[212] Mostafa Jahangirzadeh, Negin Karimzadeh Bajgiran, Sima Majidi, Jafar Azamat, Hamid Erfan-Niya, Atomistic understanding on desalination performance of pristine graphenylene nanosheet membrane at high applied pressures, J. Mol. Graph. Model. 132 (2024) 108833, http://dx.doi.org/10.1016/j.jmgm.2024.108833.

[213] Leila Mahboubian, Siamak Pakdel, Jafar Azamat, Hamid Erfan-Niya, Separation of H2/CH4 gas mixture through graphenylene membrane with functionalized nanopore: A computational study, Int. J. Hydrog. Energy 47 (65) (2022) 28025–28033, http://dx.doi.org/10.1016/j.ijhydene.2022.06.128.

[214] Johann Luder, Carla Puglia, Henrik Ottosson, Olle Eriksson, Biplab Sanyal, Barbara Brena, Many-body effects and excitonic features in 2D biphenylene carbon, J. Chem. Phys. 144 (2) (2016) http://dx.doi.org/10.1063/1.4939273.

[215] Qi Song, Bing Wang, Ke Deng, Xinliang Feng, Manfred Wagner, Julian D. Gale, Klaus Müllen, Linjie Zhi, Graphenylene, a unique two-dimensional carbon network with nondelocalized cyclohexatriene units, J. Mater. Chem. C 1 (1) (2013) 38–41, http://dx.doi.org/10.1039/c2tc00006g.

[216] E. Perim, R. Paupitz, P.A.S. Autreto, D.S. Galvao, Inorganic graphenylene: A porous two-dimensional material with tunable band gap, J. Phys. Chem. C 118 (41) (2014) 23670–23674, http://dx.doi.org/10.1021/jp502119y.

[217] Maryam S. Motallebipour, Javad Karimi-Sabet, Graphenylene and inorganic graphenylene nanopores for gas-phase 4he/3he separation: kinetic and steady-state considerations, Phys. Chem. Chem. Phys. 23 (27) (2021) 14706–14715, http://dx.doi.org/10.1039/d0cp05755j.

[218] Lei Zhu, Yakang Jin, Qingzhong Xue, Xiaofang Li, Haixia Zheng, Tiantian Wu, Cuicui Ling, Theoretical study of a tunable and strain-controlled nanoporous graphenylene membrane for multifunctional gas separation, J. Mater. Chem. A 4 (39) (2016) 15015–15021, http://dx.doi.org/10.1039/c6ta04456e.

[219] Xien Liu, Liming Dai, Carbon-based metal-free catalysts, Nat. Rev. Mater. 1 (11) (2016) http://dx.doi.org/10.1038/natrevmats.2016.64.

[220] E. Pérez-Mayoral, V. Calvino-Casilda, E. Soriano, Metal-supported carbon-based materials: opportunities and challenges in the synthesis of valuable products, Catal. Sci. & Technol. 6 (5) (2016) 1265–1291, http://dx.doi.org/10.1039/c5cy01437a.

[221] Weiguang Chen, Zhiwen Wang, Yingqi Cui, Zhaohan Li, Yi Li, Xianqi Dai, Yanan Tang, Graphenylene-supported single-atom (ru and mo) catalysts for CO and NO oxidations, New J. Chem. 44 (36) (2020) 15733–15741, http://dx.doi.org/10.1039/d0nj03842c.

[222] Yanan Tang, Weiguang Chen, Gao Zhao, Da Teng, Yingqi Cui, Zhaohan Li, Zhen Feng, Xianqi Dai, Comparative study of NO and CO oxidation reactions on single-atom catalysts anchored graphene-like monolayer, ChemPhysChem 22 (6) (2021) 606–618, http://dx.doi.org/10.1002/cphc.202001021.

[223] Yanan Tang, Weiguang Chen, Hongwei Zhang, Zhiwen Wang, Da Teng, Yingqi Cui, Zhen Feng, Xianqi Dai, Single-atom metal-modified graphenylene as a high-activity catalyst for CO and NO oxidation, Phys. Chem. Chem. Phys. 22 (28) (2020) 16224–16235, http://dx.doi.org/10.1039/d0cp01062f.

[224] Yang-Xin Yu, Graphenylene: a promising anode material for lithium-ion batteries with high mobility and storage, J. Mater. Chem. A 1 (43) (2013) 13559, http://dx.doi.org/10.1039/c3ta12639k.

[225] Guilherme da Silva Lopes Fabris, Anderson dos Reis Albuquerque, Roberto Dovesi, Julio Ricardo Sambrano, A promising carbon-based nanosheet as a suitable na-anode material, Mater. Sci. Eng.: B 268 (2021) 115121, http://dx.doi.org/10.1016/j.mseb.2021.115121.

[226] Kimal Chandula Wasalathilake, Godwin A. Ayoko, Cheng Yan, Effects of heteroatom doping on the performance of graphene in sodium-ion batteries: A density functional theory investigation, Carbon 140 (2018) 276–285, http://dx.doi.org/10.1016/j.carbon.2018.08.071.

[227] Tanveer Hussain, Marlies Hankel, Debra J. Searles, Graphenylene monolayers doped with alkali or alkaline earth metals: Promising materials for clean energy storage, J. Phys. Chem. C 121 (27) (2017) 14393–14400, http://dx.doi.org/10.1021/acs.jpcc.7b02191.

[228] Mostafa Jahangirzadeh, Jafar Azamat, Hamid Erfan-Niya, Molecular insight into water desalination through functionalized graphenylene nanosheet membranes, Comput. Mater. Sci. 203 (2022) 111126, http://dx.doi.org/10.1016/j.commatsci.2021.111126.

[229] Leonardo Villegas-Lelovsky, Ricardo Paupitz, Graphenylene-based nanoribbons for novel molecular electronic devices, Phys. Chem. Chem. Phys. 22 (48) (2020) 28365–28375, http://dx.doi.org/10.1039/d0cp04188b.

[230] R.M. Meftakhutdinov, R.T. Sibatov, A.I. Kochaev, D.A. Evseev, First-principles study of graphenylene/MoX2(X=S, Te, and Se) van der Waals heterostructures, Phys. Chem. Chem. Phys. 23 (26) (2021) 14315–14324, http://dx.doi.org/10.1039/d1cp01062j.

[231] Wei Liu, Mao-sheng Miao, Jing-yao Liu, Band gap engineering of graphenylene by hydrogenation and halogenation: a density functional theory study, RSC Adv. 5 (87) (2015) 70766–70771, http://dx.doi.org/10.1039/c5ra11208g.

[232] Ning-Jing Yang, Hai Yang, Zhigao Huang, Jian-Min Zhang, Second-order topological insulators in Kekulé-patterned hexagonal biphenylene networks, Appl. Phys. Lett. 126 (3) (2025) http://dx.doi.org/10.1063/5.0239997, URL http://dx.doi.org/10.1063/5.0239997.

[233] Wladimir A. Benalcazar, B. Andrei Bernevig, Taylor L. Hughes, Quantized electric multipole insulators, Science 357 (6346) (2017) 61–66, http://dx.doi.org/10.1126/science.aah6442, URL https://www.science.org/doi/abs/10.1126/science.aah6442.

[234] Wladimir A. Benalcazar, Tianhe Li, Taylor L. Hughes, Quantization of fractional corner charge in c_n-symmetric higher-order topological crystalline insulators, Phys. Rev. B 99 (24) (2019) http://dx.doi.org/10.1103/physrevb.99.245151.

[235] Ryo Takahashi, Tiantian Zhang, Shuichi Murakami, General corner charge formula in two-dimensional c_n -symmetric higher-order topological insulators, Phys. Rev. B 103 (20) (2021) http://dx.doi.org/10.1103/physrevb.103.205123.

[236] Ka Ho Wong, Mark R. Hirsbrunner, Jacopo Gliozzi, Arbaz Malik, Barry Bradlyn, Taylor L. Hughes, Dirk K. Morr, Higher order topological superconductivity in magnet-superconductor hybrid systems, Npj Quantum Mater. 8 (1) (2023) http://dx.doi.org/10.1038/s41535-023-00564-9.

[237] Chun-Guang Chu, Jing-Jing Chen, An-Qi Wang, Zhen-Bing Tan, Cai-Zhen Li, Chuan Li, Alexander Brinkman, Peng-Zhan Xiang, Na Li, Zhen-Cun Pan, Hai-Zhou Lu, Dapeng Yu, Zhi-Min Liao, Broad and colossal edge supercurrent in Dirac semimetal Cd3As2 josephson junctions, Nat. Commun. 14 (1) (2023) http://dx.doi.org/10.1038/s41467-023-41815-4.

[238] Qinglin Wang, Qinghua Zhou, Electronic and optical properties of biphenylene under pressure: first-principles calculations, Mol. Simul. 46 (13) (2020) 987–993, http://dx.doi.org/10.1080/08927022.2020.1797018.

[239] A.T. Balaban, C.C. Rentea, E. Ciupitu, Chemical graphs. VI. Estimation of the relative stability of several planar and tridimensional lattices for elementary carbon, Rev. Roum. Chim. 13 (1968) 231–247.

[240] R.H. Baughman, H. Eckhardt, M. Kertesz, Structure-property predictions for new planar forms of carbon: Layered phases containing sp2 and sp atoms, J. Chem. Phys. 87 (11) (1987) 6687–6699, http://dx.doi.org/10.1063/1.453405.

[241] Andrew T. Koch, Amir H. Khoshaman, Harrison D.E. Fan, George A. Sawatzky, Alireza Nojeh, Graphenylene nanotubes, J. Phys. Chem. Lett. 6 (19) (2015) 3982–3987, http://dx.doi.org/10.1021/acs.jpclett.5b01707, PMID: 26722903.

[242] Marco Bieri, Matthias Treier, Jinming Cai, Kamel Aït-Mansour, Pascal Ruffieux, Oliver Gröning, Pierangelo Gröning, Marcel Kastler, Ralph Rieger, Xinliang Feng, Klaus Müllen, Roman Fasel, Porous graphenes: two-dimensional polymer synthesis with atomic precision, Chem. Commun. (2009) 6919–6921, http://dx.doi.org/10.1039/B915190G.

[243] G.S.L. Fabris, N.L. Marana, E. Longo, J.R. Sambrano, Theoretical study of porous surfaces derived from graphene and boron nitride, J. Solid State Chem. (2017) http://dx.doi.org/10.1016/j.jssc.2017.10.025.

[244] Qi-Shi Du, Pei-Duo Tang, Hua-Lin Huang, Fang-Li Du, Kai Huang, Neng-Zhong Xie, Si-Yu Long, Yan-Ming Li, Jie-Shan Qiu, Ri-Bo Huang, A new type of two-dimensional carbon crystal prepared from 1, 3, 5-trihydroxybenzene, Sci. Rep. 7 (1) (2017) http://dx.doi.org/10.1038/srep40796.

[245] Charles F. Wilcox, Erik N. Farley, Dicycloocta[1, 2, 3, 4-def:1', 2', 3', 4'-jkl]biphenylene. Benzenoid atropism in a highly antiaromatic polycycle, J. Am. Chem. Soc. 105 (24) (1983) 7191–7192, http://dx.doi.org/10.1021/ja00362a040.

[246] Charles F. Wilcox, Erik N. Farley, Dicyclooctabiphenylene. Synthesis and properties, J. Am. Chem. Soc. 106 (23) (1984) 7195–7200, http://dx.doi.org/10.1021/ja00335a055.

[247] Chun Hui Xu, Gustavo E. Scuseria, Theoretical predictions for a two-dimensional rhombohedral phase of solid C 60, Phys. Rev. Lett. 74 (2) (1995) 274.

[248] Wenwen Li, Rui Yang, Mengtao Sun, Superior thermoelectric properties of bulk and monolayer fullerene networks, J. Mater. Chem. A 11 (8) (2023) 3949–3960.

[249] Lingxiang Hou, Xueping Cui, Bo Guan, Shaozhi Wang, Ruian Li, Yunqi Liu, Daoben Zhu, Jian Zheng, Synthesis of a monolayer fullerene network, Nature 606 (7914) (2022) 507–510.

[250] Hans Kuzmany, Rudolf Pfeiffer, Martin Hulman, Christian Kramberger, Raman spectroscopy of fullerenes and fullerene–nanotube composites, Philos. Trans. R. Soc. Lond. Ser. A Math. Phys. Eng. Sci. 362 (1824) (2004) 2375–2406.

[251] Peter C. Eklund, Apparao M. Rao, Fullerene Polymers and Fullerene Polymer Composites, vol. 38, Springer Science & Business Media, 2013.

[252] A.M. Rao, Ping Zhou, Kai-An Wang, G.T. Hager, J.M. Holden, Ying Wang, W.-T. Lee, Xiang-Xin Bi, P.C. Eklund, D.S. Cornett, et al., Photoinduced polymerization of solid C60 films, Science 259 (5097) (1993) 955–957.

[253] Hiroshi Yamamoto, Nobuyuki Iwata, Ryoji Hashimoto, Shingo Ando, Photon-assisted synthesis of C60 polymers by laser irradiation, Appl. Surf. Sci. 253 (19) (2007) 7977–7980.

[254] Masato Nakaya, Tomonobu Nakayama, Masakazu Aono, Fabrication and electron-beam-induced polymerization of C60 nanoribbon, Thin Solid Films 464 (2004) 327–330.

[255] Noboru Takahashi, Henrik Dock, Nobuyuki Matsuzawa, Masafumi Ata, Plasma-polymerized C60/C70 mixture films: electric conductivity and structure, J. Appl. Phys. 74 (9) (1993) 5790–5798.

[256] Minh Xuan Tran, Ryanda Enggar Anugrah Ardhi, Guicheng Liu, Ji Young Kim, Joong Kee Lee, Plasma-polymerized C60-coated CNT interlayer with physical and chemical functions for lithium–sulfur batteries, Chem. Eng. J. 401 (2020) 126075.

[257] Y. Iwasa, T. Arima, R.M. Fleming, T. Siegrist, O. Zhou, R.C. Haddon, L.J. Rothberg, K.B. Lyons, H.L. Carter Jr., A.F. Hebard, et al., New phases of C60 synthesized at high pressure, Science 264 (5165) (1994) 1570–1572.

[258] C.S. Sundar, P.Ch. Sahu, V.S. Sastry, G.V.N. Rao, V. Sridharan, M. Premila, A. Bharathi, Y. Hariharan, T.S. Radhakrishnan, D.V.S. Muthu, et al., Pressure-induced polymerization of fullerenes: a comparative study of C 60 and C 70, Phys. Rev. B 53 (13) (1996) 8180.

[259] B. Narymbetov, V. Agafonov, V.A. Davydov, L.S. Kashevarova, A.V. Rakhmanina, A.V. Dzyabchenko, V.I. Kulakov, Rene Ceolin, The crystal structure of the 2D polymerized tetragonal phase of C60, Chem. Phys. Lett. 367 (1–2) (2003) 157–162.

[260] Bo Peng, Michele Pizzochero, Monolayer C60 networks: a first-principles perspective, Chem. Commun. (2025) http://dx.doi.org/10.1039/d5cc02473k.

[261] Douglas L. Strout, Robert L. Murry, Chunhui Xu, Wade C. Eckhoff, Gregory K. Odom, Gustavo E. Scuseria, A theoretical study of buckminsterfullerene reaction products: C60+ C60, Chem. Phys. Lett. 214 (6) (1993) 576–582.

[262] Madhu Menon, K.R. Subbaswamy, Majid Sawtarie, Structure and properties of c 60 dimers by generalized tight-binding molecular dynamics, Phys. Rev. B 49 (19) (1994) 13966.

[263] Gary B. Adams, John B. Page, Otto F. Sankey, Michael O'Keeffe, Polymerized C 60 studied by first-principles molecular dynamics, Phys. Rev. B 50 (23) (1994) 17471.

[264] Mark R. Pederson, Andrew A. Quong, Fullerene dimers: Cohesive energy, electronic structure, and vibrational modes, Phys. Rev. Lett. 74 (12) (1995) 2319.

[265] Dirk Porezag, Mark R. Pederson, Th. Frauenheim, Th. Köhler, Structure, stability, and vibrational properties of polymerized C 60, Phys. Rev. B 52 (20) (1995) 14963.

[266] Susumu Okada, Susumu Saito, Atsushi Oshiyama, New metallic crystalline carbon: three dimensionally polymerized C 60 fullerite, Phys. Rev. Lett. 83 (10) (1999) 1986.

[267] Manuel Nunez-Regueiro, L. Marques, J.-L. Hodeau, O. Béthoux, M. Perroux, Polymerized fullerite structures, Phys. Rev. Lett. 74 (2) (1995) 278.

[268] Susumu Okada, Susumu Saito, Electronic structure and energetics of pressure-induced two-dimensional C 60 polymers, Phys. Rev. B 59 (3) (1999) 1930.

[269] V.A. Davydov, V. Agafonov, A.V. Dzyabchenko, R. Céolin, H. Szwarc, Packing models for high-pressure polymeric phases of C60, J. Solid State Chem. 141 (1) (1998) 164–167.

[270] Raphael M. Tromer, Luiz A. Ribeiro Junior, Douglas S. Galvão, A DFT study of the electronic, optical, and mechanical properties of a recently synthesized monolayer fullerene network, Chem. Phys. Lett. 804 (2022) 139925.

[271] L.A. Ribeiro Junior, M.L. Pereira Junior, W.F. Giozza, R.M. Tromer, Douglas S. Galvao, Thermal stability and fracture patterns of a recently synthesized monolayer fullerene network: A reactive molecular dynamics study, Chem. Phys. Lett. 807 (2022) 140075.

[272] Linfeng Yu, Jinyuan Xu, Bo Peng, Guangzhao Qin, Gang Su, Anisotropic optical, mechanical, and thermoelectric properties of two-dimensional fullerene networks, J. Phys. Chem. Lett. 13 (50) (2022) 11622–11629.

[273] Bo Peng, Monolayer fullerene networks as photocatalysts for overall water splitting, J. Am. Chem. Soc. 144 (43) (2022) 19921–19931.

[274] Yujing Tong, Hongjun Liu, Sheng Dai, De-en Jiang, Monolayer fullerene membranes for hydrogen separation, Nano Lett. 23 (16) (2023) 7470–7476.

[275] Wenjing Miao, Li Wang, Jingang Wang, Mengtao Sun, Simulation studies on external electric field-dependent anisotropy of two-dimensional fullerene nanomaterials qTP C_{60} and qHP C_{60}: Implications for photoelectric nanodevices, ACS Appl. Nano Mater. 6 (21) (2023) 20074–20081.

[276] Bo Peng, Stability and strength of monolayer polymeric C60, Nano Lett. 23 (2) (2023) 652–658.

[277] Bohayra Mortazavi, Structural, electronic, thermal and mechanical properties of C60-based fullerene two-dimensional networks explored by first-principles and machine learning, Carbon 213 (2023) 118293.

[278] Shahram Ajori, Mohsen Eghbalian, Fatemeh Sadeghi, Graphullerene: a fully atomistic analysis of the tensile characteristics under temperature variation, Adv. Eng. Mater. 26 (5) (2024) 2301128.

[279] Tiago S.A. Cassiano, M.L. Pereira, G.M. e Silva, Pedro Henrique de Oliveira Neto, L.A. Ribeiro, Large polarons in two-dimensional fullerene networks: the crucial role of anisotropy in charge transport, Nanoscale 16 (5) (2024) 2337–2346.

[280] Amedeo Capobianco, Julia Wiktor, Alessandro Landi, Francesco Ambrosio, Andrea Peluso, Electron localization and mobility in monolayer fullerene networks, Nano Lett. 24 (27) (2024) 8335–8342.

[281] Aurélie Champagne, María Camarasa-Gómez, Francesco Ricci, Leeor Kronik, Jeffrey B. Neaton, Strongly bound excitons and anisotropic linear absorption in monolayer graphullerene, Nano Lett. (2024).

[282] Kesai Shi, Yushun Zhao, Weizhe Hao, Yuna Sang, Junjiao Li, Linlin Miao, Jiaxuan Li, Chao Sui, Xiaodong He, Chao Wang, Tunable viscoelasticity of bulk fullerene network via high-temperature annealing, Diam. Relat. Mater. 144 (2024) 111030.

[283] Ruipeng Wang, Haipeng Li, Muhammad Asif Shakoori, Xuechao Cheng, Yuxiao Hu, Leyang Wang, Strain engineering of electronic structure and thermoelectric properties of quasi-hexagonal fullerene monolayer, J. Appl. Phys. 136 (1) (2024).

[284] Haoyong Suo, Manfu Li, Guang Yang, Yuxin Du, Xingju Zhao, Xiaoyan Ren, Shunfang Li, Covalent-bond-linked monolayer fullerene network as a spin sponge for spin-triplet O 2 activation and CO oxidation, Phys. Rev. B 110 (12) (2024) 125405.

[285] Qiang Xu, Daniel Weinberg, Mahmut Sait Okyay, Min Choi, Mauro Del Ben, Bryan M. Wong, Photoinduced electron–nuclear dynamics of fullerene and its monolayer networks in solvated environments, J. Am. Chem. Soc. 146 (51) (2024) 35313–35320.

[286] Daniil Alekseev, Mikhail Logunov, Mikhail Lazarev, Sergey Zhukov, Nikita Orekhov, Thermal stability of monolayer fullerene networks: A molecular dynamics study with machine-learning potential, Comput. Mater. Sci. 248 (2025) 113572.

[287] Bohayra Mortazavi, Xiaoying Zhuang, Low and anisotropic tensile strength and thermal conductivity in the single-layer fullerene network predicted by machine-learning interatomic potentials, Coatings 12 (8) (2022) 1171.

[288] Penghua Ying, Haikuan Dong, Ting Liang, Zheyong Fan, Zheng Zhong, Jin Zhang, Atomistic insights into the mechanical anisotropy and fragility of monolayer fullerene networks using quantum mechanical calculations and machine-learning molecular dynamics simulations, Extrem. Mech. Lett. 58 (2023) 101929.

[289] Yanbo Han, Mengyang Li, Masahiro Ehara, Xiang Zhao, Unveiling fullerene formation and interconversion through molecular dynamics simulations with deep neural network potentials, Phys. Chem. Chem. Phys. 27 (18) (2025) 9767–9773.

[290] V.A. Davydov, L.S. Kashevarova, A.V. Rakhmanina, V.N. Agafonov, R. Ceolin, H. Szwarc, Pressure-induced polycondensation of C 60 fullerene, J. Exp. Theor. Phys. Lett. 63 (1996) 818–824.

[291] V.A. Davydov, L.S. Kashevarova, A.V. Rakhmanina, V. Agafonov, H. Allouchi, R. Ceolin, A.V. Dzyabchenko, V.M. Senyavin, H Szwarc, Tetragonal polymerized phase of C 60, Phys. Rev. B 58 (22) (1998) 14786.

[292] Xuean Chen, Shoji Yamanaka, Single-crystal X-ray structural refinement of thetetragonal'C60 polymer, Chem. Phys. Lett. 360 (5–6) (2002) 501–508.
[293] Xuean Chen, Shoji Yamanaka, Kohta Sako, Yuhta Inoue, Masahiro Yasukawa, First single-crystal X-ray structural refinement of the rhombohedral C60 polymer, Chem. Phys. Lett. 356 (3–4) (2002) 291–297.
[294] Takeo Oku, Masaki Kuno, Hidehiko Kitahara, Ichihito Narita, Formation, atomic structures and properties of boron nitride and carbon nanocage fullerene materials, Int. J. Inorg. Mater. 3 (7) (2001) 597–612.
[295] Z.-T. Zhu, J.L. Musfeldt, Katalin Kamarás, G.B. Adams, J.B. Page, V.A. Davydov, L.S. Kashevarova, A.V. Rakhmanina, Far-infrared vibrational properties of tetragonal C 60 polymer, Phys. Rev. B 65 (8) (2002) 085413.
[296] V.P. Kazachenko, I.V. Ryazanov, Structure of C 60 polymer coatings deposited via electron-beam dispersion of fullerite, Phys. the Solid State 51 (2009) 870–875.
[297] D.W. Murphy, M.J. Rosseinsky, R.M. Fleming, R. Tycko, A.P. Ramirez, R.C. Haddon, T. Siegrist, G. Dabbagh, J.C. Tully, R.E. Walstedt, Synthesis and characterization of alkali metal fullerides: AxC60, J. Phys. Chem. Solids 53 (11) (1992) 1321–1332.
[298] Peter J.F. Harris, Fullerene polymers: A brief review, C 6 (4) (2020) 71.
[299] Xingmao Chang, Youzhi Xu, Max von Delius, Recent advances in supramolecular fullerene chemistry, Chem. Soc. Rev. 53 (1) (2024) 47–83, http://dx.doi.org/10.1039/d2cs00937d.
[300] Taotao Wang, Li Zhang, Jinbao Wu, Muqing Chen, Shangfeng Yang, Yalin Lu, Pingwu Du, Few-layer fullerene network for photocatalytic pure water splitting into H_2 and H_2O_2, Angew. Chem. Int. Ed. 62 (40) (2023) e202311352.
[301] Elena Meirzadeh, Austin M Evans, Mehdi Rezaee, Milena Milich, Connor J. Dionne, Thomas P. Darlington, Si Tong Bao, Amymarie K. Bartholomew, Taketo Handa, Daniel J. Rizzo, et al., A few-layer covalent network of fullerenes, Nature 613 (7942) (2023) 71–76.
[302] Xiaofang Chen, Yifang Mu, Chunxin Jin, Yayu Wei, Jinlin Hao, Huanting Wang, Jürgen Caro, Aisheng Huang, Ultrathin two-dimensional porous fullerene membranes for ultimate organic solvent separation, Angew. Chem. 136 (18) (2024) e202401747.
[303] Fei Pan, Kun Ni, Tao Xu, Huaican Chen, Yusong Wang, Ke Gong, Cai Liu, Xin Li, Miao-Ling Lin, Shengyuan Li, Xia Wang, Wensheng Yan, Wen Yin, Ping-Heng Tan, Litao Sun, Dapeng Yu, Rodney S. Ruoff, Yanwu Zhu, Long-range ordered porous carbons produced from C60, Nature 614 (7946) (2023) 95–101, http://dx.doi.org/10.1038/s41586-022-05532-0.
[304] Meng He, Yehui Ding, Xue Liu, Nanoporous amorphous carbon monolayer derived from fullerene film, Adv. Sci. 11 (10) (2023) http://dx.doi.org/10.1002/advs.202308187.
[305] Yuxuan Zhang, Yifan Xie, Hao Mei, Hui Yu, Minjuan Li, Zexiang He, Wentao Fan, Panpan Zhang, Antonio Gaetano Ricciardulli, Paolo Samorì, et al., Electrochemical synthesis of 2d polymeric fullerene for broadband photodetection, Adv. Mater. 37 (14) (2025) 2416741.
[306] Samiul Islam, S.S.Z. Ashraf, Point and space groups of graphene, Resonance 24 (4) (2019) 445–457, http://dx.doi.org/10.1007/s12045-019-0797-1.
[307] Ke Cao, Shizhe Feng, Ying Han, Libo Gao, Thuc Hue Ly, Zhiping Xu, Yang Lu, Elastic straining of free-standing monolayer graphene, Nat. Commun. 11 (1) (2020) http://dx.doi.org/10.1038/s41467-019-14130-0.
[308] Li Yang, Excitonic effects on optical absorption spectra of doped graphene, Nano Lett. 11 (9) (2011) 3844–3847, http://dx.doi.org/10.1021/nl201928g.
[309] Xu Du, Ivan Skachko, Anthony Barker, Eva Y. Andrei, Approaching ballistic transport in suspended graphene, Nature Nanotechnology 3 (8) (2008) 491–495, http://dx.doi.org/10.1038/nnano.2008.199.
[310] K.S. Novoselov, A.K. Geim, S.V. Morozov, D. Jiang, M.I. Katsnelson, I.V. Grigorieva, S.V. Dubonos, A.A. Firsov, Two-dimensional gas of massless Dirac fermions in graphene, Nature 438 (7065) (2005) 197–200, http://dx.doi.org/10.1038/nature04233.
[311] Marie-Luise Braatz, Lothar Veith, Janis Köster, Ute Kaiser, Axel Binder, Martin Gradhand, Mathias Kläui, Impact of nitrogen doping on the band structure and the charge carrier scattering in monolayer graphene, Phys. Rev. Mater. 5 (8) (2021) http://dx.doi.org/10.1103/physrevmaterials.5.084003.
[312] Valentin N. Popov, Philippe Lambin, Theoretical Raman fingerprints of α–, β–, and γ–graphyne, Phys. Rev. B 88 (7) (2013) http://dx.doi.org/10.1103/physrevb.88.075427.
[313] Shuting Lei, Qiang Cao, Xiao Geng, Yang Yang, Sheng Liu, Qing Peng, The mechanical properties of defective graphyne, Crystals 8 (12) (2018) 465, http://dx.doi.org/10.3390/cryst8120465.
[314] Qing Peng, Wei Ji, Suvranu De, Mechanical properties of graphyne monolayers: a first-principles study, Phys. Chem. Chem. Phys. 14 (38) (2012) 13385, http://dx.doi.org/10.1039/c2cp42387a.
[315] Behrouz Rouzkhash, Alireza Salehi, Mohammad Taghi Ahmadi, γ-Graphyne-1 band structure modeling and simulation, Solid State Commun. 325 (2021) 114164, http://dx.doi.org/10.1016/j.ssc.2020.114164.
[316] Xun Hou, Zhongjing Xie, Chunmei Li, Guannan Li, Zhiqian Chen, Study of electronic structure, thermal conductivity, elastic and optical properties of α, β, γ-graphyne, Materials 11 (2) (2018) 188, http://dx.doi.org/10.3390/ma11020188.
[317] Heyu Ding, Hongcun Bai, Yuanhe Huang, Electronic properties and carrier mobilities of 6, 6, 12-graphyne nanoribbons, AIP Adv. 5 (7) (2015) http://dx.doi.org/10.1063/1.4927497.
[318] Patrick Serafini, Alberto Milani, Matteo Tommasini, Chiara Castiglioni, Carlo S. Casari, Raman and IR spectra of graphdiyne nanoribbons, Phys. Rev. Mater. 4 (1) (2020) http://dx.doi.org/10.1103/physrevmaterials.4.014001.
[319] Yang Pei, Mechanical properties of graphdiyne sheet, Phys. B 407 (22) (2012) 4436–4439, http://dx.doi.org/10.1016/j.physb.2012.07.026.
[320] Lu Zhang, Wencai Yi, Junfang Li, Guoying Wei, Guangcheng Xi, Lanqun Mao, Surfactant-free interfacial growth of graphdiyne hollow microspheres and the mechanistic origin of their SERS activity, Nat. Commun. 14 (1) (2023) http://dx.doi.org/10.1038/s41467-023-42038-3.
[321] Hongyu Ge, Guo Wang, Yi Liao, A theoretical prediction on huge hole and electron mobilities of 6, 6, 18-graphdiyne nanoribbons, Chem. Phys. Lett. 633 (2015) 30–34, http://dx.doi.org/10.1016/j.cplett.2015.05.009.
[322] Xin-Wei Chen, Zheng-Zhe Lin, Xi-Mei Li, Biphenylene network as sodium ion battery anode material, Phys. Chem. Chem. Phys. 25 (5) (2023) 4340–4348, http://dx.doi.org/10.1039/d2cp04752g.
[323] Yinlong Hou, Kai Ren, Yu Wei, Dan Yang, Zhen Cui, Ke Wang, Opening a band gap in biphenylene monolayer via strain: A first-principles study, Molecules 28 (10) (2023) 4178, http://dx.doi.org/10.3390/molecules28104178.
[324] Changhong Zhang, Chengyi Hou, Yi Lu, Le Zhao, Haorong Wu, Hongyuan Song, Ju Rong, Lan Yu, Xiaohua Yu, Thermal and electrical transport properties of two-dimensional Dirac graphenylene: a first-principles study, Phys. Chem. Chem. Phys. 25 (45) (2023) 31301–31311, http://dx.doi.org/10.1039/d3cp04512a.
[325] Linfeng Yu, Jinyuan Xu, Bo Peng, Guangzhao Qin, Gang Su, Anisotropic optical, mechanical, and thermoelectric properties of two-dimensional fullerene networks, J. Phys. Chem. Lett. 13 (50) (2022) 11622–11629, http://dx.doi.org/10.1021/acs.jpclett.2c02702.
[326] Rizwan Ur Rehman Sagar, Xiaozhong Zhang, Chengyue Xiong, Yi Yu, Semiconducting amorphous carbon thin films for transparent conducting electrodes, Carbon 76 (2014) 64–70, http://dx.doi.org/10.1016/j.carbon.2014.04.049.
[327] Chunya Wang, Kailun Xia, Huimin Wang, Xiaoping Liang, Zhe Yin, Yingying Zhang, Advanced carbon for flexible and wearable electronics, Adv. Mater. 31 (9) (2018) http://dx.doi.org/10.1002/adma.201801072.
[328] J.V.N. Sarma, Rajib. Chowdhury, R. Jayaganthan, Graphyne-based single electron transistor: Ab initio analysis, Nano 09 (03) (2014) 1450032, http://dx.doi.org/10.1142/s1793292014500325.
[329] Utkarsh Kumar, Pei-Ying Wu, Chun-En Lin, Zu-Yin Deng, Ren-Jang Wu, Kuen-Lin Chen, Wen-Min Huang, Chiu-Hsien Wu, γ-Graphyne as a functional 2D nanoarchitectonics for room-temperature chemiresistive–potentiometric sensing interfaces, ACS Sensors 10 (10) (2025) 7508–7520, http://dx.doi.org/10.1021/acssensors.5c01507.
[330] K. Srinivasu, Swapan K. Ghosh, Graphyne and graphdiyne: Promising materials for nanoelectronics and energy storage applications, J. Phys. Chem. C 116 (9) (2012) 5951–5956, http://dx.doi.org/10.1021/jp212181h.
[331] Krishnanshu Basak, Mainak Ghosh, N. Bedamani Singh, Rajkumar Mondal, Debnarayan Jana, Functionalised biphenylene and graphenylene: excellent choices for supercapacitor electrodes, Phys. Chem. Chem. Phys. 26 (48) (2024) 29759–29772, http://dx.doi.org/10.1039/d4cp03624g.
[332] Luzhen Xie, Tong Chen, Xiansheng Dong, Guogang Liu, Hui Li, Ning Yang, Desheng Liu, Xianbo Xiao, A comparative study of the electronic transport and gas-sensitive properties of graphene+, T-graphene, net-graphene, and biphenylene-based two-dimensional devices, ACS Sensors 8 (9) (2023) 3510–3519, http://dx.doi.org/10.1021/acssensors.3c01087.
[333] K.A. Lopes Lima, L.A. Ribeiro, Unveiling the CO_2 adsorption capabilities of biphenylene network monolayers through DFT calculations, Comput. Mater. Sci. 232 (2024) 112673, http://dx.doi.org/10.1016/j.commatsci.2023.112673.
[334] Yi Ren, Yun Lu, Dong Zhang, Enhanced hydrogen storage capacity in two-dimensional fullerene networks, J. Phys. Chem. Lett. 14 (49) (2023) 11051–11057, http://dx.doi.org/10.1021/acs.jpclett.3c02488.
[335] Jiguang Du, Mingyang Shi, Xuying Zhou, Xiujuan Cheng, Kunyang Cheng, Gang Jiang, Monolayer fullerene networks for high-performance lithium–sulfur and sodium–sulfur batteries, ACS Catal. 15 (11) (2025) 9949–9961, http://dx.doi.org/10.1021/acscatal.4c07268.
[336] Xiao Chang, Xianghong Liu, Wei Zheng, Lihao Zhou, Jun Zhang, Monolayer fullerene network: A promising material for VOCs sensor, Appl. Surf. Sci. 637 (2023) 157909, http://dx.doi.org/10.1016/j.apsusc.2023.157909.
[337] Wenwen Li, Rui Yang, Mengtao Sun, Superior thermoelectric properties of bulk and monolayer fullerene networks, J. Mater. Chem. A 11 (8) (2023) 3949–3960, http://dx.doi.org/10.1039/d2ta08537b.

Further reading

[1] Andre Geim, Konstantin Novoselov, The nobel prize in physics 2010, Nat. Phys. 6 (2010) 836.